Master's thesis

NTNU
Norwegian University of Science and Technology
Faculty of Natural Sciences
Department of Biotechnology and Food Science

Silje Trå Hervig

A study of AlgE-type mannuronan C-5-epimerases from *Azotobacter chroococcum* and *Azotobacter vinelandii*

Master's thesis in Biotechnology (MBIOT5)
Supervisor: Helga Ertesvåg
Co-supervisor: Finn Lillelund Aachmann
May 2022

NTNU
Kunnskap for en bedre verden

Silje Trå Hervig

A study of AlgE-type mannuronan C-5-epimerases from *Azotobacter chroococcum* and *Azotobacter vinelandii*

Master's thesis in Biotechnology (MBIOT5)
Supervisor: Helga Ertesvåg
Co-supervisor: Finn Lillelund Aachmann
May 2022

Norwegian University of Science and Technology
Faculty of Natural Sciences
Department of Biotechnology and Food Science

NTNU
Kunnskap for en bedre verden

Abstract

Alginate is a biopolymer consisting of β-D-mannuronic acid (M) and α–L-guluronic acid (G), linked by 1→4 glycosidic bonds. The polymer is biocompatible and has the ability to form hydrogels, which for instance makes it useful for medical applications and in the food industry. Structurally, alginate consist of G-blocks, M-blocks and MG-blocks of variable lengths and frequencies. The structure affects its physiochemical properties. G-blocks can for instance crosslink with calcium ions, leading to gelation. The G-content and the length of the G-blocks are therefore important factors for the properties of alginate. Mannuronan C-5-epimerases and alginate lyases are capable of epimerizing M residues to G and cleave the alginate, respectively. This alters the properties of the polymer, making these enzymes interesting tools for modification of alginate.

In this project, AlgE-type mannuronan C-5-epimerases from *Azotobacter* were studied. The main objective of the study was to improve the understanding of the function of these enzymes and how their activity can be altered. In a larger perspective, the aim is to open for further use of bacterial epimerases and lyases for modification of industrial alginate. The mode of action of two mannuronan C-5-epimerases, AcAlgE1 and AlgE1, was studied and compared by NMR. Two bifunctional mannuronan C-5-epimerases and alginate lyases, AcAlgE2 and AcAlgE3, were studied to measure kinetics and salt dependency of their lyase activity. The effect of calcium was tested and compared for calcium binding sites in the A-modules of AlgE6 and AlgE7. For this purpose, an optimized epimerase assay was developed and tested. Additionally, a C-terminal His-tag was tested for purification of AcAlgE1-3.

In this work, it was found that AcAlgE1 produce higher G-content than AlgE1, but shorter G-blocks. AcAlgE2 and AcAlgE3 were both dependent on calcium and the lyase activity was affected by the NaCl concentration. It was also demonstrated that the studied calcium binding site from AlgE7 had different calcium dependency than the same amino acid sequence in AlgE6. In addition, it was found that a C-terminal His-tag could not be used for purification of AcAlgE1-3 and that *E. coli* SHuffle T7 express was better than *E. coli* RV308 for production of these enzymes.

Sammendrag

Alginat er en biopolymer bestående av β-D-mannuronsyre (M) og α-L-guluronsyre (G), bundet sammen med 1→4 glykosidbindinger. Alginat er biokompatibelt og kan danne hydrogeler, som for eksempel kan brukes i medisinsk sammenheng og i matindustrien. Polymeren består av G-blokker, M-blokker og MG-blokker av ulik lengde og hyppighet. Strukturen påvirker de fysiokjemiske egenskapene til alginatet. G-blokker kan for eksempel kobles sammen ved hjelp av kalsiumioner, som fører til geldannelse. Andelen G og lengden på G-blokkene er derfor viktige faktorer for egenskapene til alginat. Mannuronan C-5 epimeraser og alginat lyaser er enzymer som henholdsvis epimeriserer og kløyver alginat og er derfor interessante verktøy for modifisering av alginat.

I dette prosjektet ble AlgE-type mannuronan C-5-epimeraser studert. Hovedmålet ved denne studien var å oppnå en bedre forståelse for funksjonen til disse enzymene og hvordan aktiviteten deres kan endres. Hensikten med dette er i det store bildet å legge til rette for videre bruk av bakterielle epimeraser og lyaser for modifisering av industrielt alginat. NMR ble brukt for å studere epimeriseringsmønstrene for to mannuronan C-5-epimeraser (AcAlgE1 og AlgE1). Lyaseaktiviteten til to bifunksjonelle mannuronan C-5-epimeraser og alginat lyaser, AcAlgE2 og AcAlgE3, ble studert for å måle enzymkinetikk og salt-avhengighet. Effekten av kalsium ble også testet og sammenliknet for kalsiumbindende seter i A-modulene til AlgE6 og AlgE7. En kvantitativ metode for å måle epimerase-aktivitet ble utviklet og testet i denne sammenhengen. I tillegg ble det forsøkt å rense AcAlgE1-3 med C-terminale His-tagger.

Det ble observert at AcAlgE1 produserte en større andel G enn AlgE1, men kortere G-blokker. Både AcAlgE2 og AcAlgE3 var avhengige av kalsium og ble påvirket av konsentrasjonen av NaCl. I tillegg ble det vist at et kalsium-bindende sete fra AlgE7 ble påvirket av kalsium annerledes enn den samme aminosyresekvensen i AlgE6. Det ble også funnet at C-terminale His-tagger ikke kunne brukes til rensing av AcAlgE1-3 og at *E. coli* SHuffle T7 express var bedre enn *E. coli* RV308 for produksjon av disse enzymene.

Preface

This master project was conducted at the Department of Biotechnology and Food Science at the Norwegian University of Science and Technology (NTNU) in Trondheim. The experimental work was was done in collaboration with the molecular genetics group with Helga Ertesvåg as supervisor and the biopolymer NMR group with Finn L. Aachmann as co-supervisor. Some of the experimental work was also done in collaboration with SINTEF – Department of Biotechnology and Nanomedicine.

First of all, I would like to thank my supervisor Helga Ertesvåg for excellent guidance and for always making time for me. Thank you to Finn Lillelund Aachmann for your guidance and for conducting some of the experimental work. I would also like to express my gratitude to Agnes Beenfeldt Petersen for great collaboration and for conducting some of the work presented in this project. Thank you to Randi Aune and Deni Koseto at SINTEF for conducting some of the experimental work and including me in the process. The work conducted by Wenche Iren Strand is much appreciated too. I would also like to thank Gerd Inger Sætrom for your encouragement and for training me in experimental procedures. Additionally, thank you to all the members of both research groups for assistance in the laboratory and for providing a good learning environment.

Finally, a special thanks to my mother for your endless support and to my friends for making these five years at NTNU the best.

Silje Trå Hervig
May 2022

Table of Contents

Symbols and abbreviations

α	Alpha
Abs	Absorbance
AlgE	AlgE-type mannuronan C5 epimerase
Amp	Ampicillin
β	Beta
bp	Base pair
CV	Column volume
Δ	Delta
ddNTP	Dideoxynucleoside triphosphate
DMSO	Dimethyl sulfoxide
DNA	Deoxyribonucleic acid
DO	Dissolved oxygen
DPn	Number average degree of polymerization
dNTP	Deoxynucleotide
dsDNA	Double stranded DNA
DTT	1,4-dithiothreitol
ε_M	Molar extinction coefficient
F_G	Fraction of G residues
F_M	Fraction of M residues
FPLC	Fast protein liquid chromatography
G	α-L-guluronic acid
GDP	Guanosin diphosphate
HCDC	High-cell-density cultivation
I	Angular momentum quantum number
IPTG	Isopropyl β-D-1-thiogalactopyranoside
Kb	Kilobase
Kan	Kanamycin
λ	Lambda
L	Light path length
LA	Luria broth with agar
LB	Luria broth

M	β-D-mannuronic acid
mAU	Milli Absorbance unit
Min	Minuttes
MOPS	4-morpholinepropanesulfonic acid
MQ	Milli-Q® water
M_W	Molecular weight
NMR	Nuclear magnetic resonance spectroscopy
OD	Optical density
ON	Overnight
PCR	Polymerase chain reaction
RO	Reverse osmosis
rpm	Revolutions per minute
SDS	Sodium dodecyl sulphate
SDS-PAGE	Sodium dodecyl sulphate – polyacryl amide gel electrophoresis
SEC	Size exclusion chromatography
Sec	Seconds
SOC	Super optimal catabolite-repression medium
TAE	Tris-acetate-EDTA
Tm	Melting temperature
TOPO-cloning	Topoisomerase cloning

1 Introduction

1.1 Alginate

Alginate is a family of linear copolymers with several desirable biological and physiochemical properties. It is chemically stable, biocompatible, renewable, biodegradable, non-toxic and has gel-forming abilities (1). The biopolymer has therefore become industrially important with a wide range of applications in food industry, water treatment, medical and pharmaceutical sectors (2, 3). Alginate is FDA-approved and is used in development of drug delivery systems (4). Brown algae is the main source of alginate, but it is also produced by two families of heterotroph bacteria, *Azotobactericeae* and *Pseudomonadaceae* (5). The cell wall of brown algae is built up of a network of alginate, cross-linked by Ca^{2+}. In *Azotobacter*, alginate surround the vegetative cells and is used as cyst coat, whereas *Pseudomonas* produce alginate as a response to cell wall stress and as a part of their biofilm and loose capsule (6). Alginate is a polysaccharide composed of the isomeric residues β-D-mannuronic acid (M) and α–L-guluronic acid (G), linked by 1→4 glycosidic bonds (7). The carboxyl group on the C5 carbon of the saccharide ring has different orientation in the two epimers (Figure 1A). In the M unit, the carboxyl group is above the plane of the ring, whereas it is below the plane in the G unit. Alginates consist of three different block-types, depending on the organization of the monomers: homopolymeric G blocks, homopolymeric M blocks and heteropolymeric MG-blocks. The length and frequency of each block type varies. Due to the diaxial linkages between G monomers, G blocks form a conformation with cavities (Figure 1B). These cavities can bind calcium ions and make the alginate form hydrogels (8). Two antiparallel alginate molecules with G-blocks can form a dimer with calcium-ions in the cavities between them. Several alginate molecules can bind to each other in the same way, forming a multimer, leading to the gelation. MG-blocks also form cavities and can therefore similarly contribute to crosslinking with calcium, leading to gel formation (8).

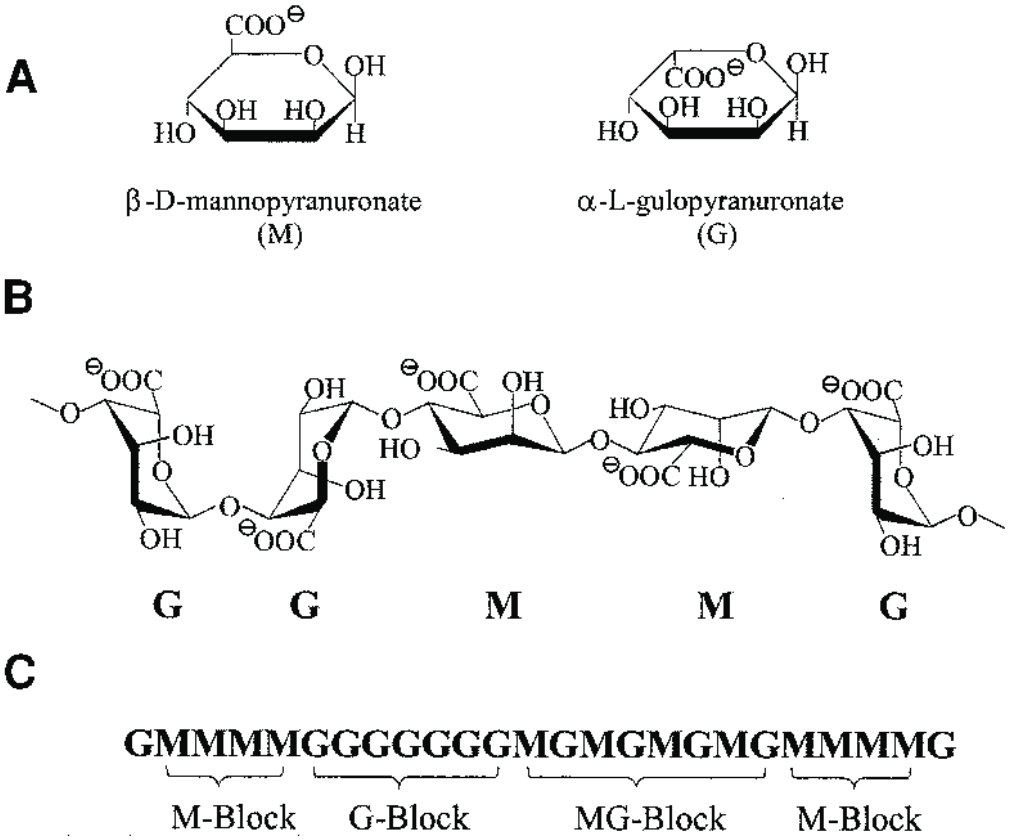

Figure 1: Chemical structures of alginate. **A:** Haworth formula of β-D mannuronate (M) and its epimer α-L guluronate (G). **B:** Chair formation of G and M residues, linked by 1→4 glycosidic bonds. **C:** Chain structure of alginate, showing homopolymeric M- and G-blocks and heteropolymeric M/G-block. The Copied from (9).

1.2 Alginate modifying enzymes

Alginate is initially synthetized as the homopolymer mannuronan, consisting of only M residues, by polymerization of guanosin diphosphate (GDP)-mannuronic acid. Mannuronan is further modified by enzymes: alginate acetylases, alginate deacetylases, alginate lyases, and mannuronan C-5-epimerases. Acetylation of alginate increase water-binding capacity and the viscosity of alginate (6). Alginate lyases cleave the alginate and mannuronan C-5-epimerases epimerize M to G. The physiochemical properties of alginate can be altered by modifying the polysaccharide. The chain length, frequency and distribution of M and G residues are important factors for the properties of alginate. For this reason, alginate modifying enzymes are industrially relevant. Alginates with a high content of G-block form gels by crosslinking with divalent cations such as Ca^{2+}, which is an industrially valuable property (3). It has also been found that a high fraction of M is immunogenic, which was not observed for G-blocks, making C-5-epimerases especially relevant for medical and pharmaceutical purposes (10).

1.2.1 Alginate lyases

Alginate lyases are enzymes that degrade alginate by β-elimination. The alginate is degraded to monosaccharides or oligosaccharides. Alginate oligosaccharides (AOs) have attracted attention by the pharmaceutical industry due to proposed antimicrobial, antitumour, antidiabetic and immunomodulatory activity of some AOs (5). There is also a great potential for AOs in agriculture since they can be used as growth promoters (11). Compared to chemical and physical degradation of alginate, lyases degrade alginate in a more specific and efficient way due to the substrate specificity and high enzyme activity (5). Alginate lyases can therefore be a useful biotechnological tool for processing of alginate. Endolytic alginate lyases cleave the glycosidic linkages within the alginate chain, releasing alginate oligosaccharides, while exolytic alginate lyases degrade the alginate to monosaccharides. The majority of the alginate lyases that have been studied cleave alginate within M-blocks, but some G-specific lyases have also been characterized (7).

All alginate producing bacteria encode a periplasmic alginate lyase. This lyase is likely involved in clearing alginate from the periplasm. Due to the negative charge of alginate, free alginate molecules in the periplasm can increase the osmotic pressure and lead to cell lysis (12, 13). Alginate lyases are therefore necessary for survival of the bacterial cells. Alginate lyases are also produced by organisms that utilize alginate as carbon source, e.g., marine organisms such as *Zobellia galactanivorans* that use alginate from brown algae or by soil bacteria, e.g., *Sphingomonas* sp. A1 that use alginate from *Azotobacter* or *Pseudomonas* (13, 14).

1.2.2 Mannuronan C5-epimerases

The G residues in alginates originate from epimerization of M residues. This epimerization is catalysed by mannuronan C5-epimerases (15). Some mannuronan C5-epimerases introduce long G-blocks and are thus industrially relevant for making stiff hydrogels (16).

The main sources of mannuronan C5-epimerases are brown algae, *Azotobacter* and *Pseudomonas.* Both brown algae and *Azotobacter* can produce G-blocks, while *Pseudomonas* only produce single G residues. The reason for this difference could be that brown algae and *Azotobacter* need strong gel networks for their cell wall and cyst coat, whereas *Pseudomonas*

does not have the same need for structural strength in their loose capsule and biofilm (6). Different species have mannuronan C5-epimerases with specific structural and functional characteristics. A family of AlgG-type epimerases have been found in all alginate-producing species (6). Moreover, there is a strong sequence homology between AlgGs from different species (Figure 2). AlgG epimerases are periplasmic enzymes that are produced in the matrix between the inner and outer membrane. Brown algae also encode a family of mannuronan C5-epimerases related to bacterial AlgGs (Figure 2). AlgE epimerases are secreted, unlike the AlgG-type epimerases. The secretion of AlgE epimerases from A*zotobacter vinelandii* has been found to be facilitated by a type I secretion machineries, composed of an ABC transporter, a membrane fusion protein, and an outer membrane protein (17).

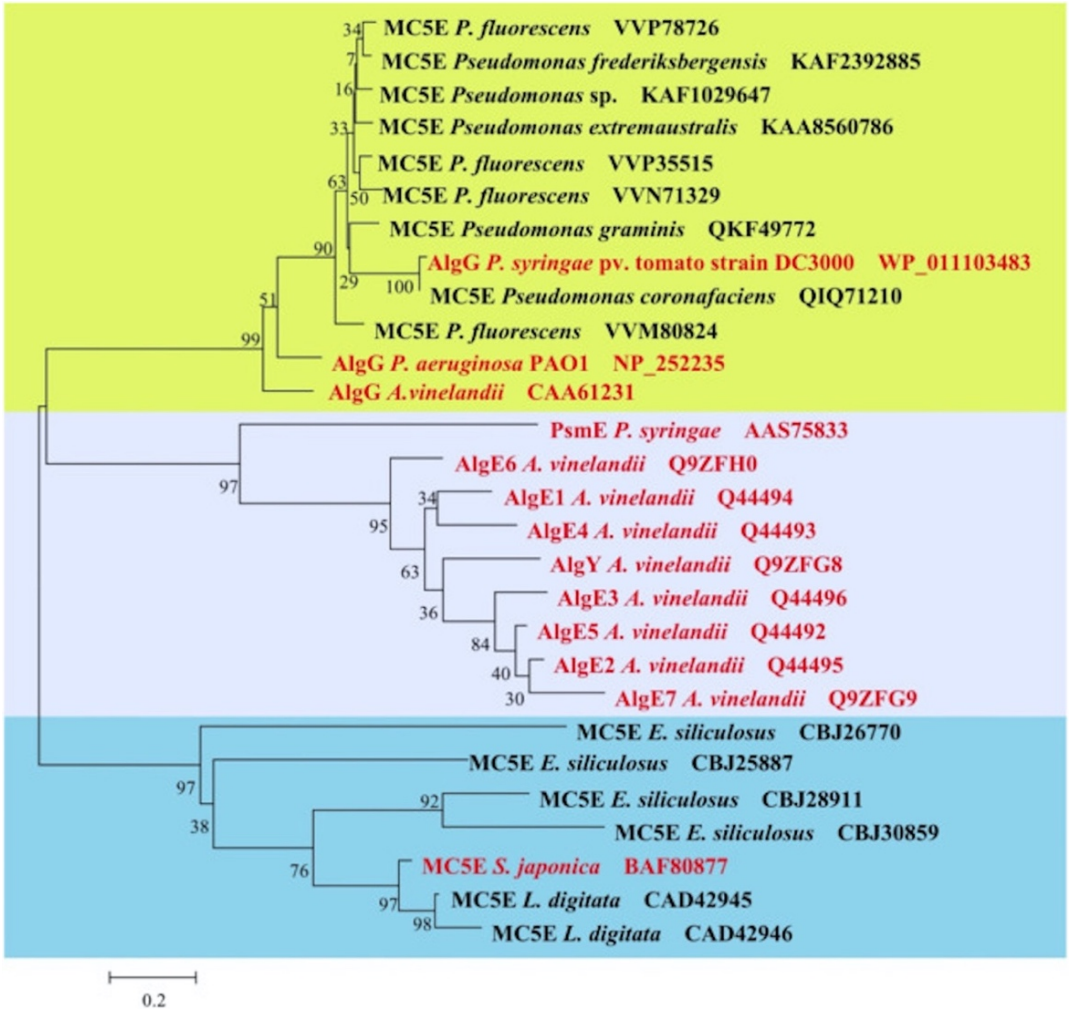

Figure 2: Phylogenetic tree of putative (black) and expressed (red) mannuronan C-5-epimerases from different species, constructed by MEGA 6.0. The colours green, light blue and turquoise represent epimerases mainly from *Pseudomonas*, *Azotobacter*, and brown algae respectively. Mannuronan C-5-epimerases are denoted MC5E. Copied from (15).

AlgE epimerases have attracted interest because they enable formation of G residues *in vitro* (18). Different AlgE epimerases introduce variable distributions of G residues and are expressed at particular stages of the bacterial life cycle (19). AcAlgE1, a mannuronan C5-epimerase found in *Azotobacter chroococcum,* can catalyse epimerization of alginate up to 87% G residue content, and produce G-blocks (20). AlgE1, AlgE2 and AlgE6 are also examples of typical G-block-forming enzymes, whereas AlgE4 form alginate with strictly alternating sequences (21, 22). AlgE-type epimerases consist of one to two catalytic parts (A-modules) and one to seven R-modules. The R-modules are necessary for full activity and have been found to be involved in substrate- and calcium binding (6).

Three AlgE-type epimerases from *A. chroococcum* have been identified: AcAlgE1, AcAlgE2 and AcAlgE3 (20). Their amino acid sequence has been sequenced and compared to different AlgE-type epimerases. It was found that the A-modules of the bifunctional alginate lyases and mannuronan C5-epimerases AcAlgE2 and AcAlgE3 from *A. chroococcum* were related to the A-module of the bifunctional lyase and mannuronan C5-epimerase AlgE7 from *A. vinelandii* (Figure 3). Moreover, it was found that the A-module of AcAlgE1 from *A. chroococcum* was related to A-modules in AlgE1, AlgE2, AlgE3 and AlgE5 from *A. vinelandii*.

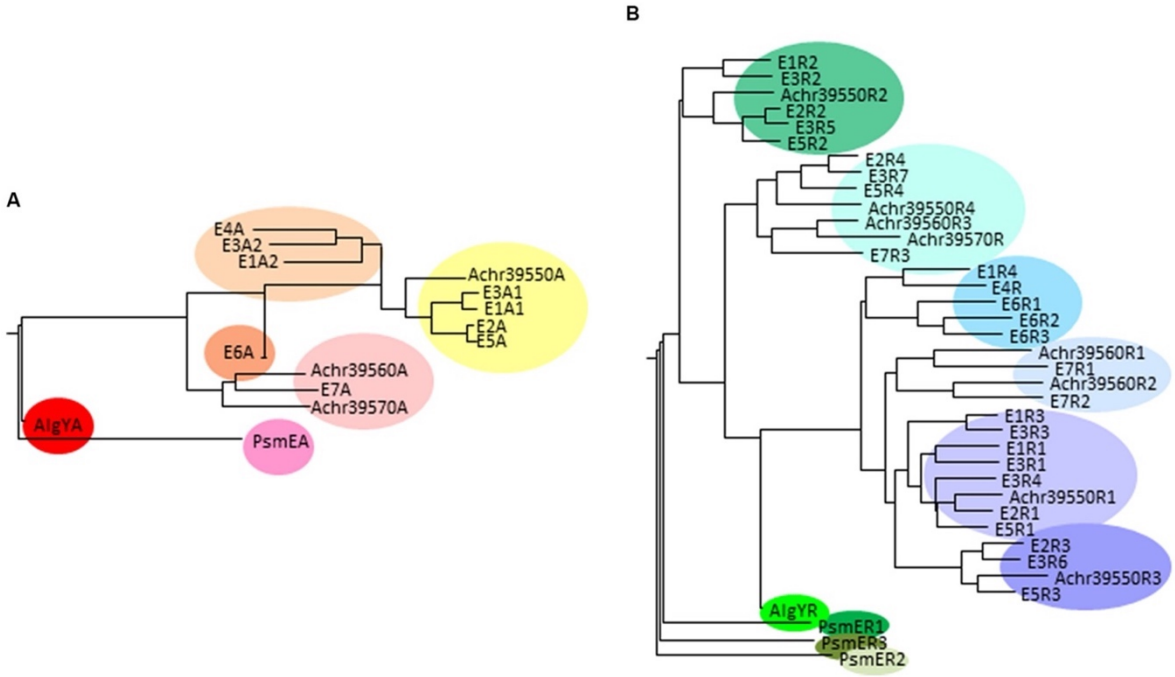

Figure 3: Phylogenetic trees of the A-modules **(A)** and R-modules **(B)** from different AlgE-type C-5-epimerases. Epimerases from *A. vinelandii* are denoted by E+enzyme number. AlgY from *A. vinelandii* and is a homologous protein to AlgE-type C-5-epimerases. PsmE is a secreted epimerase from *P. syringae*. AcAlgE1, AcAlgE2 and AcAlgE3 are denoted Achr39550, Achr39560 and Achr39570, respectively. Enzymes with several A- or R-modules are numbered according to Figure 4A. Copied from (6).

Based on a sequence alignment, it was found that AcAlgE1 was homologous to AlgE2, consisting of one catalytic A-module and four R-modules (Figure 4) (6). AlgE2 introduce G residues adjacent to pre-existing G-blocks, but not within MG sequences. It has also been shown that AlgE2 is strongly dependent on Ca^{2+} for epimerization (23). Both AcAlgE2 and AcAlgE3 show sequence homology to the bifunctional mannuronan C-5-epimerase and alginate lyase AlgE7 (6). AlgE7 consists of one A-module and three R-modules (Figure 4), and the A-module of the enzyme catalyse both epimerization and lyase reactions. Likewise, AcAlgE2 has one A-module and three R-modules in the same position relative to the A-module as AlgE7. AcAlgE3, on the other hand, has only one R-module, which shows homology to the third R-module of AlgE7 (20).

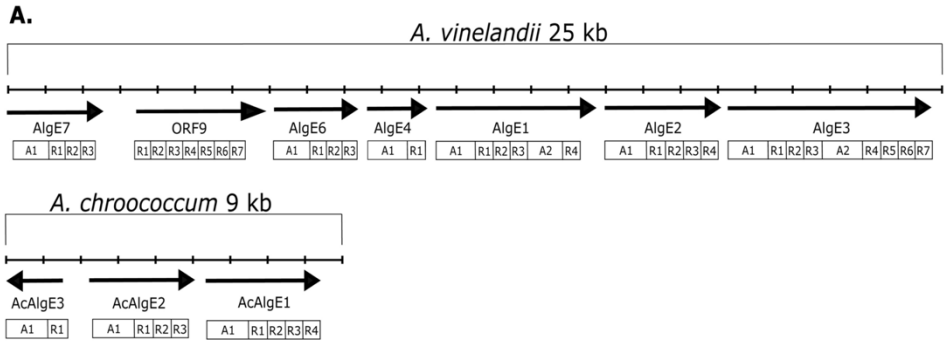

B.

```
ConA          MDYNVKDFGALGDGVSDDTAAIQAAIDAAHAAGGGTVYLPAGEYRVSGGEEPSDGCLTIKSNVYIVGAGMGETVIKLVDGWDQNVTGIVRSAYGEETSNF   100
AlgE2         ............................Y.................................H...................D.................   100
AcAlgE1       ..F....Y.......T.....................................M......M..D..............K...M.............   100
AlgE7         .E........K...KT...D..........K.........S........D.A...A.I.......................EKL...I...N..K.HDY   100
AcAlgE2       .EF.......K...RT...D..........SK..................D.A...A.M......M..................KL...I..KN..K.HDY   100
AcAlgE3       ..FD......K...K....E.........YE......R.S.........D.A...A.M.....MD.................KL...I..KN..K.HDY   100

ConA          GMSDLTLDGNRDNTSGKVDGWFNGYIPGQDGADRDVTLERVEIREMSGYGFDPHEQTINLTIRDSVAHDNGLDGFVADYQIGGVFENNVSYNNDRHGFNI   200
AlgE2         ............................E.....................................................F.....................   200
AcAlgE1       ..............VTA.............V.....................................................L.DS......A..........   200
AlgE7         .I....I...Q...E.E...FYT.....KN...YN..V.......V.R.A.....................K......F...A..........G......   200
AcAlgE2       .I........Q...E.E...FYT....EK....YN..V.......V.R.A.....................K......F..DST.........G......   200
AcAlgE3       .IR.......Q...E.E...FYT....RE....YN..A.......V.R.....................N..K....G.F..DST......HD.G......   200

ConA          VTSTNDFVLSNNVAYGNGGAGLVVQRGSXDLAHFYNILIDGGAYYDNGLEGVQIKMAHDVTLQNAEIYGNGLYGVRVYGAQDVQILDNQIHDNSQNGAYA   300
AlgE2         ............................S.V....D.....................................................E.......Y........S..   300
AcAlgE1       ....H..TMTG..........V.......Y.....................S.........L..L.D.......D.....SS.....................A.....P   300
AlgE7         ...SH.I.FT........AN........E.RDFV..VE.E..SFH...Q...L...ST.....G.......YA....Q.VE..R....Y....A.SK.N.   300
AcAlgE2       T..SH.I.FR........AN......N.E.RDL....Q.ED...H...M...L...ST.....G....N..AA....Q..EN......Y....A....N.   300
AcAlgE3       ...SH.IL.RD.......AN........E.I.....Q.E....H...A...L...TSNAS..G......DAA....R.VDGM.L...D....A.G.GK.   300

ConA          EVLLQSYDDTAGVSGNFYTTTGTWIEGNTISGSANSTYGIQERADGTDYSSLYANSISGVQXGAVRLYGXNSV-VSDXXGTGQQAT    385
AlgE2         .I.....................V.............D.............V.N..N.S.....A...-...LP.......    385
AcAlgE1       .IT.....VN.......V.T.............N.......R.......D.A.R...L.Q.A..T-...QA.......    385
AlgE7         ..IVE...RD.P.DDY.E.QNVTVK....V.................T.IGN..V..T.R.I.Q.S.T..T-F.GRS.DAY.F-    384
AcAlgE2       .I..DA.....A...Y.E.LSATVQ....V.........VL.....S...TVSG.....T.R.T.L.S.SH.TY.ASSQ.FAGD.Q    386
AcAlgE3       .IV.ED...RD.....Y.E.LNATVQ..RVA.A.Q-----------------------------------------------------    335
```

Figure 4: (A) Gene clusters encoding six AlgE epimerases in *A. vinelandii* and three AlgE epimerases in *A. chroococcum*. The A-modules and R-modules are shown for each enzyme. (B) Sequence alignment of the A-modules of AlgE2 and AlgE7 from *A. vinelandii*, AcAlgE1, AcAlgE2 and AcAlgE3 from *A. chroococcum*. The amino acid residues in the active site are underlined. The conserved amino acid residues Tyr^{235} and Tyr^{307} are marked with brackets. Copied from (20).

Mannuronan C-5-epimerases have conserved Tyr^{149}, Asp^{152}, His^{154}, and Asp^{178} amino acids residues in their catalytic site. These amino acids residues are also conserved in the *A. chroococcum* mannuronan C-5-epimerases (Figure 4) (6). Moreover, it has been found that mannuronan C-5-epimerases that can insert G residues adjacent to pre-existing G residues have conserved Tyr^{235} and Tyr^{307} amino acids residues. As seen in in Figure 4, these amino acid residues are also conserved in the three *A. chroococcum* mannuronan C-5-epimerases, indicating that they are able to form G-blocks (20).

1.2.3 Reaction mechanisms of mannuronan C-5-epimerases and alginate lyases

The first steps of the alginate lyase reaction mechanism are the same as for mannuronan C5-epimerization. The negatively charged carboxylate anion of mannuronan is neutralized by an amino acid residue (AA_1) or Ca^{2+} (Figure 5). The C5-proton is taken up by a second amino acid residue (AA_2), resulting in a double bond between C5 and C6. For the epimerase reaction, a third amino acid residue (AA_3) is needed. AA_3 donate a proton to C5 from the opposite side of the sugar ring, leading to an epimerization. In the lyase reaction, an electron is transferred from the carboxylic group. This results in a double band between C4 and C5, as seen in Figure 5, which lead to cleavage of the glycosidic bond. This reaction is often facilitated by an amino acid residue acting as an electron donor (20). The bifunctional alginate lyases and mannuronan C5-epimerases can catalyse both the epimerase- and lyase reaction.

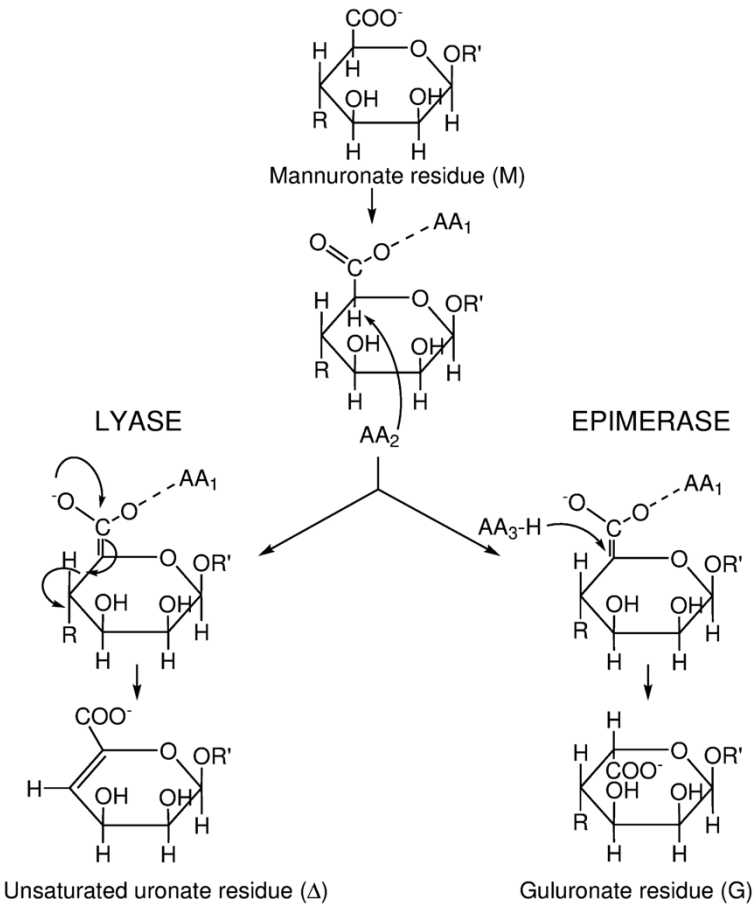

Figure 5: Alginate lyase and mannuronan C-5-epimerase reaction mechanisms. AA_1, AA_2 and AA_3 are catalytic active amino acid residues. AA_1 neutralize the carboxylate group. AA_2 abstract the proton on C5. In the lyase reaction, an electron is transferred from the carboxyl group. This leads to formation of a double bond between C4 and C5 and a cleavage of the glycosidic linkage to R. In the epimerase reaction, AA_3 donate a proton to the opposite side of the plane of the sugar ring, which flips the ring from $^4C_1$ (M) to $^1C_4$ (G). Copied from (20).

1.2.4 Salt dependency of alginate modifying enzymes

The concentration of salt can affect enzyme activity. High salt concentration increases the ionic strength which can lead to denaturation by disruption of intramolecular interactions. This can result in confirmation transformations, rendering the enzyme inactive (24). The ionic strength can also affect the interactions between the enzyme and the ligand, resulting in a reduction of enzyme activity. However, salt can also have a positive effect on enzyme activity by stabilizing the protein. Calcium ions can for instance stabilize the R-module of mannuronan C5-epimerases and thus increase enzyme activity (25).

The reaction mechanism of mannuronan C5-epimerases can be Ca^{2+}-dependent or Ca^{2+}-independent. The epimerases AlgE1-7 from *A. vinelandii* and AcAlgE1-3 from *A. chroococcum* are all Ca^{2+}-dependent (15, 20). AlgE epimerases need calcium ions for neutralization of the negatively charged carboxylate anion (Figure 5). It has been found that the N-terminal end of the R-modules of epimerases are involved in calcium-binding (25). Ca^{2+}-independent epimerases, AlgG epimerases, can neutralize the negatively charged carboxylate anion by positively charged amino acid residues, for instance arginine, instead (26).

The effect of NaCl has been analysed for AlgE1 and its two catalytic domains (27). It was found that 100-200 mM NaCl gave optimal enzyme activity, but that the first catalytic site alone is more sensitive to high ionic strength (27). Similarly, a poly-G lyase was found to be dependent of the NaCl concentration, the activity increasing alongside the NaCl concentration, peaking at 0.3 M (28). However, NaCl can also inhibit lyase activity at high concentrations, which was found in a study of AlgE7 (29). In the same study it was observed that increasing the calcium concentration reduced the negative effect of NaCl.

Additionally, NaCl can affect gelation of alginate since the Na^{+}-ions compete with Ca^{2+} for the junction sites in G-blocks. This leads to a decrease in stiffness of the alginate gels, due to loss of crosslinking (30). The degree of gelation can also affect the alginate modifying enzymes because high viscosity can inhibit enzyme activity (31).

1.3 Enzyme kinetics

Enzymes are catalysts of chemical reactions and decrease the activation energy needed (32). They speed up the reaction without being consumed themselves and are therefore only needed in small amounts. Enzyme kinetics is the study of enzymatic reactions and the factors that influence their reaction rates (33). The catalytic activity of an enzyme can be expressed in several ways. The catalytic constant for the conversion of substrate to product (k_{cat}), also referred to as turnover rate, is one example. k_{cat} is a measure of the number of substrate molecules that can be converted by one enzyme molecule per time unit (32, 34). Michaelis and Menten's theory of enzyme kinetics describe enzymatic reactions by the equation

$$E + S \underset{k_{-1}}{\overset{k_1}{\rightleftharpoons}} E - S \underset{k_{-2}}{\overset{k_2}{\rightleftharpoons}} E + P$$

where E is the enzyme, S is the substrate, P is the product, k_1 and k_{-1} are the forward and reverse rate constant of the substrate binding and k_2 and k_{-2} are the forward and reverse rate constant of the product formation (32). Michaelis and Menten also defined the initial turnover rate of enzymes, V_0, and described the relationship between V_0 and the substrate concentration [S] as

$$V_0 = \frac{V_{max}\,[S]}{[S] + K_m}$$

where V_{max} is k_{cat} times the total enzyme concentration (32). V_{max} is the maximum velocity of the system. The Michaelis-Menten constant K_m is defined as the substrate concentration at which the initial rate is one-half of the maximum velocity (35, 36).

1.4 Heterologous gene expression

Industrial microbiology enables large scale production of proteins and other desired products (37). Commercially relevant proteins, such as alginate modifying enzymes, can be produced in different host organisms to control the protein production. This is possible due to genetic engineering and heterologous gene expression. Heterologous gene expression systems are often used for overexpression of proteins (38). Genes or part of a gene that encode a protein is expressed in a different host species (37). *Escherichia coli* is often used for this purpose due to its rapid growth, inexpensive growth conditions, easy DNA transformation and high yield of overexpression (38).

E. coli are rod-shaped bacteria, normally living in the gut of vertebrates, but can easily be grown in the laboratory on nutrient broth (37). Several *E. coli* strains have also been developed specifically for cloning purposes, e.g., *E. coli* DH5α, which is a derivative of *E. coli* K-12 (39). *E. coli* DH5α is optimal for cloning because the strain has a stable DNA amplification and yields high-quality unmethylated plasmid DNA due to the lack of nonspecific endonuclease I

and disruption of endonuclease EcoKI (40). Additionally, it is capable of recombining linear DNA fragments with homologous ends, enabling *in vivo* fragment assembly (41).

Moreover, *E. coli* K-12 and *E. coli* B derived strains are commonly used for recombinant protein expression (42), e.g., the K-12 derived strain *E. coli* RV308 and the B derived strain *E. coli* SHuffle T7 Express. One of the challenges with protein production is to produce correctly disulphide-bonded proteins. The strain *E. coli* SHuffle was therefore developed to improve the production of disulphide bonds to achieve high yields of active protein (43). This strain also expresses a T7 RNA polymerase, which enables use of the LacI/P_{T7}*lac* regulator/promoter system (Section 1.5.1).

Expression vectors are used to control the protein production in heterologous gene expression. The native promoter might not work optimally in the host organism, and the expression vector can therefore be designed so that the genes are under the control of a more optimal promoter instead (37). This can be useful to achieve production of a large amount of the desired protein.

1.5 Recombinant protein expression systems

1.5.1 LacI/P_{T7}*lac* regulator/promoter system

The LacI/P_{T7}*lac* regulator/promoter system is an example of a system for overexpression of proteins that was used in this project. The gene expression is controlled by a bacteriophage T7 promoter. An expression vector is constructed as illustrated in Figure 6, with a T7 RNA promoter located nearby a *lac* operator (*lacO*). The expression vector also contains *lacI*, encoding the lactose repressor LacI (44). The wild type *lac* operon regulate genes involved in lactose metabolism in *E. coli*. The gene expression in this operon is regulated by the level of lactose and glucose. In the presence of lactose, allolactose bind allosterically to the lactose repressor LacI. The lac repressor undergoes a confirmation transformation and diffuses from *lacO.* Isopropyl β-D-1-thiogalactopyranoside (IPTG) is a chemical reagent that mimics allolactose and can bind allosterically to LacI. This leads to a dissociation of the repressor, allowing the T7 RNA polymerase to attach to the T7 promoter in the expression vector (Figure 6). The genes regulated by the T7 promoter can then be expressed (37). IPTG can therefore be used to induce protein production by the LacI/P_{T7}*lac* regulator/promoter system.

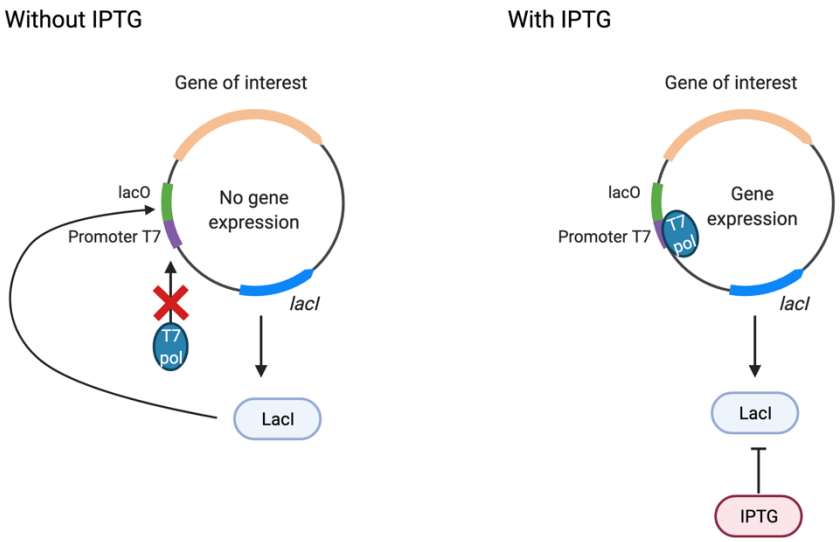

Figure 6: Schematic overview of the LacI/P_{T7}*lac* regulator/promoter system. The lac repressor (LacI) binds to the lac operator (lacO). The T7 promoter is located close to lacO and when LacI is bound, the polymerase (T7 pol) cannot bind to the promoter and there is therefore no gene expression. In the presence of IPTG, IPTG binds allosterically to LacI. This leads to a conformational change of LacI, and it will dissociate from lacO. T7 pol can therefore bind to the T7 promoter and gene transcription is allowed. The figure is created in BioRender.

1.5.2 XylS/P_m regulator/promoter system

P_m is an inducible promoter that is useful for expression of recombinant proteins. This promoter originates from the TOL plasmid from *Pseudomonas putida*, where it regulates the gene *xylS*, which encode an AraC family positive transcription factor, XylS (45). This plasmid encodes enzymes that are involved in the catabolism of toluene and xylenes, the TOL *meta*-cleavage pathway (46, 47). These enzymes are organized in operons, or regulatory blocks. In the presence of an inducer, activated XylS induces gene expression from the P_m promoter. XylS can be activated by several different effector molecules, for instance *m*-Toluate. Activated XylS dimerizes and binds to the activator-binding site, which induces transcription from P_m (Figure 7) (45). XylS appears to consist of two domains, a C-terminal domain that binds to DNA and interacts with the RNA polymerase, and a N-terminal domain that binds to the effector molecule and plays a role in the protein dimerization (45).

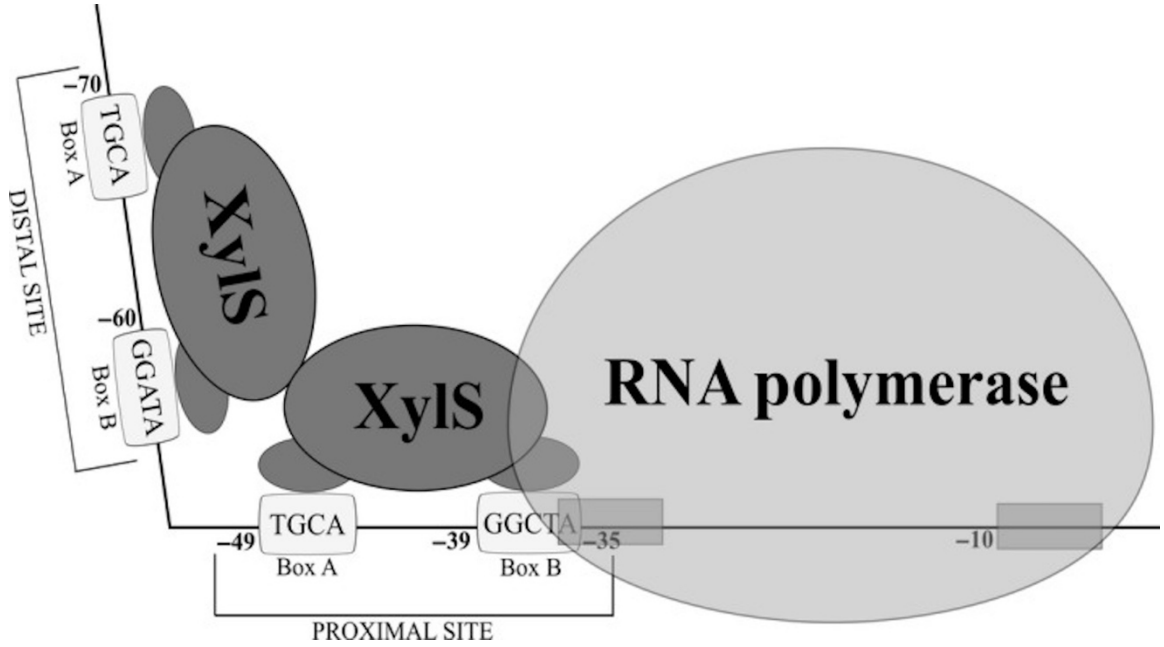

Figure 7: Schematic model of induced activation of the XylS/P_m regulator/promoter system. XylS binds as a dimer to the upstream region of the binding site of the RNA polymerase. The activated XylS dimer bind to the RNA polymerase, initiating transcription. The XylS dimerization leads to a curvature of the DNA. Copied from (45).

1.6 Purification of proteins by column liquid chromatography

Column liquid chromatography is a commonly used method for separation of molecules in a liquid phase. A mixture of molecules in solution pass through a column filled with a solid, porous matrix (39). Different molecules are retarded at a different degree through the porous matrix based on their interactions with the solid phase. Originally, the liquid phase moved through the solid phase by gravity, whereas modern methods use mechanical pumps to elute the liquid and on-line systems to detect the analytes. This makes liquid chromatography less time-consuming and enables higher resolution (35). High performance liquid chromatography (HPLC) is the dominant modern analytical method, which generates quantitative results. Fast protein liquid chromatography (FPLC) is another modern LC-method, with several similarities to HPLC. FPLC is more used as a method for protein purification, whereas HPLC is used to achieve analytical quantitative results. A wide range of aquatic buffers and stationary phases can be used in the FPLC-system, for instance ion exchange, affinity and gel filtration chromatography (48).

1.6.1 Ion exchange chromatography

Ion-exchange chromatography is a method for separating molecules based on their net charge. The net charge of a protein depends on the charged amino acids it consists of and the pH and buffer that is used (49). Charged proteins can adsorb onto a matrix with oppositely charged groups. Negatively charged proteins will adsorb onto a cationic matrix whereas an anionic matrix is used for purification of positively charged proteins. One example of an anion exchange column that is used for purification of anionic proteins is HiTrap Q HP. This column has a resin with the positively charged group $CH_2N^+(CH_3)_3$ (50). Negatively charged proteins adsorb onto the matrix of the column and can then be eluted by adjusting the pH or ionic strength. The ionic strength can be adjusted by applying a linear gradient of salt during the elution to separate proteins with different isoelectric points (pI) (51).

1.6.2 Metal ion affinity chromatography (IMAC)

Histidine tagged proteins can be purified with immobilized metal ion affinity chromatography (IMAC), which is a type of affinity chromatography. A histidine tag often consists of six histidine residues and can be attached to the C- or N-terminus of the protein of interest. It is possible to have longer His-tags to achieve an increased purification, but this increases the risk of the tag affecting the functionality of the protein (52). In IMAC, the matrix of the stationary phase contains metal ions that bind selectively to specific groups. To purify His-tagged proteins, a matrix with NiSepharose can be used, since histidine can form complexes with the Ni^{2+}-ions (53). Protein purification by IMAC is more specific than ion exchange chromatography and can therefore give a purer yield (54). The His-tagged proteins will bind to the column during the sample application. To remove nonspecific proteins, the column is washed with buffer. To elute the protein, the pH can be lowered (to protonate histidine, lowering its affinity to Ni^{2+}) or an increasing gradient of imidazole can be added (55). Imidazole is a histidine analogue, which also bind to Ni^{2+}. Imidazole will therefore react competitively. When the concentration of imidazole increases, the His-tagged proteins will eventually be eluted.

1.6.3 Gel filtration chromatography

Gel filtration chromatography, also known as size exclusion chromatography (SEC), is a method for separating molecules in a solution based on size (48). The column is packed with a matrix consisting of porous beads, forming a gel. This gel is equilibrated with a buffer that fills the pores. The liquid inside the pores forms the stationary phase, whereas the liquid outside of the beads is the mobile phase. Large molecules will not be able to enter the pores and will therefore be eluted first, whereas small molecules will be retarded. The conditions are kept constant throughout the elution, using only one buffer. The porosity determines the exclusion limit. Columns with different pore-sizes can therefore be used to fractionate molecules of different molecular mass (48).

1.7 Aims and Approaches

Alginate is a family of industrially important polymers, consisting of M and G residues. The chain length, frequency and distribution of M and G residues are important factors for the properties of alginate. Alginate lyases cleave alginate and mannuronan C-5-epimerases catalyse the epimerization of M to G, and they are therefore important tools for modification of alginate. The main objective of this study is to improve the understanding of the function of AlgE-type mannuronan C-5-epimerases and how their enzyme activity can be altered. By providing more knowledge, the aim is to open up for further use of bacterial epimerases and lyases for modification of industrial alginate.

In this study, AcAlgE1, AcAlgE2 and AcAlgE3 from *A. chroococcum* were characterised as a continuation of the work done by Gawin et. al (20) and Sønsteby (56). Additionally, a study of AlgE6/AlgE7 hybrids was continued (56). The enzymes that were characterised in this work are shown in the left panel of Figure 8. The initial objective was to achieve pure protein. For this purpose, different expression systems and purification methods were tested, as indicated in the middle panel of Figure 8. The left panel demonstrates how the enzymes were characterized.

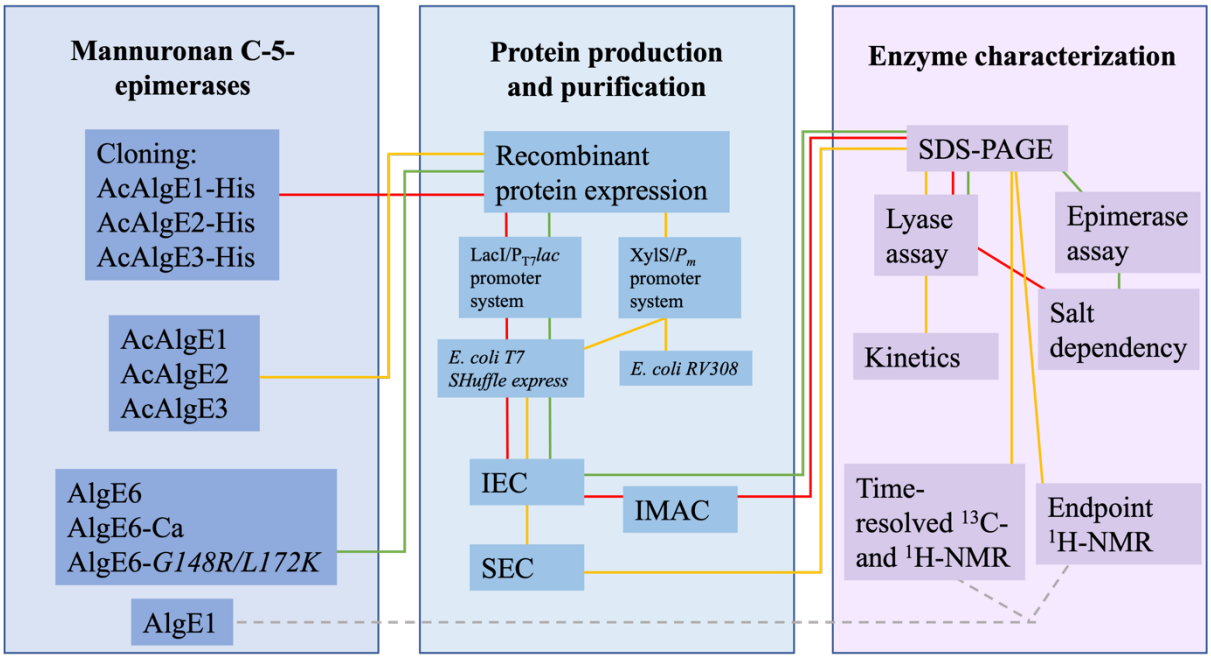

Figure 8: Flow chart of the experimental work in this project. The lyases (AcAlgE2 and AcAlgE3) and putative lyases (AlgE6-Ca and AlgE6-*G148R/L172K*) were analysed by lyase assays, whereas the epimerases were analysed by epimerase assays or NMR. The enzyme kinetics of the lyase activity of AcAlgE2 and AcAlgE3 were analysed. The salt dependency of AcAlgE2, AcAlgE3, AlgE6 and AlgE6-Ca was tested. AlgE1 was produced and purified previously but was analysed by NMR in this study.

The epimerization pattern of AcAlgE1 was characterised by analysing the mode of action on mannuronan compared to AlgE1 from *A. vinelandii*. AcAlgE1 has one catalytic site and has been shown to introduce a high G-content and short G-blocks (20). AlgE1 has two catalytic sites and introduce both poly-G and single G residues, which has been shown to result in long G-blocks (57). It is therefore interesting to compare the G-content and G-block length of the two enzymes at the same conditions. Based on previous research, it was expected that AcAlgE1 would introduce a higher fraction of G residues than AlgE1, but that AlgE1 would introduce longer G-blocks.

Next, the bifunctional mannuronan C-5-epimerases and alginate lyases AcAlgE2 and AcAlgE3 were characterised. The aim was to test salt dependency and enzyme kinetics of the lyase activity. To study enzyme kinetics, a higher protein purity was needed than in the study of salt dependency, which is the reason why different purification methods were tested, as seen in Figure 8. In a previous study, it was found that the activity of AcAlgE2 and AcAlgE3 depend on Ca^{2+} (20). Additionally, in a study of AlgE7, it was demonstrated high concentrations of NaCl reduced lyase activity and that the negative effect of NaCl was reduced at high calcium concentrations (29). Based on previous research, it was therefore expected that the lyase activity

of AcAlgE2 and AcAlgE3 would increase with increasing calcium and be reduced at high NaCl concentration. It was also expected to see a reduced effect of NaCl at high calcium concentration.

AlgE7 is a bifunctional mannuronan C-5-epimerase and alginate lyase from *A. vinelandii.* The amino acids that are responsible for the lyase activity of these bifunctional enzymes are yet to be discovered. A study of AlgE6/AlgE7 hybrids (56) was therefore completed in this work. It has been demonstrated in previous studies that calcium promotes lyase activity of AlgE7 (29) and it was therefore interesting to compare calcium binding sites of AlgE7 and AlgE6. For this purpose, the activity of an AlgE6 mutant with a proposed calcium binding site from AlgE7 was tested and compared to AlgE6 at different calcium concentrations. To measure epimerase activity quantitatively, a coupled epimerase/lyase assay was optimized. The optimized epimerase assay was tested and used in this project.

2 Materials and Methods

2.1 Kits

Table 1 describes the kits that were used in this project.

Table 1: The kits that were used in this work.

Kit	Utilization	Components	Manufacturer
Monarch® DNA gel extraction kit and PCR and DNA Cleanup kit	Purification of DNA extracted from agarose gel or PCR-product.	DNA Wash Buffer DNA Cleanup Binding buffer Monarch Gel Dissolving Buffer DNA Elution Buffer	New England BioLabs (58).
Zymo Research Plasmid Miniprep™ -*Classic*	Plasmid purification.	P1 Buffer P2 Buffer P3 Buffer Endo-Wash Buffer Plasmid Wash Buffer Collection tubes Zymo-Spin™ IIN Columns	Zymo Research (59).
Zero Blunt® TOPO® PCR Cloning Kit	TOPO-cloning.	Salt Solution pCR™II-Blunt-TOPO®	Life Technologies (60).

2.2 Software

The software and bioinformatic tools that were used in this project are described in Table 2.

Table 2: Software and bioinformatic tools that were used in this work.

Software	Utilization	Reference
Benchling	Construction of plasmid maps. Simulation of plasmid digestion for selection of restriction enzymes. Simulation of TOPO-cloning. Analysing results from Sanger sequencing by sequence alignment.	Benchling
BioRender	Creating simplified schematics.	BioRender
Excel	Planning setup for enzyme assays. Analysis of results from enzyme assays and time-resolved NMR.	Microsoft
ImageLab 6.0.1	Visualization and photographing DNA- and protein gels.	BioRad
PowerPoint	Editing images and constructing flowcharts.	Microsoft
ProtParam	Finding theoretical protein parameters: molecular mass, extinction coefficient and pI.	ExPASy
SoftMaxPro 4.7.1	Conducting spectrophotometric enzyme assays.	Molecular Devices LLC.
TopSpin 4.0.7	Recording, processing, and analysing NMR-spectra.	Bruker BioSpin
Unicorn 7.5	Controlling FPLC runs and analysing chromatograms.	GE Healthcare Life Sciences

2.3 Growth media and buffers

The growth media and buffers that were used in this project are listed below.

Luria broth (LB) medium
10 g/l Tryptone
5 g/l Yeast extract
5 g/l NaCl
Autoclaved at 121°C for 20 min

3xLB
30 g/l Tryptone
15 g/l Yeast extract
5 g/l NaCl
Autoclaved at 121°C for 20 min

Luria broth with agar (LA) medium
10 g/l Tryptone
5 g/l Yeast extract
5 g/l NaCl
15 g/l Agar bacteriological
Autoclaved at 121°C for 20 min
Stored at 4°C

Psi medium
20 g/l Tryptone
5 g/l Yeast extract
5 g/l $MgSO_4$
pH adjusted to 7.6 using KOH
Autoclaved at 121°C for 20 min

Super optimal catabolite-repression (SOC) medium
20 g/l Tryptone
5 g/l Yeast extract
0.5 g/l NaCl
2.5 mM KCl
3.6 g/l Glucose
5.08 g/l $MgCl_2$
Sterile filtered
Stored at -20°C

MOPS ((3-(*N*-morpholino) propanesulfonic acid)) buffer
0.5 M MOPS
pH adjusted to 6.9 using NaOH
Sterile filtered
Stored at 4°C

TFB1

30 mM KAc

100 mM RbCl

10 mM $CaCl_2$ x 2 H_2O

10 mM $MnCl_2$ x 4 H_2O

pH adjusted to 5.8 using CH_3COOH

Sterile filtered

TFB2

10 mM MOPS buffer

75 $CaCl_2$ x 2 H_2O

10 mM RbCl

15% v/v Glycerol

pH adjusted to 6.5 using NaOH

Sterile filtered

Buffer A

50 mM MOPS buffer

5 mM $CaCl_2$

pH adjusted to 6.9 using NaOH

Sterile filtered

Stored at 4°C

Buffer B

50 mM MOPS buffer

5 mM $CaCl_2$

1 M NaCl

pH adjusted to 6.9 using NaOH

Sterile filtered

Stored at 4°C

Buffer C

50 mM MOPS buffer

5 mM $CaCl_2$

0.5 M NaCl

20 mM Imidazole

pH adjusted to 6.9 using NaOH

Sterile filtered

Stored at 4°C

Buffer D

50 mM MOPS buffer

5 mM $CaCl_2$

0.5 M NaCl

500 mM Imidazole

pH adjusted to 6.9 using NaOH

Sterile filtered

Stored at 4°C

Buffer E

50 mM MOPS buffer

5 mM $CaCl_2$

0.25 M NaCl

pH adjusted to 6.9 using NaOH

Sterile filtered

Stored at 4°C

2.4 Alginate solutions

Sodium alginate ($F_{G,}$ = 0.41, F_M = 0.59, F_{GG} = 0.23, F_{MG} = F_{GM} = 0.18, [η] = 5.7 dl/g from *Macrocystis pyrifera* (Sigma V-90)) was used in the lyase assays of this project. High molecular weight mannuronan (F_G = 0 from *Pseudomonas fluorescens* strain PF20118) was used as substrate in the coupled epimerase/lyase assays, the optimized epimerase assay and endpoint ^{1}H-NMR. ^{13}C1-enriched mannuronan polymers (degree of polymerization (DPn) ≈ 70) was used for time-resolved NMR.

2.5 Bacterial strains and plasmids

The bacterial strains that were used in this project are listed in Table 3.

Table 3: The bacterial strains that were used in this work.

Strain	Description	Source
E. coli DH5α	General cloning host.	(41)
E. coli SHuffle T7 Express	Used for recombinant protein expression using the LacI/P_{T7}*lac* regulator/promoter system or the XylS/P_m regulator/promoter system.	(NEB)
E. coli RV308	Used for recombinant protein expression using the XylS/P_m regulator/promoter system.	(61)

The plasmids that were used or constructed in this project are listed in Table 4.

Table 4: The plasmids that were used in this work.

Plasmid	Description	Reference
pAG550	Derivative of pVB1-251-bla_Kan (Vectron Biosolutions AS, Trondheim). *acalgE1*, $P_{m,}$ Kan^r.	Gawin (20).
pAG560	Derivative of pVB1-251-bla_Kan. *acalgE2*, $P_{m,}$ Kan^r.	Gawin (20).

pAG570	Derivative of pVB1-251-bla_Kan. *acalgE3*, P_m, Kan^r.	Gawin (20).
pCR™- BluntII- TOPO	TOPO®-cloning vector. Kan^r.	Life Technologies (60).
pMEJ18	Derivative of pVB1 mCherry Kan271. His-tag, Kan^r.	Jakobsen (62).
TOPO560	Derivative of pCR™- BluntII- TOPO. *acalgE2,* Kan^r.	Moghaddam (63).
pTYB1	*E. coli* expression vector used in IMPACT™. Encodes a C-terminal *Sce* VMA intein/chitin-binding domain, P_{T7}, *lacI*, ori M13 and Amp^r.	New England Biolabs Inc (58).
pSTS1	Derivative pf pTYB1AlgE6ds. *algE6,* Amp^r.	Sønsteby (56).
pSTS5	Derivative of pSTS1. *algE6-G148/L172K,* Amp^r.	Sønsteby (56).
pSTS10	Derivative of pSTS1. *algE6-Ca2,* Amp^r.	Sønsteby (56).
pSTS21	Derivative of pTYB1. *acalgE1,* Amp^r.	Sønsteby (56).
pSTS22	Derivative of pTYB1. *acalgE2,* Amp^r.	Sønsteby (56).
pSTS23	Derivative of pTYB1. *acalgE3,* Amp^r.	Sønsteby (56).
pSTH1	Derivative of pSTS23, where the BamHI-KpnI 7.3 kb fragment is ligated to the BamHI-KpnI 1 kb fragment of pSTH18. Amp^r.	This work.
pSTH2	Derivative of pSTH1, where the NotI-PstI 6.7 kb fragment is ligated to the NotI-PstI 1 kb fragment of pSTH21. Amp^r.	This work.
pSTH3	Derivative of pSTH2, where the SacI-XbaI 5.9 kb fragment is ligated to the SacI-XbaI 3 kb fragment of pSTS21. Amp^r.	This work.

pSTH4	Derivative of TOPO560, where the Acc65I-BspEI 5.4 fragment is ligated to the Acc65I-BspEI 753 bp fragment of pSTH22. Kan^r.	This work.
pSTH5	Derivative of pSTH3, where the NdeI-NotI 6.6 kb fragment is ligated to the NdeI-NotI 2.6 kb fragment of pSTH4. Amp^r.	This work.
pSTH6	Derivative of pSTH1, where the PstI-NotI 6.7 kb fragment is ligated to the SbfI-NotI 0.6 kb fragment of pSTH23. Amp^r.	This work.
pSTH7	Derivative of pCR™- BluntII- TOPO where an overlap extension PCR product of pTYBalgE6ds with the primers pTYB1algE6F1, algE65994C, algE66025 and algE66090C was cloned with topoisomerase (56). Kan^r.	This work.
pSTH8	Derivative of pCR™- BluntII- TOPO where an overlap extension PCR product of pTYBalgE6ds with the primers algE66133 and algE6R2 was cloned with topoisomerase (56). Kan^r.	This work.
pSTH18	Derivative of pCR™- BluntII- TOPO where the PCR product of pMEJ18 with the primers His18Kpn and His18Bam was cloned with topoisomerase. Kan^r.	This work.
pSTH21	Derivative of pCR™- BluntII- TOPO where the PCR product of pSTS21 with the primers Ac550F2 and AcAlgE1 HR was cloned with topoisomerase. Kan^r.	This work.

pSTH22	Derivative of pCR™- BluntII- TOPO where the PCR product of pSTS22 with the primers AcAlgE2 sjekk 1 and AcAlgE2 HR was cloned with topoisomerase. Kan^r.	This work.
pSTH23	Derivative of pCR™- BluntII- TOPO where the PCR product of pSTS23 with the primers AcAlge3sjekk and AcAlgE3 HR was cloned with topoisomerase. Kan^r.	This work.

2.6 Primers

The primers that were used in this study are listed in Table 5. The nucleotide sequence, length (bp) and melting temperature (Tm) of the primers are given.

Table 5: The primers that were used for PCR and sequencing in this project.

Primer name	**Sequence (5' → 3')**	**Length [bp]**	**Tm [°C]**
AcAlgEn HF	GGGAATTGTGAGCGGATAAC	20	60
AcAlgE1 HR	ATTCTTGCGGCCGCGGCGACCTGCTCGGGCTGCGTGG	37	78
AcAlgE2 HR	ATTCTTGCGGCCGCCAGGTCGGTC	24	67
AcAlgE3 HR	TAACAAGCGGCCGCGGCGACCTGGTCGGTCTG	32	66
AcAlgE2 sjekk1	GCACCTACCTGAGGAGCTAC	20	63
AcAlgE3sjekk	CCCACGAGCAGACCATCAAC	20	65
Ac550F2	TCTCCCTCGACGGCAACTAC	20	65
AlgE1sjekkF	CCTCTACGCCAACAGCATCGAC	22	65

algE6F1	CCGCCATAAACTGCCAGGAATTG	23	66
His18Kpn	ATTCTTGGTACCGCGCCGAAGGTGGCCAAC	30	73
His18Bam	TCTAGGATCCACTAGTCTCGACTTAGCAGCCGGATCTC	38	70
M13F	GTAAAACGACGGCCAG	16	50
M13R	CAGGAAACAGCTATGAC	17	46

2.7 Polymerase Chain Reaction (PCR)

Polymerase Chain Reaction (PCR) is a method for in vitro DNA amplification. PCR makes it possible to generate billions of copies of a specific DNA-sequence from a small amount of DNA (64). PCR can also be used for detection of specific DNA fragments, for instance to detect and identify pathogens in a sample or to identify people in forensic medicine (65). To perform a PCR assay, template DNA, primers, nucleotides, DNA polymerase and buffer is needed. The template DNA is the DNA that is being analysed, which can be isolated from a variety of organisms. The primers are specific for the PCR assay and are designed based on the DNA sequence that should be amplified. The nucleotides are deoxynucleotides (dNTPs) which are the substrate of the new DNA strands that are synthetized. The polymerase is an enzyme that bind to the template DNA and catalyse the synthesis of the PCR DNA. Polymerases used for PCR need to be thermostable due to the heating that is needed for the PCR assay. The buffer contains salts and is necessary to achieve favourable conditions for the reaction. PCR can be divided in three steps: denaturation, annealing and extension. Denaturation is a heat-induced separation of the two strands of the template DNA. The next step is the annealing, where the primers bind to the template DNA. The forward and reverse primers bind to each of the two strands. The annealing happens as the temperature is lowered. The temperature needed depends on the melting temperature of the primers that are used. The final step is the extension, which is induced by raising the temperature to 72°C. This makes the polymerase bind to the DNA, extending the primers by adding nucleotides. This leads to an extension of a complementary strand to the template DNA, resulting in double stranded DNA (dsDNA) again. These three steps are repeated in the desired number of cycles. (65, 66)

In this project, PCR was performed with Q5® High-Fidelity DNA Polymerase (M0491). For each sample, 50 µl reaction mix was made. 10 µl 5X Q5 Reaction buffer, 1 µl 10 mM dNTPs, 1.25 µl 20 µM Forward Primer, 1.25 µl 20 µl Reverse Primer, 0.5 µl template DNA, 0.5 µl Q5 High-Fidelity DNA Polymerase, 10 µl 5X Q5 High GC Enhancer and 25.5 µl Nuclease-Free Water was mixed gently. The samples were spun down quickly. The general PCR settings that were used are shown in Table 6. The annealing temperature that was used was three degrees below the lowest melting temperature of the primers that were used.

Table 6: Thermocycler conditions used for PCR.

Step	Temperature	Time	Cycles
Initial denaturation	98°C	30 sec	
Denaturation	98°C	5-10 sec	35
Annealing	50-72°C	10-30 sec	
Extension	72°C	20-45 sec/kb DNA	
Final extension	72°C	2 min	
Hold	4°C		

2.7.1 PCR cleanup

PCR products were purified with Monarch® PCR and DNA Cleanup kit. The PCR reaction mix was diluted with DNA Cleanup Binding Buffer. If the PCR product was larger than 2 kb, the buffer to sample ratio was 2:1, whereas it was 5:1 for smaller DNA fragments. The sample was loaded on a column in a collection tube and centrifuged for 1 min. All centrifugation steps were carried out at 13000 revolutions per min (rpm). The flow through was discarded. 200 µl DNA Wash Buffer was added, and the sample was centrifuged for 1 min. This wash-step was repeated once. The column was transferred to a new 1.5 ml Eppendorf tube, and 15 µl DNA Elution Buffer was added to the centre of the matrix. The tube was incubated at room temperature for 1 min before 1 min centrifugation to elute the DNA.

2.8 Agarose gel electrophoresis

Agarose gel electrophoresis is a method that can be used to separate DNA fragments of different size. The agarose polymers form non-covalent bonds, resulting in pores, where the size of the pores depend on the concentration of the agarose. Small DNA fragments will migrate faster through these pores than larger fragments (67). The backbone of DNA is negatively charged due to phosphate groups, and the DNA will therefore migrate towards the positive anode when a current is applied. DNA has a uniform mass/charge ratio, making it possible to elucidate the molecular weight of the fragments based on how far they migrate. The samples are compared to a standard with fragments of known molecular weight. To visualize the bands on the gel, a loading dye is added to the samples. The dye binds to the DNA, making it possible to visualize the fragments. The dye also makes the samples sink into the wells of the gel (68).

In this project, 0.8% agarose with Tris-acetate-EDTA (TAE) buffer and 20 µl GelGreen dye was used. The agarose was kept at 60°C and poured in trays for casting the gel. Wells were made with a comb that were placed at one end of the gel. The DNA samples were mixed with 2µl 6x Purple gel loading dye (NEB) before the samples were loaded in the wells of the gel. A current of 100 V was applied for at least 30 min. The running time depended on the separation requirements of the DNA fragments. The gels were photographed and edited with ImageLab (Bio-Rad). In this project, HindIII and PstI standards were used (Appendix A: DNA and protein standards). The standards were made by digesting 10 µl 500 µg/µl λ-DNA with 2 µl enzyme. 10 µl buffer (3.1 for PstI and CutSmart for HindIII) and 78 µl reverse osmosis (RO) water were added to the reaction.

2.8.1 DNA gel extraction

DNA fragments that were to be used further were excised from the agarose gel after separation by agarose gel electrophoresis. The DNA fragment was cut with a scalpel under UV light and transferred to a 1.5 ml Eppendorf tube. The DNA was extracted with Monarch® DNA gel extraction kit. 600 µl Gel Dissolving Buffer was added and the sample was incubated at 50 ºC for 10 min. The sample was mixed periodically during the incubation to dissolve the gel before it was loaded on a column in a collection tube and centrifuged for 1 min. All centrifugation steps were carried out at 13000 rpm. The flow through was discarded, 200 µl DNA Wash Buffer

was added, and the sample was centrifuged for 1 min. This wash-step was repeated once. The column was transferred to a new 1.5 ml Eppendorf tube, and 15 µl DNA Elution Buffer was added to the centre of the matrix. Finally, the tube was incubated at room temperature for 1 min before 1 min centrifugation to elute the DNA.

2.9 Restriction reactions

Restriction enzymes are a category of endonucleases that recognize specific double stranded DNA sequences and cleave it (69). The discovery of restriction enzymes made recombinant DNA technology possible and transformed molecular biology (70). Some restriction enzymes (e.g. EcoRV) cut the dsDNA at the same position of each strand, leaving a blunt end, whereas some restriction enzymes (e.g. HindIII) produce a staggered cut. The recognition sites are symmetric. The most used recognition sites are typically palindromes, or inverted repeats, and fragments cut with the same restriction enzyme can therefore religate. This thus opens possibilities for recombinant DNA technology and cloning (70).

100-200 ng DNA, 2 µl 10 X buffer (i.e., CutSmart or 3.1 buffer) and 0.5 µl enzyme was mixed in RO water, to a total volume of 20 µl. The reaction was incubated at 37ºC (which was the optimal temperature for all restriction enzymes used in this work) for at least one hour.

2.10 Ligation

DNA ligases are enzymes that can ligate DNA strands together under specific conditions (71). In nature, they are essential in DNA repair, replication and recombination. Ligases also make it possible to join DNA-fragments with complementary “sticky-ends” to construct recombinant DNA (70).

17 µl digested and purified DNA (3 µl vector DNA and 14 µl insert DNA) was mixed with 2 µl 10 X ligase buffer and 0.5 µl T4 ligase. The reaction was incubated 3-20 hours at 16 ºC.

2.11 Cultivation of *Escherichia coli*

E. coli DH5α was used for cloning in this project, whereas *E. coli* SHuffle T7 Express and *E. coli* RV308 were used for recombinant protein production (Section 1.4).

The bacteria were grown on LA plates with the selective antibiotics for the plasmid (200 µg/µl ampicillin (Amp) or 50 µl/µg kanamycin (Kan)) at 37°C overnight (ON) or in liquid LB medium with the selective antibiotics for the plasmid at 37°C with 225 rpm shaking ON.

2.12 Isolation of plasmid

One approach for performing cloning is to insert a DNA fragment into a plasmid vector (39). Plasmid vectors are self-replicating genetic elements derived from plasmids that occur in nature. They are extrachromosomal replicons found in most bacteria and some archaea and eukaryotes and are essential for genetic communication between bacteria. They can transfer small (20-200 kb), conjugative, self-replicating plasmids by conjugation to share traits, leading to rapid evolution and adaptation (72, 73). Plasmid vectors have become an important tool in molecular biology for genetic engineering (74). The plasmid vectors are constructed to enable molecular cloning and can for instance contain antibiotic resistance for selection, a multiple cloning site (MCS) with restriction sites for different restriction enzymes and different systems for regulating gene expression (37).

In this work, plasmid isolation was performed using Zymo Research Plasmid Miniprep™ - *Classic* kit (59). Bacteria were cultivated in LB medium at 37°C with 225 rpm shaking for 16-20 hours. 1.5 ml bacterial culture was centrifuged in 1.5 ml tubes for 2 min. All centrifugation steps were carried out at 13000xg in a microcentrifuge. 200 µl P1 buffer was added, and the pellet was resuspended by pipetting. Buffer P1 contain RNase A to degrade RNA. 200 µl P2 buffer was added, and the tubes were inverted 2-4 times. The P2 buffer contain NaOH and sodium dodecyl sulphate (SDS) for alkaline cell lysis. After 1-2 min, 400 µl P3 buffer was added and mixed by inversion. The P3 buffer neutralize the lysate and renature dsDNA. The lysate was incubated at room temperature for 4-5 min before 5 min centrifugation. The supernatant was transferred to a Zymo-SpinTM IIN column in a collection tube and centrifuged for 2 min. The DNA in the column was washed in two steps with 200 µl Endo-Wash Buffer

and 400 µl Plasmid Wash Buffer. The wash buffers were eluted during centrifugation for 1 and 2 min, respectively. The column was transferred to a clean 1.5 ml tube and 50 µl elution buffer was added. The sample was incubated at room temperature for 1 min before 1 min centrifugation to elute the DNA.

2.13 Spectrophotometry

Spectrophotometry is a quantitative measurement of the interaction between radiation (e.g. UV or visible light at a specific wavelength) and a material. The transmission or absorbance properties of the material is given as a function of wavelength (75).

2.13.1 OD measurements of cell cultures

Optical density (OD) measurements can be used to estimate the microbial growth of a culture. The spectrophotometer measures the turbidity based on light scattering. The unscattered light that emerge through the suspension is detected and measured. The microbial growth is indicated based on the assumption that the OD-value is proportional to the number of cells (76). Within certain limits, this is true for unicellular organisms, and OD-measurements are therefore a useful tool for estimating the cell number (37).

In this project, the OD of bacterial cultures were measured at 600 nm using a 1 ml cuvette. The media of the culture was used as blank. The same spectrophotometer was used every time for each measurement. If necessary, the samples were diluted with culture media to ensure that all OD_{600} measurements were below 0.4.

2.13.2 Measurement of DNA- and protein concentration

DNA- and protein concentrations were measured using NanoDrop One with wavelength 260 nm and 280 nm, respectively. When measuring DNA concentration, elution buffer was used as blank. For protein concentration measurements, Buffer A was used as blank. The molar extinction coefficient (ε_M) 0.020 µg/ml was used for all measurements of DNA concentration.

The extinction coefficient was adjusted at the NanoDrop before measuring protein concentration. Abs_{280} depends on the amount of the amino acids tryptophan (Trp), tyrosine (Tyr) and cystine (Cys) (77). For folded proteins in water, this equation gives a prediction of ε_M:

$$\varepsilon_M = nTrp(5500) + nTyr(1490) + nCys(125)$$

This results in ε_M of 68 650 $M^{-1}cm^{-1}$, 57 190 $M^{-1}cm^{-1}$ and 33 810 $M^{-1}cm^{-1}$ for AcAlgE1, AcAlgE2 and AcAlgE3, respectively. AlgE6 has an ε_M of 50 200 $M^{-1}cm^{-1}$.

ε_M is used to calculate the molar protein concentration by the equation

$$[P] = A_{280}/\varepsilon_M L$$

when [P] is the protein concentration in mole/litre (M), A_{280} is the absorbance at 280 nm and L is the light path length in centimetres (77). The molecular weight of the proteins is used to determine the protein concentration in mg/ml.

When the protein concentration of crude extract was measured in this work, this was done based on the assumption that 1 Abs_{280} = 1mg/ml.

2.14 Making competent *E. coli* cells

Competent cells are bacterial cells that are treated to make them able to take up DNA from bacteriophages or plasmid DNA from the surroundings (78). This can be done by altering the cell membrane permeability by electroporation or chemical modification. It is possible to change the cell wall permeability by exposing to cells to ice cold $CaCl_2$ followed by heat-treatment (79). The divalent cations neutralize the negatively charged bacterial cell, reducing the repulsion between negatively charged DNA and the bacterial cell (80). This makes the cells competent to take up extracellular DNA by heat-shock transformation.

A preculture of *E. coli* was made in a 250 ml Erlenmeyer flask with 10 ml Psi medium which was incubated at 37ºC, 225 rpm ON. The next day, a 1% culture was made in 200 ml Psi medium. The culture was incubated at 37ºC, 225 rpm until OD_{600} reached 0.4. The flask was

incubated on ice for 15 min. The culture was transferred to a sterile centrifuge tube and centrifuged at 4000 rpm, 4ºC for 5 min. The supernatant was discarded. The pellet was dissolved carefully in 80 ml TFB1, before the resuspension was incubated on ice for 5 min and centrifuged again at 4000 rpm, 4ºC for 5 min. The supernatant was discarded, and the pellet was dissolved in 6 ml TFB2. 100 µl of the resuspension was aliquoted in Eppendorf tubes that were kept on ice. The tubes were frozen by 5-10 sec in liquid nitrogen.

The competent cells were tested by performing a heat-shock transformation (Section 2.15) with a plasmid of known size (in this project, a TOPO-vector was used) and a negative sample without DNA. A dilution series was made, and the bacteria were counted. The transformation efficiency of the competent DH5α cells that were constructed and used in this project was $8x10^5$ bacteria per 100 µl competent cells.

2.15 Heat-shock transformation

Heat-shock transformation is a method for inserting a plasmid into bacteria (81). Competent cells are mixed with the plasmid. By incubating the competent cells on ice and then giving them a heat-shock, it is possible for the cells to take up the DNA. The heat-shock lowers the membrane potential of the cells, which can facilitate the uptake of negatively charged DNA. After the heat shock, the cells are incubated on ice, raising the membrane potential again (82).

100 µl competent cells were thawed on ice. 10 µl DNA was added and mixed gently with the cells, before incubation on ice for 30-60 min. The cells were heat-shocked at 37°C for 1-2 min before an incubation on ice for 2 min. Next, 900 µl SOC-medium (37°C) was added. The cells were incubated for 1 hour or more at 37°C, 225 rpm. During this incubation, the bacteria generate antibiotic resistance proteins encoded by the plasmid, which enables selection in the subsequent incubation step. Finally, the cells were plated on LA with an antibiotic that was selective for the plasmid.

2.16 TOPO®-cloning

TOPO-cloning is a method that allows insertion of a blunt end PCR product in a plasmid vector. The enzyme DNA Topoisomerase I is essential for TOPO cloning. In nature, this enzyme cleaves and religates DNA during replication. The Topoisomerase that is used for TOPO cloning originates from *Vaccinia* virus, which binds to dsDNA and cleaves one strand after recognizing the sequence 5'CCCTT. This leads to the unwinding of DNA. Next, the enzyme religates the DNA strands. The vector pCR™II-Blunt-TOPO® contains a TOPO-cloning site where both strands have a 5'CCCTT sequence adjacent to each other. This makes a DNA Topoisomerase I recognize each strand, leading to a double strand blunt end cut. The PCR product can then be ligated in the vector, as illustrated in Figure 9 (60, 83).

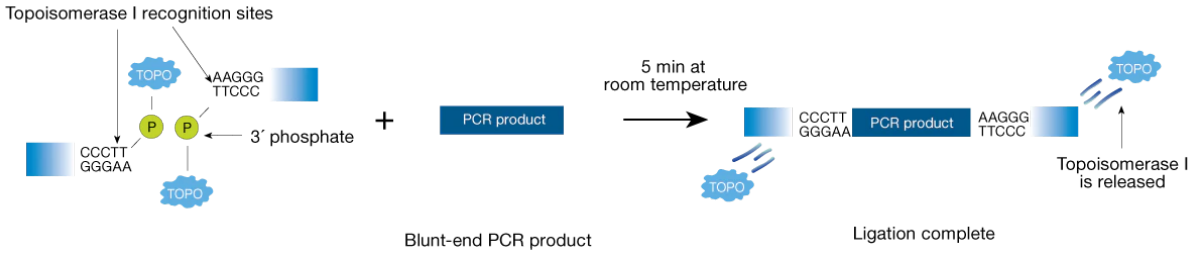

Figure 9: Simplified illustration of blunt end TOPO cloning. Topoisomerase I (TOPO) recognize the pentameric sequence 5'(C/T) CCTT3' and bind to the phosphate group (P) of the 3' thymidine (T). The enzyme functions as a restriction enzyme and cleave the DNA-strand to unwind the DNA. The enzyme also functions as a ligase and religate the ends. A blunt end PCR product can be ligated between the two ends by incubation at room temperature for 5 min. Copied from (83).

The vector contains the gene *ccd*B, which is used for positive selection since it encodes a lethal toxin for *E. coli* strain K-12. The gene is fused to the C-terminal end of a LacZα fragment. If a blunt end PCR product is inserted, this disrupts the fusion, and the toxin is not expressed. Bacteria without insert are therefore killed upon plating (60). pCR™II-Blunt-TOPO® also encodes Kan and Zeocin resistance, to select for bacteria that has taken up the plasmid.

TOPO-cloning was performed using the ZERO Blunt® TOPO® PCR Cloning Kit (Invitrogen by life technologies). 2 µl purified PCR product was mixed gently with 0.5 µl Salt Solution and 0.5 µl pCR™II-Blunt-TOPO®, and incubated at room temperature for about 20 min. Next, the plasmid was taken up by *E. coli* DH5α by heat-shock transformation.

2.17 Sanger sequencing

Sanger sequencing is a method for determining the nucleotide sequence of a DNA fragment. A labelled DNA primer is added to a reaction with the DNA fragment of interest. The primer hybridizes with the DNA so that a DNA polymerase can bind and elongate the complementary strand. Deoxyribonucleoside triphosphates (dNTPs) are added. Next, the polymerase is added, and the reaction is divided in four tubes. Additionally, each tube is added a small amount of dideoxyribonucleoside triphosphate (ddNTPs), in one tube each. When the ddNTPs are incorporated in the growing complementary DNA strand, the elongation is terminated due to the lack of a 3' OH-group. Because there is only a small amount of ddNTPs compared to dNTPs, they will be incorporated occasionally, and the result will be several strands of different lengths. These fragments can be separated on a polyacrylamide gel with one well for each of the four bases. The sequence can then be elucidated by the gel. Sanger sequencing can also be automated by loading the DNA-products on a capillary gel to separate them by size. The ddNTPs are labelled with a fluorescent tag so that the sequence can be read by a camera. The sequence can then be assembled by computers, making the method less time-consuming. (39)

400-500 ng purified DNA was mixed with 0.75 µl dimethyl sulfoxide (DMSO) and 1.25 µl 20 pmole/µl sequencing primer. Only one primer was added to each sample. RO water was added to achieve a total volume of 15 µl. The samples were sequenced by automated Sanger sequencing using the LightRun service at Eurofins Genomic GATC.

2.18 Recombinant protein expression

2.18.1 Recombinant protein expression in *E. coli* RV308

The inducible P_m promoter can be used to control protein production, as explained in Section 1.5.2. This system can for instance be used in *E. coli* RV308, which is a commonly used strain for protein production.

E. coli RV308 was cultivated in 25 ml LB with an antibiotic that was selective for the plasmid in 250 ml Erlenmeyer flasks ON at 37°C, 225 rpm. 2 ml of the precultures were transferred to 200 ml 3x LB with Amp (200 mg/ml) and $CaCl_2$ (5mM) in 1L baffled Erlenmeyer flasks. The

cultures were incubated at 37°C, 225 rpm until the OD_{600nm} reached 0.7-1.2. Next, *m*-Toluate was added to a total concentration of 0.75 mM to induce protein production. The cultures were incubated at 30°C, 225 rpm for 8 hours. The cells were harvested by centrifugation at 5500 g at 4°C for 5 min. The supernatant was discarded, and the pellets were kept at -20°C.

2.18.2 Recombinant protein expression in *E. coli* SHuffle T7 express

A T7 RNA polymerase is necessary to produce proteins where the gene expression is regulated by the LacI/P_{T7}*lac* promoter/regulator system, as explained in Section 1.5.1. *E. coli* SHuffle T7 Express, a strain that encodes T7 RNA polymerase was used for this purpose.

E. coli SHuffle T7 Express was cultivated in 25 ml LB with an antibiotic that was selective for the plasmid in 250 ml Erlenmeyer flasks ON at 37°C, 225 rpm. 4 ml of the precultures were transferred to 400 ml 3x LB with Amp (200 mg/ml) and $CaCl_2$ (5mM) in 2L baffled Erlenmeyer flasks. The cultures were incubated at 37°C, 225 rpm until the OD reached 0.8. Next, the cultures were incubated on ice for 5 min before 500 µl IPTG (0.5 M) were added. The cultures were incubated at 16°C, 225 rpm for 20 hours. The temperature is lowered to produce protein at a rate that allows them to be processed and folded correctly. The next day, the culture was transferred to two 250 ml centrifuge tubes and centrifuged at 5500 g at 4°C for 5 min. The supernatant was discarded, and the pellets were kept at -20°C or used directly for protein purification.

This strain was also used for recombinant protein expression using the XylS/P_m regulator/promoter system. The procedure was identical apart from the inducer, instead of IPTG, *m*-Toluate was added to a total concentration of 0.75 mM.

2.19 Cell lysis by sonication

To purify proteins produced intracellularly, the cells must be lysed. Sonication is a commonly used method for this, where the cells are broken by the use of ultrasonic vibrations (39). This leads to the disruption of the cellular membranes so the proteins can be released. The sonication

is performed in cycles (ON and OFF) with the sample submerged in ice water to avoid rapid heating of the sample.

The pellet with harvested cells was dissolved in 25 ml cold buffer A (50 mM MOPS with 5 mM $CaCl_2$). The resuspension was split in two 50 ml tubes. Next, the cells were lysed by sonication for 6 min. The settings were pulse ON = 10 sec, pulse OFF = 20 sec, amplitude (amp) = 40%. The 50 ml tubes were submerged in ice water with the microtip 1 cm below the sample surface. Next, the crude extract was transferred to smaller centrifuge tubes and centrifuged at 16 000 rpm, 4 °C for 30 min. The supernatant was sterile filtered and transferred to new 50 ml tubes. The filtrate was then purified by ion exchange chromatography.

2.20 Protein purification by liquid chromatography

2.20.1 Protein purification by ion-exchange chromatography

Ion-exchange chromatography a category of liquid chromatography and can be used to separate proteins based on their net charge. Mannuronan C5-epimerases are negatively charged and can therefore be purified using a column with a positively charged resin, as explained in Section 1.6.1.

The samples were partially purified by FPLC with an ion exchange column. The sterile filtered crude extract from sonication was loaded on a 5 ml anion exchange chromatography column (HiTrap Q HP, GE Healthcare), and purified by FPLC (ÄKTA FPLC system, GE Healthcare). 5 column volumes (CV) buffer A was used to equilibrate the system. The sample was added using an air sensor. During sample application, the elution was collected in a 50 ml tube. The sample path flow was washed with buffer A. The protein was eluted in 15 ml tubes during a stepwise gradient of NaCl. The gradient increased more rapidly in the beginning and end, and slower between 25 and 60% buffer B. The flow rate was kept at 5 ml/min. The column was washed with 5 CV buffer B after elution and then equilibrated with 5 CV buffer A. Before and after each time the column was used, it was washed with 1 CV RO water followed by 1 CV 20% ethanol. The column was stored at 4°C with 20% ethanol.

In some cases, a second purification was also done by IEC with a smaller column. The samples were loaded on a 1 ml anion exchange chromatography column (HiTrap Q HP, GE Healthcare), and purified by FPLC (ÄKTA FPLC system, GE Healthcare). The purification was performed the same way as the first round, apart from using a flow rate of 1 ml/min instead of 5 ml/min and collecting the samples in 2 ml tubes.

2.20.2 Protein purification by immobilized metal ion affinity chromatography

IMAC is a form of affinity chromatography and can be used to purify His-tagged proteins, as explained in Section 1.6.2.

The partially purified enzyme was loaded on a 1 ml immobilized metal ion affinity chromatography column (HisTrap HP, GE Healthcare), and purified by FPLC (ÄKTA FPLC system, GE Healthcare). 5 CV buffer C was used to equilibrate the system. The sample was added using an air sensor. During sample application, the elution was collected in a 50 ml tube. The sample path flow was washed with buffer C. The binding buffer had 0.5 M NaCl and 40 mM imidazole to reduce nonspecific protein binding. An increasing gradient of imidazole was loaded on the column by adding buffer D. The column was washed with 5 CV buffer D after elution and then equilibrated with 5 CV buffer C. The flow rate was kept at 1 ml/min. Before and after each time the column was used, it was washed with 1 CV RO water followed by 1 CV 20% ethanol. The column was stored at 4°C with 20% ethanol.

2.20.3 Gel filtration chromatography

Gel filtration, or size exclusion chromatography (SEC) is a method that is used to separate molecules in a solution based on their size, as explained in paragraph 1.6.3. In this project, gel filtration chromatography was used as a final purification step after IEC. In addition, gel filtration was used for desalting of protein samples.

Protein purification by gel filtration

A size exclusion chromatography column with Superdex 200 pg resin (HiLoad 26/600 Superdex 200 pg, Cytiva) was used for protein purification by FPLC (ÄKTA FPLC system, GE Healthcare). Initially, the column was washed with 1 CV filtered RO water. The column

was equilibrated with 2 CV buffer E. Next, the partially purified enzyme was loaded on the column. The maximum sample size of the column was 13 ml, and the sample was therefore up concentrated using centrifugal concentrators (Vivaspin® 6 Polyethersulfone, 100 kDa) by centrifugation at 4 000 xg with swing out rotor at 10ºC. The samples were up concentrated to a total volume of about 5 ml.

At least 1 CV buffer E was run through the column after sample application. The fractionation was controlled manually. When the UV_{280} increased, 5 ml were fractionated, whereas 40 ml were fractionated otherwise. The column was equilibrated with 2 CV buffer E between each run. The flow rate was kept at 2.6 ml/min apart from the sample application, where the flow rate was lowered to 1 ml/min. The column was washed with 1 CV filtered RO water after elution followed by 2 CV 20% ethanol. The column was stored at room temperature with 20% ethanol.

Desalting of protein samples by gel filtration

Protein samples were desalted, using 10 ml Thermo Scientific™ Zeba™ Spin Desalting Columns to remove salt and small molecules. The storage solution was removed by centrifugation at 1000xg for 2 min. 5 ml buffer with 50 mM MOPS and 2 mM $CaCl_2$ was loaded on the column before centrifugation at 1000xg for 2 min. This step was repeated four times. The column was placed in a new tube and the sample was loaded before centrifugation at 1000xg for 2 min to collect the sample.

2.21 Enzyme assays to measure activity of alginate lyases and mannuronan C-5-epimerases

The activity of alginate lyases can be measured by a UV-spectrophotometer. When an alginate lyase cleave alginate, an unsaturated uronic acid unit will be formed at the non-reducing end of the alginate. Unsaturated uronic acid has a strong absorbance at 230-240 nm. Cleavage of alginate can therefore be seen as increase in Abs_{230} by UV-spectrophotometer (84).

2.21.1 Lyase assay

The enzyme activity of alginate lyases can be determined quantitively by measuring Abs_{230} over a period where the product concentration increases linearly. The Abs_{230} was therefore plotted as a function of time and the slope of the linear region was found by linear regression in Excel. Enzyme activity can be measured in U, which is defined as the amount of enzyme that gives a rise of 1 Abs_{230} in 1 min in a 1 cm cuvette, according to (27). U in the added enzyme solution is found by

$$U_{sample} = \frac{1}{tAbs_{230}} L$$

where t Abs_{230} is how many min it would take to rise Abs_{230} by 1 and L is the light pathlength measured in cm. U/ml is found by

$$\frac{U}{ml} = \frac{U_{sample}}{V_{sample}}$$

where V_{sample} is the volume of enzyme solution added in the reaction, measured in ml. The enzyme activity of purified protein was also found in U/mole by

$$\frac{U}{mole} = \frac{U}{ml}\frac{M_W}{[P]}$$

where M_W is the molar weight of the protein measured in g/mole and [P] is the protein concentration measured in g/ml, found by NanoDrop according to Section 2.13.2.

The lyase activity was determined by measuring ΔAbs_{230}. Sodium alginate (Sigma V-90) (1 mg/ml), buffer (50 mM MOPS, pH 6.9 with variable $CaCl_2$ and NaCl concentrations) and enzyme solution was added in the wells of a UV-transparent acrylic plate, 200 µl in each well. The pathlength was found to be 0.451 cm in average. Buffer A was used as blank. Abs_{230} was measured every min for an hour or every 10 sec for 20 min using SpectraMaxPlus and the software SoftMaxPro 4.7.1 (Molecular Devices LLC.).

Initially, when samples were tested for lyase activity to identify fractions with active enzyme, 50 µl of the fractions and 5 ul crude extract were used. The $CaCl_2$ concentration was 2 mM, and no additional NaCl was added to the NaCl already present in the fractions. When the activity was tested at variable concentrations of $CaCl_2$ and NaCl, a smaller sample volume was used to achieve a linear increase in Abs_{230}. The samples were tested in triplicates and the Abs_{230} of the blank was deducted from the raw values.

2.21.2 Coupled epimerase/lyase assay

Epimerase activity can be measured by a coupled epimerase/lyase assay (85). The first step is epimerization of mannuronan, and the second step is cleavage by a G-specific lyase (AlyA). If there is active epimerase in the sample, some of the M residues will be epimerized to G residues. As a result, the G-specific lyase will be able to cleave the alginate, which can be seen as an increase in Abs_{230}. The G-specific lyase will not cleave poly-M, only G-G or G-M linkages, thus samples without active epimerase would not give a significant increase in absorbance (85, 86). The enzyme activity can be determined qualitatively by measuring Abs_{230} before and after addition of the G-specific lyase.

Mannuronan (1 mg/ml) was used as substrate in the coupled epimerase/lyase assay, dissolved in 50 mM MOPS, pH 6.9, 1.5 mM $CaCl_2$. 50 µl enzyme solution was added, resulting in a total volume of 200 µl in each well of a UV-transparent acrylic plate. Buffer A was used as blank. The samples were incubated at 37ºC for 18 hours. Abs_{230} was measured with SpectraMaxPlus and the software SoftMaxPro 4.7.1 (Molecular Devices LLC.). NaCl was added to a total concentration of 0.2 M before 8 µl G-specific lyase was added. The reaction was incubated at room temperature with shaking for 4 hours, before Abs_{230} was measured again. ΔAbs_{230} of the blank was subtracted from the calculations, to exclude the contribution from the lyase-solution itself.

2.21.3 Optimized epimerase assay

Because the coupled epimerase/lyase assay is an endpoint measurement, this assay was optimized to quantitatively measure and compare epimerase activity. Instead of performing epimerization and β-elimination separately, the two enzymes were added simultaneously.

Mannuronan (1 mg/ml) was used as substrate in 50 mM MOPS, pH 6.9, 75 mM NaCl, 1.5 mM $CaCl_2$. 8 µl G-specific lyase and 8 µl enzyme solution was added, resulting in a total volume of 200 µl in each well of a UV-transparent acrylic plate. An identical reaction without enzyme solution was used as blank. Abs_{230} was measured every min for an hour at 37ºC with SpectraMaxPlus and the software SoftMaxPro 4.7.1 (Molecular Devices LLC.). ΔAbs_{230} of the blanks was subtracted from the calculations to exclude the contribution from the lyase-solution itself.

2.21.4 Michaelis-Menten kinetics

Lyase assays were performed at different substrate concentrations estimate the initial velocity of the reaction (Section 1.3). V_0 was calculated for each substrate concentration by the equation:

$$V_0 = \Delta[P]\left(\frac{M}{min}\right) = \frac{\Delta Abs_{230}(min^{-1})}{\varepsilon_M\left(\frac{l}{mol\ cm}\right)\ L\ (cm)}$$

where ΔP is the change in product concentration, ε_M is the extinction coefficient of uronate and L is the path length. The extinction coefficient of unsaturated uronates is 5200 $M^{-1}cm^{-1}$ (87, 88) and was used to convert absorbance to product concentration. The path length was found to be 0.451 cm. V_0 was plotted as a function of substrate concentration [S] according to Michaelis-Menten kinetics.

A Lineweaver Burk-plot can be used to estimate K_m, V_{max} and k_{cat}. This plot is a linear transformation of the Michaelis-Menten equation by taking reciprocals on both sides to obtain

$$\frac{1}{v} = \frac{K_m}{[S]\,V_{max}} + \frac{1}{V_{max}}$$

Where v is V_0 at given substrate concentrations (34). The reciprocal velocity is plotted as a function of the reciprocal substrate concentration. The graph should, in accordance with Lineweaver Burk, be linear with the equation y = mx + C, where the slope m = K_m/ V_{max} and the intercept C = 1/ V_{max}. k_{cat} can also be calculated by the equation

$$k_{\text{cat}} = \frac{V_{max}}{[\text{E}]}$$

where [E] is the molar enzyme concentration.

2.22 SDS-PAGE

Sodium dodecyl-sulphate polyacrylamide gel electrophoresis (SDS-PAGE) is a commonly used method for separation of proteins in a mixture (39). By applying an electric field to a solution of proteins, they can be separated based on their electrical charge and size. A strongly cross-linked polyacrylamide gel is used as the solid matrix that the proteins migrate through. Initially, the proteins are denatured to unfold their three-dimensional structure, forming extended polypeptides. This is done by the negatively charged detergent SDS, which binds to the hydrophobic regions of the proteins. β-mercaptoethanol, or the less hazardous chemical dithiothreitol (DTT), is also often added to break S-S bonds within proteins and between different polypeptides in multisubunit proteins (39). Disulphide bridges can make the proteins more densely packed, which can make them migrate faster than expected. Due to the large amount of negatively charged SDS-molecules bound to the proteins, they will have a negative charge regardless of their intrinsic charge. Because of their unfolded structure, the proteins will have a uniform mass to charge ratio and proteins with similar size will therefore migrate the same distance through the polyacrylamide gel. They will migrate towards the positive electrode when an electric field is applied. To visualize the protein bands, the proteins can be stained with a dye, such as Coomassie blue, and compared to a standard with proteins of known molecular weight. (39)

9.5 µl protein sample was mixed with 5 µl 3xSDS sample buffer and 0.5 µl 30xDTT in a 1.5 ml tube. When cell mass was analysed, a small amount of the pellet was dissolved in 50 µl solution of SDS sample buffer and DTT. The samples were heated at 95ºC for 10 min before it was centrifuged using a microcentrifuge for about 10 min to avoid debris.

A polyacrylamide gel (RunBlue, 4-12% gradient (Expedeon) or TruPAGE™, 12%, no gradient (Sigma-aldrich)) with 12 or 17 wells was placed in a chamber filled with RunBlue 1x SDS Running Buffer (Expedeon). Alternatively, a SurePAGE 12% polyacrylamide gel, no gradient with 15 wells (GenScript) was used with either tris(hydroxymethyl)aminomethane 2-(*N*-morpholino) ethanesulfonic acid (TRIS-MES) or TRIS-MOPS buffer.

15 µl sample and 5 µl protein standard (Blue Prestained Protein Standard, Broad Range (NEB), (Appendix A: DNA and protein standards)) were loaded on the gel. A current of 150 V was applied for at about 1.5-2 hours. When the SurePAGE gels were used, the current was 200 V for 20-35 min.

The polyacrylamide gel was rinsed with 100 ml RO water three times for 5 min, followed by staining with SimplyBlue™ SafeStain (Invitrogen) for one hour at room temperature with gentle shaking. Next, the gel was washed with 100 ml RO water ON at room temperature with gentle shaking, followed by washing for one more hour to get a clear gel background. Alternatively, the gel was stained and washed with a different, less time-consuming method. This involved an initial wash for a few min in RO water before staining and washing with eStain L1 Protein Staining Device (GenScript) for 9.5 min (89). This method is less time-consuming due to mechanical pumping of the stain and washing solution. The gel was photographed and edited with ImageLab (Bio-Rad).

2.23 High-cell-density cultivation of *E. coli*

When recombinant proteins are produced at industrial scale, a large biomass is necessary to increase protein production. This can be achieved by high-cell-density cultivation (HCDC) (90). HCDC is performed in bioreactors where environmental factors are controlled to achieve a high OD and a high product yield. The fermentation protocol that was used for HCDC in this project was developed and optimized at SINTEF (91). The fermentation was performed by

Randi Aune and Deni Koseto at SINTEF- Department of Biotechnology and Nanomedicine, who kindly demonstrated to me the setup and how the different parameters were controlled in the bioreactors during the fermentation.

In this project, the fermentation inoculum was prepared by growing *E. coli* RV308 on LA with selective antibiotics (50 µl/µg Kan) at 37ºC ON. Single colonies were transferred to 100 ml LB(g) with 50 µl/µg Kan in 500 ml baffled flasks and incubated for 7 hours at 30ºC, 200 rpm. A 0.5% culture was made in 100 ml Hi-media with 50 µl/µg Kan, where growth was continued at 30ºC for 16 hours. This culture was used to inoculate 0.75 litres Hf-production media in a 3 litre Applicon fermentor. The fermentation was performed without antibiotic selection. The temperature was kept at 30º C and pH was maintained at 6.8 by adding 8.33% ammonia. Airflow was kept at 1 l/min to keep dissolved oxygen (DO) above 10% throughout the fermentation. Stirring was kept at 500 rpm from start but was increased to 1800 rpm after 2-3 hours. 25 g/l glucose was added at the start of the fermentation and growth was continued until all glucose had been consumed. 13 g reactor^{-1} hour^{-1} feeding solution was added to achieve a specific growth rate of 0.2 hour^{-1}. Feeding was increased to 25 g reactor^{-1} hour^{-1} before it was lowered and kept at 22 g reactor^{-1} hour^{-1}. *m*-toluate inducer (0.5 M) was added when the OD_{600} was between 70 and 90. pH, DO, feeding rate, airflow, and molar fraction of CO2 in the exhausted gas was monitored during the whole fermentation process.

A sample was taken after 3.5 hours. 1.00 g fermentate was centrifuged and the pellet and supernatant and pellet was kept at -20ºC. The rest of the cells were harvested by centrifugation after 8 hours. The cell-pellets were kept at -20ºC.

2.24 NMR

Nuclear magnetic resonance (NMR) spectroscopy is an often-used method for structural identification of organic compounds (92, 93). NMR is a form of absorption spectrometry where atomic nuclei absorb energy in a magnetic field. The absorption is governed by the chemical environment of the nuclei. The atomic nucleus can in principle be seen as a charged, rotating sphere. The nuclei therefore behave like a magnetic dipole with the angular momentum quantum number, or nuclear spin *I*, which can have values from 0, ½, 1, 1 ½ etc. up to 8. Both ^{1}H and ^{13}C have quantum spin number ½, meaning there are two possible spin orientations in a

strong magnetic field, either towards or against the magnetic field. The energy (E) of each spin state is different and ΔE depends on the intensity of the applied magnetic field. By applying a radiofrequency (RF) pulse equal to ΔE, the nuclei will absorb energy in the magnetic field. This will make the spin state of the nuclei change from lowest to highest energy state before they return to their initial spin state by relaxation. The relaxation leads to irradiation of energy which is detected by the NMR instrument and transformed to frequency. (93)

In the NMR spectra, the frequency of the absorption peaks are plotted against the peak intensity. Because the atoms in chemically different groups are surrounded by different electron clouds with different electron density distribution, they give rise to different peaks. In ^{1}H-NMR, the ^{1}H nuclei absorb the electromagnetic radiation, and each peak in the NMR-spectra will represent protons in a particular chemical environment. The ^{13}C isotope nuclei absorb the electromagnetic radiation in ^{13}C-NMR, and the peaks therefore represent carbon atoms in particular chemical environments. (93)

2.24.1 Time-resolved NMR to study mode of action on mannuronan over time

Time-resolved NMR is usually based on several one-dimensional spectra over time. This enables measurements of the structural changes of organic compounds over time. It can for instance be useful to study chemical reactions, macromolecular changes or phase transitions (94).

The experimental procedures were conducted by Professor Finn Lillelund Aachmann and PhD. candidate Agnes Beenfeldt Petersen at the Department of Biotechnology and Food Science, NTNU. A BRUKER Avance III HD 800 MHz instrument with a 5 mm Z-gradient CP-TCI (H/C/N) cryogenic probe was used to record the NMR spectra at the NV NMR centre. All reactions were performed at 25ºC.

A substrate solution of 9 mg/ml ^{13}C1-enriched mannuronan polymers (DPn ≈70) was prepared in 5 mM MOPS pH 6.9, 2,5 mM $CaCl_2$, 75 mM NaCl, 99.9% D_2O. 160 µl substrate solution was transferred to a 3 mM LabScape Stream NMR tube (Bruker Labscape Store). The substrate was preheated in the NMR instrument before addition of 20 µl enzyme solution. The tube was inverted to achieve a homogenous solution. Next, the tube was inserted in the NMR-instrument

and the experiment was started. A pseudo-2D type spectrum was created by recording a 1D ^{13}C-NMR spectrum every 10 min with a total run time of 16 hours. The spectra were captured, processed, and analysed by Agnes Beenfeldt Petersen using TopSpin 4.0.7 software (Bruker BioSpin). The same procedure was also performed with ^{1}H-NMR, with a 1D ^{1}H-NMR spectra being captured every 5 min for a total run time of 17 hours.

2.24.2 Endpoint NMR to study mode of action on long chain mannuronan

Endpoint NMR was performed after an epimerization reaction to analyse the structure of the final product. The experimental procedures of the epimerization were conducted in collaboration with Agnes Beenfeldt Petersen. 20 mg mannuronan were dissolved in 4 ml 5 mM MOPS, pH 6.9, 2.5 mM $CaCl_2$, 75 mM NaCl in 99.9% D_2O. 80 µl 45.6 µM epimerase was added. The tubes were incubated at shaking at 25ºC for 24 hours. Next, the reaction was split in two tubes per enzyme. One of the reactions was stopped by freezing the sample. The other sample was added 20 µl 1mM $CaCl_2$ and 40 µl enzyme before continued incubation another 24 hours. To remove Ca^{2+} and dissolve the gels, 1.6 ml 50 mM EDTA, pH 7 was added. The samples were dissolved in 20 ml Milli-Q® (MQ) water and stirred for a few hours before storage at 4ºC.

Dialysis and acid hydrolysis was performed by Agnes Beenfeldt Petersen to remove the EDTA and Ca^{2+} and cleave the alginate before NMR. Dialysis was performed with a MWCO 12-14 kD membrane. The dialysis tubes were initially submerged in 50 mM NaCl in MQ water, which was changed two times with at least 4.5 hours in between. Next, the dialysis was performed in MQ water which was changed two times over three days. Acid hydrolysis was performed according to the method described by ASTM (95). The samples were freeze-dried and prepared for NMR by Agnes Beenfeldt Petersen. Endpoint ^{1}H-NMR was performed by overengineer Wenche Iren Strand at the Department of Biotechnology and Food Science, NTNU, again according to ASTM (95).

3 Results

3.1 Construction of His-tagged AcAlgE1, AcAlgE2 and AcAlgE3

In a previous study of AcAlgE1-3, the Intein Mediated Purification with an Affinity Chitin-binding Tag (IMPACT) system was used for isolation of the epimerases (56). This resulted in a high and pure yield, but the enzyme activity was very low. In this project, it was tested if a His-tag could be used for purification of the proteins.

A simplified overview of the plan for production and purification of AcAlgE1-3 in this work, is outlined in Figure 10. The first step was to construct three plasmids encoding the His-tagged epimerases regulated by the LacI/P_{T7}*lac* promoter/regulator system. The proteins were produced by recombinant protein production before purification by IEC and IMAC.

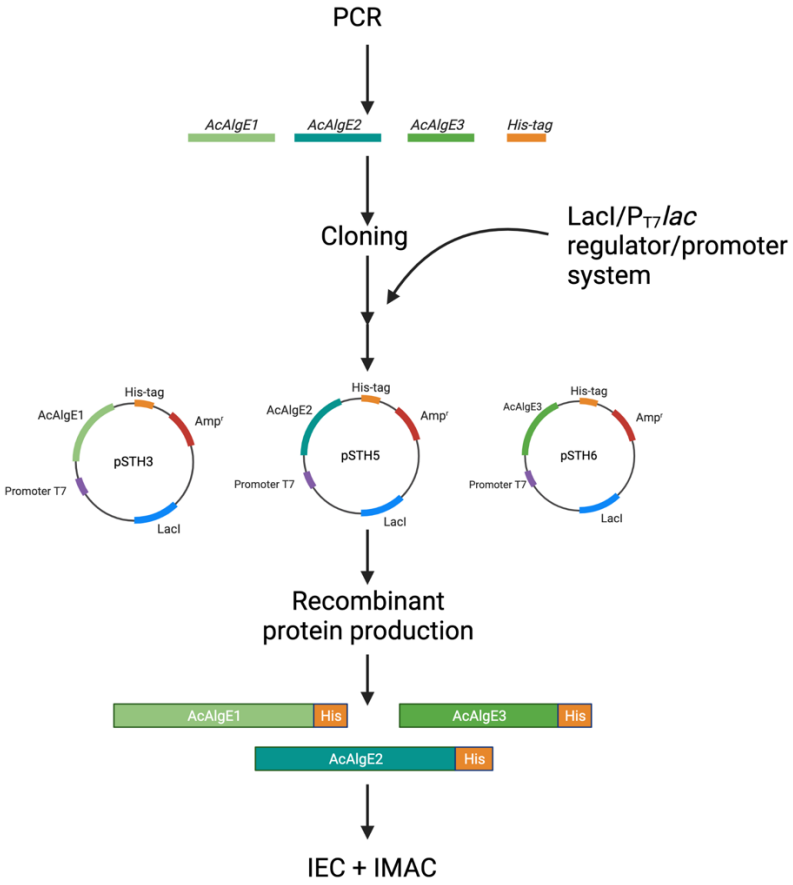

Figure 10: Simplified overview of the production of AcAlgE1, AcAlgE2 and AcAlgE3 with His-tags. The figure is created in BioRender.

3.1.1 Construction of plasmids encoding epimerases with His-tag

Construction of initial plasmids containing *acalgE1, acalgE2, acalgE3* and a His-tag

Firstly, *acalgE1*, *acalgE2*, *acalgE3* and a gene with a His-tag were cloned separately into four TOPO-vectors. These four TOPO-vectors were transformed into *E. coli* DH5α by heat-shock transformation. To check if the PCR products had been inserted correctly, the plasmids were digested by EcoRI and analysed by gel electrophoresis. TOPO-vectors without insert would give one fragment at 3.5 kilo bases (kb), whereas correct transformants would have an additional fragment of the size of the PCR product. There was at least one correct transformant for each plasmid (Figure 11). Next, the inserts were verified by Sanger sequencing (Appendix B: Sequencing of TOPO-vectors). All TOPO-vectors had correct inserts of reverse orientation. One transformant was selected for each, and the plasmids were named pSTH18, pSTH21, pSTH22 and pSTH23 (Table 4).

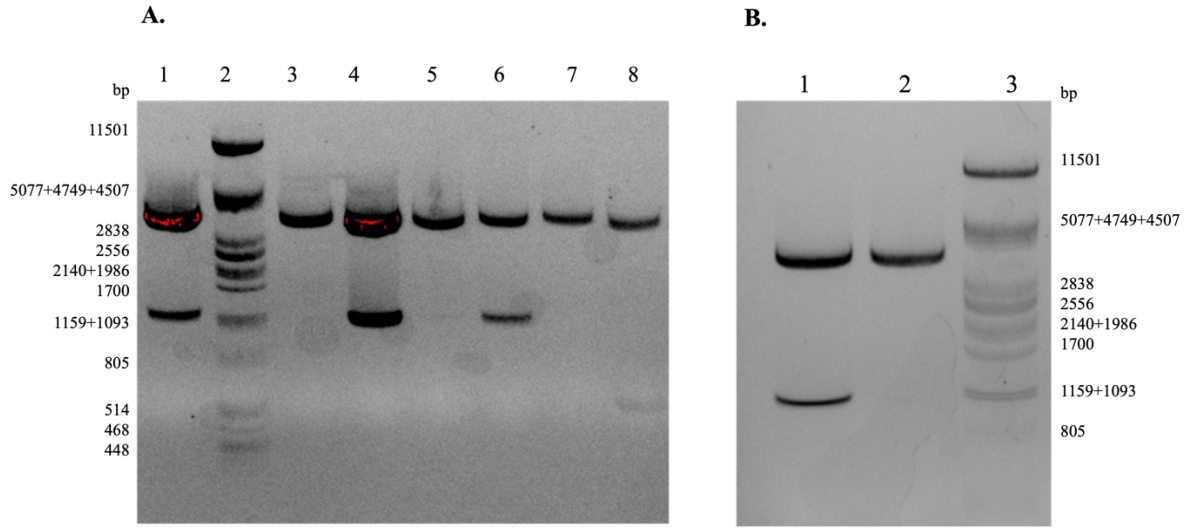

Figure 11: Gel electrophoresis of digested plasmids. **(A)** Lanes: 1) A TOPO-vector with a 997 bp PCR product of pSTS21 constructed with the primers Ac550F2 and AcAlgE1 HR. The plasmid was selected and named pSTS21. 2) λ-DNA digested by PstI. 3, 5 and 7) TOPO-vectors without insert. 4 and 6) TOPO-vectors with a 1100 bp PCR product of pSTS22 constructed with the primers AcAlgE2 sjekk 1 and AcAlgE2 HR. The transformant in lane 4 was selected and the plasmid was named pSTH22. 8) TOPO-vector with a 540 bp PCR product of pMEJ18 with the primers His18Kpn and His18Bam. The plasmid was named pSTH18 **(B)** Lanes: 1) A TOPO-vector with a 1012 bp PCR product of pSTS23 constructed with the primers AcAlge3sjekk and AcAlgE3 HR. The plasmid was named pSTH23. 2) A TOPO-vector without insert. 3) λ-DNA digested by PstI.

In the second step, pSTH18 was used to insert the His-tag into a plasmid vector containing the LacI/P_{T7}*lac* promoter/regulator system, as illustrated in Figure 12, which would facilitate subsequent cloning steps.

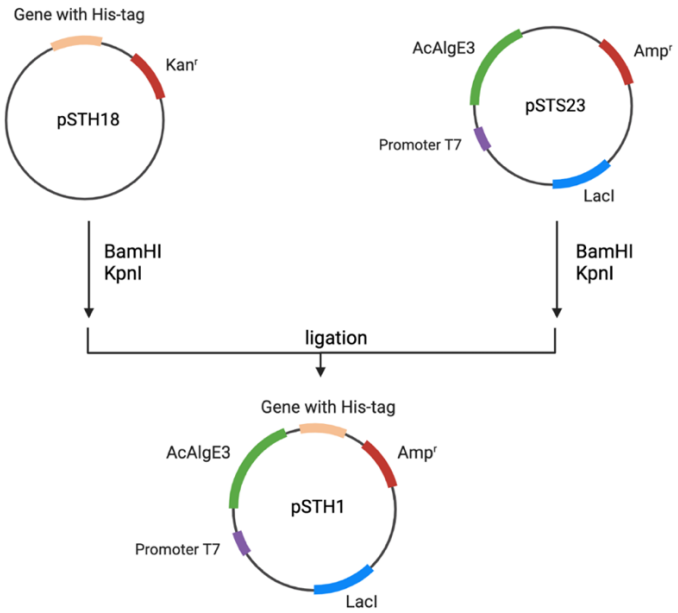

Figure 12: Schematic overview of the construction of pSTH1, encoding AcAlgE3 and a gene containing a His-tag. pSTH18 and pSTS23 were digested by BamHI and KpnI. The 7.3 kb fragment from pSTS23 and the 0.5 kb fragment from pSTH18 were purified and ligated to construct pSTH1. The figure is created in BioRender.

The ligation product of pSTS23 and pSTH18 (Figure 12) was transformed into *E. coli* DH5α and tested by digestion with XbaI and NotI, which indicated that a transformant was correct (Figure 13). The plasmid was named pSTH1.

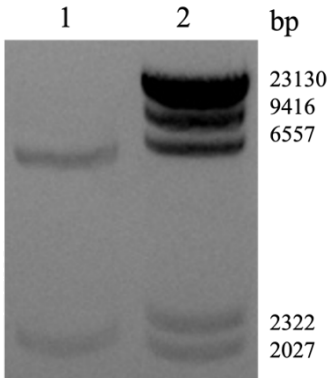

Figure 13: Gel electrophoresis of digested plasmid. Lanes: 1) PSTH1, a ligation product of a BamHI-KpnI 7.3 kb fragment from pSTS23 and a BamHI-KpnI 1 kb fragment from pSTH18. The ligation product was digested by XbaI and NotI. Correct insert would give two fragments (5.9 kb and 2 kb), whereas the parental plasmid pSTS23 would give only one fragment at 8.9 kb. 2) λ-DNA digested by HindIII.

AcAlgE1

The plasmid pSTH1 was used to construct the plasmid pSTH3, encoding AcAlgE1 with a His-tag. This was done in two steps (Figure 14).

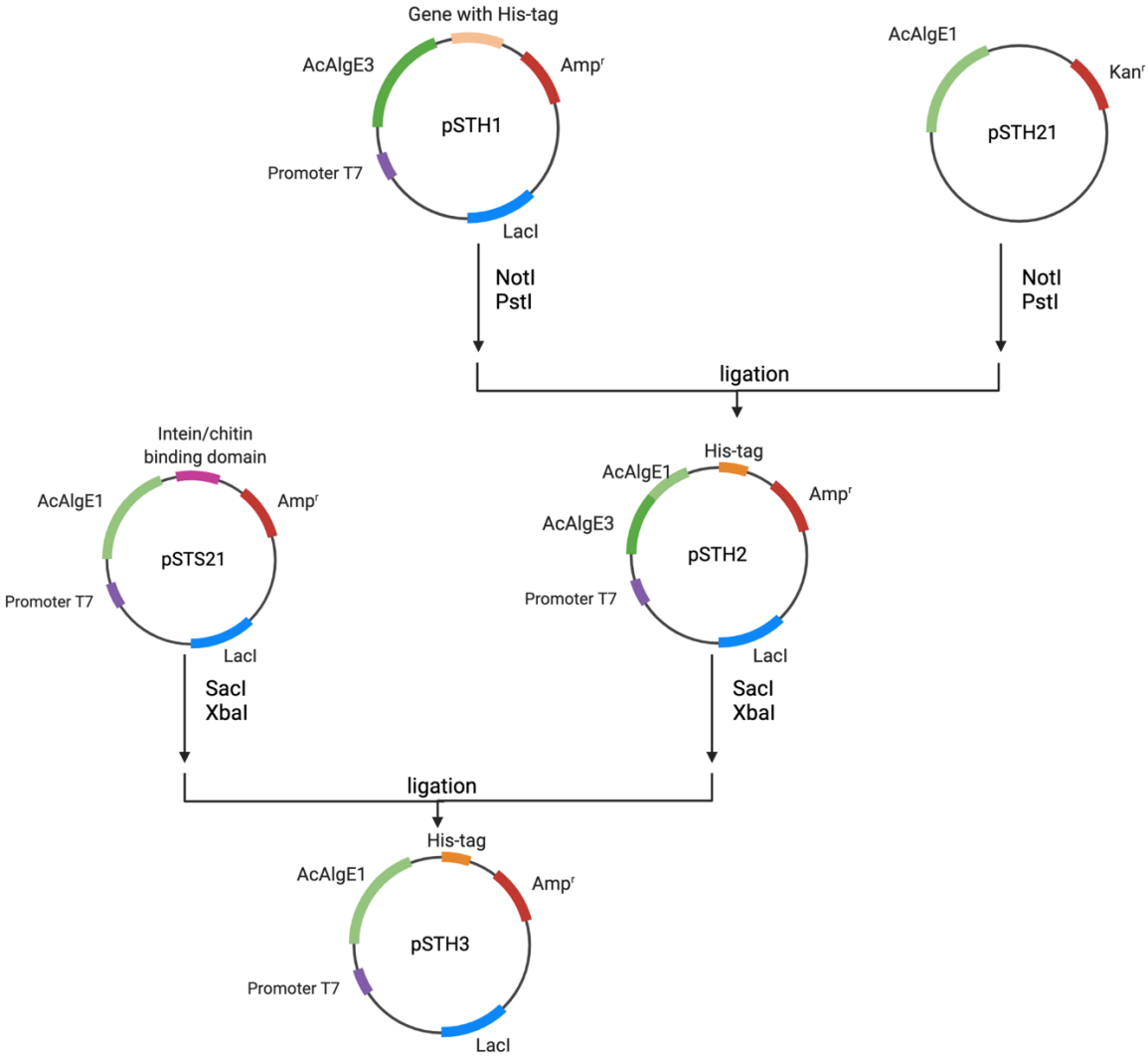

Figure 14: Schematic overview of the construction of pSTH3, encoding AcAlgE1 with a His-tag, regulated by the LacI/P_{T7}*lac* promoter/regulator system. pSTH1 and pSTH21 were digested by NotI and PstI. The 6.7 kb fragment from pSTH1 and the 1 kb fragment from pSTH21 were ligated to construct pSTH2. Next, pSTH2 and pSTS21 were digested by SacI and XbaI. The 5.9 kb fragment from pSTH2 was ligated with the 3 kb fragment from pSTS21 to construct pSTH3. The figure is created in BioRender.

Firstly, the ligation product of pSTH1 and pSTH21 (Figure 14) was transformed into *E. coli* DH5α and tested by digestion with BamHI. The gel electrophoresis indicated that a transformant was correct (Figure 15). Its plasmid was named pSTH2.

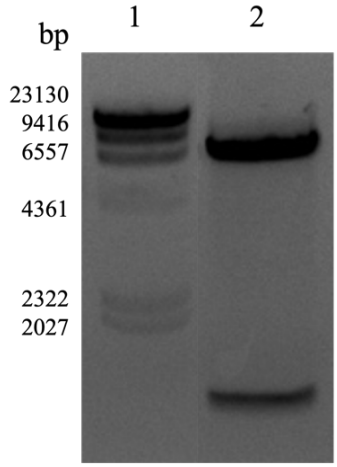

Figure 15: Gel electrophoresis of digested plasmid. Lanes: 1) λ-DNA digested by HindIII. 2) pSTH2, a ligation product of a NotI-PstI 6.7 kb fragment from pSTH1 and a NotI-PstI 1 kb fragment of pSTH21. The plasmid was digested by BamHI. A correct plasmid would give two fragments (6.7 and 1 kb), whereas the parental plasmid pSTH1 would give only one fragment of 7.9 kb.

Subsequently, the ligation product of pSTH2 and pSTS21 (Figure 14) was transformed into *E. coli* DH5α and tested by digestion with BspEI. A transformant with correct plasmid was selected and named pSTH3 (Figure 16).

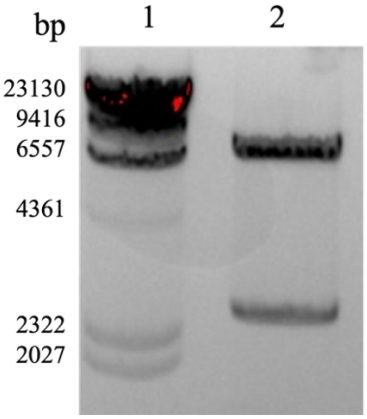

Figure 16: Gel electrophoresis of digested plasmid. Lanes: 1) λ-DNA digested by HindIII. 2) pSTH3, a ligation product of a SacI-XbaI 5.9 kb fragment from pSTH2 and a SacI-XbaI 3 kb fragment from pSTS21. The plasmid was digested by BspEI. Correct insert would give two fragments (6.6 and 2.3 kb), whereas the parental plasmid pSTH2 only would give one fragment (7.7 kb).

AcAlgE2

To produce AcAlgE2 with His-tag, the plasmid pSTH5 was constructed as illustrated in Figure 17.

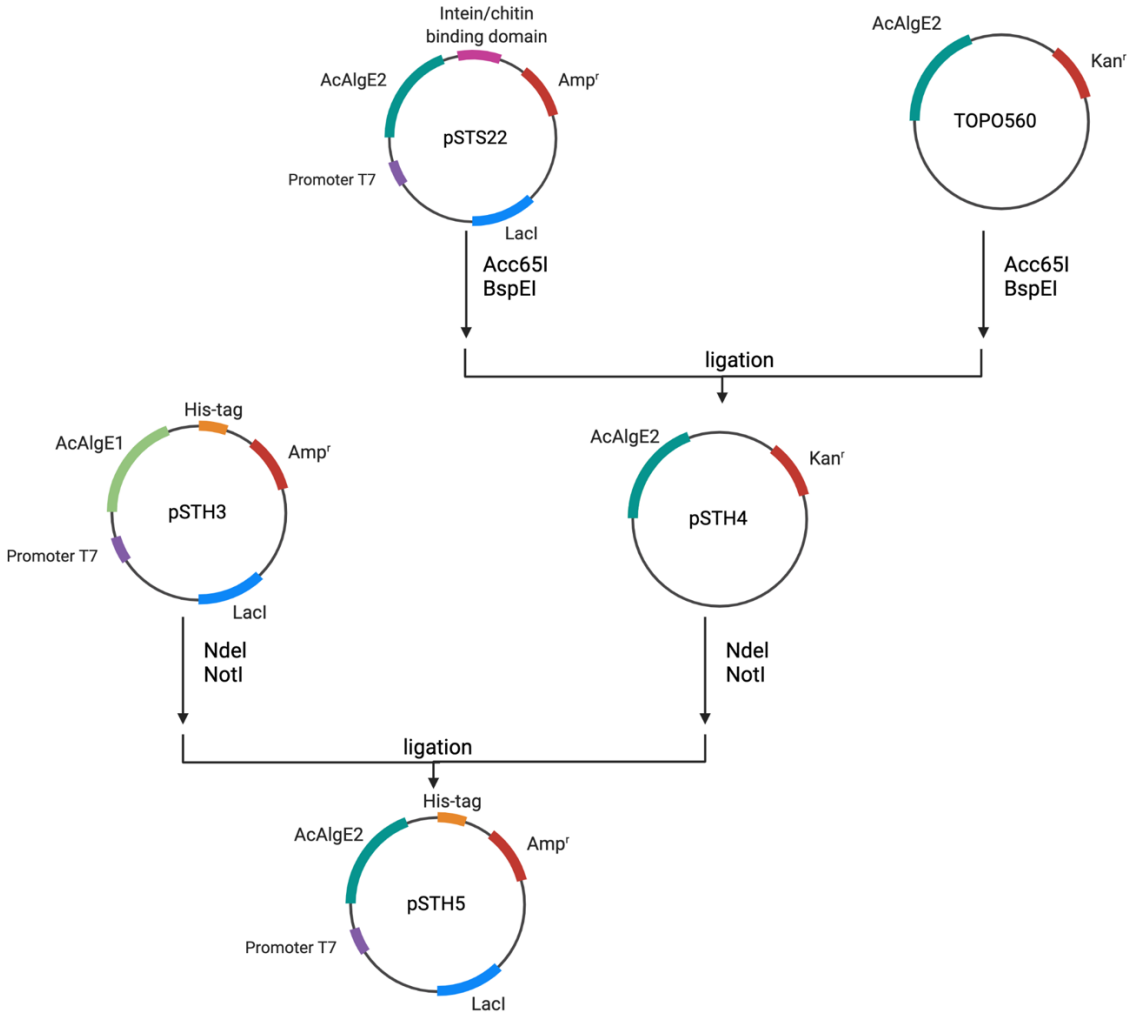

Figure 17: Schematic overview of the construction of pSTH5, encoding AcAlgE2 with a His-tag, regulated by the LacI/P$_{T7}$*lac* promoter/regulator system. TOPO560 and pSTS22 were digested by Acc65I and BspEI. The 5.4 kb fragment from TOPO560 was ligated with the 753 bp fragment from pSTS22 to construct pSTH4. Next, pSTH3 and pSTH4 were digested by NdeI and NotI. The 2.6 kb fragment from pSTH4 was ligated with the 6.6 kb fragment from pSTH3 to construct pSTH5. The figure is created in BioRender.

Firstly, the ligation product of TOPO560 and pSTS22 (Figure 17) was transformed into *E. coli* DH5α and tested by digestion with NdeI and NotI. A transformant showed the correct fragments and its plasmid was named pSTH4 (Figure 18). This plasmid was constructed to obtain the restriction sites that were to be used in the second cloning step.

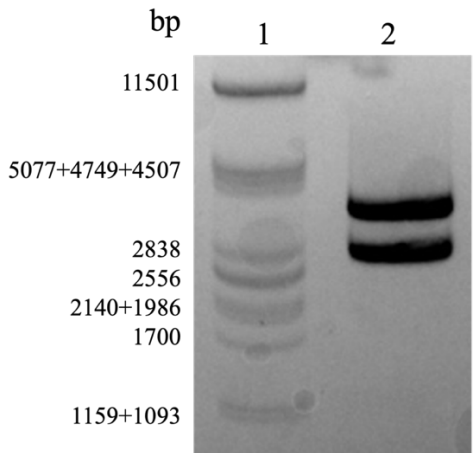

Figure 18: Gel electrophoresis of digested plasmid. Lanes: 1) λ-DNA digested by PstI. 2) pSTH4, a ligation product of a Acc65I-BspEI 5.4 kb fragment from TOPO560 and a Acc65I-BspEI 753 bp fragment from pSTH22. The plasmid was digested by NdeI and NotI. Correct insert would give rise to two fragments of 3.5 and 2.6 kb, whereas pSTS22 would give rise to two fragments of 3.5 and 1.1 kb. TOPO560 would result in one fragment of 6.1 kb.

Next, the ligation product of pSTH4 and pSTH3 (Figure 17) was transformed into *E. coli* DH5α. To test if the correct fragment was inserted, the plasmid was digested by BspEI. A correct transformant was identified, and its plasmid was named pSTH5 (Figure 19).

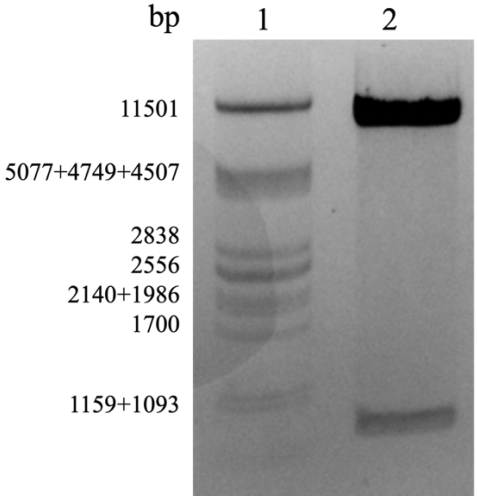

Figure 19: Gel electrophoresis of digested plasmid. Lanes: 1) λ-DNA digested by PstI. 2) pSTH5, a ligation product of a NdeI-NotI 6.6 kb fragment from pSTH3 and a NdeI-NotI 2.6 kb fragment of pSTH4. The plasmid was digested by BspEI. Correct plasmid would result in two bands (7.6 and 0.9 kb), whereas the parental plasmids pSTH3 and pSTH4 would give two bands at 6.6 and 2.3 kb or one band at 6.1 kb, respectively.

AcAlgE3

Although pSTH1 encodes both the epimerase AcAlgE3 and the His-tag, the plasmid had to be processed further to encode epimerases with C-terminal His-tag. The gene upstream of the His-tag had to be removed, as outlined in Figure 20.

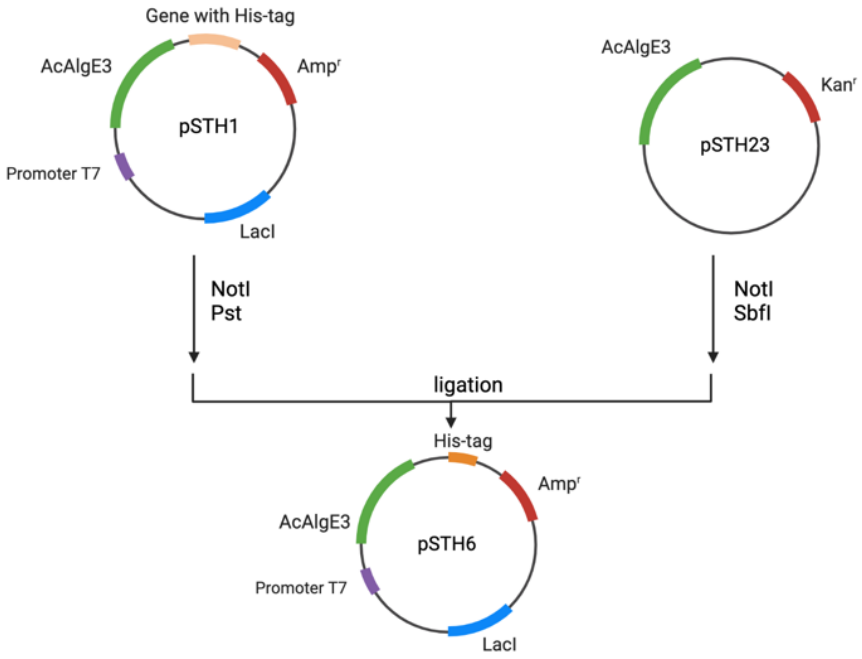

Figure 20: Schematic overview of the construction of pSTH6, encoding AcAlgE3 with a His-tag, regulated by the LacI/P$_{T7}$*lac* promoter/regulator system. pSTH1was digested by NotI and PstI. pSTH23 was digested by NotI and SbfI. The 6.7 kb fragment from pSTH1 and the 0.6 kb fragment from pSTH23 was ligated to construct pSTH6. The figure is created in BioRender.

The ligation product of pSTH1 and pSTH23 was transferred to *E. coli* DH5α and tested by restriction enzyme digestion, which indicated a correct transformant (Figure 21). Its plasmid was named pSTH6.

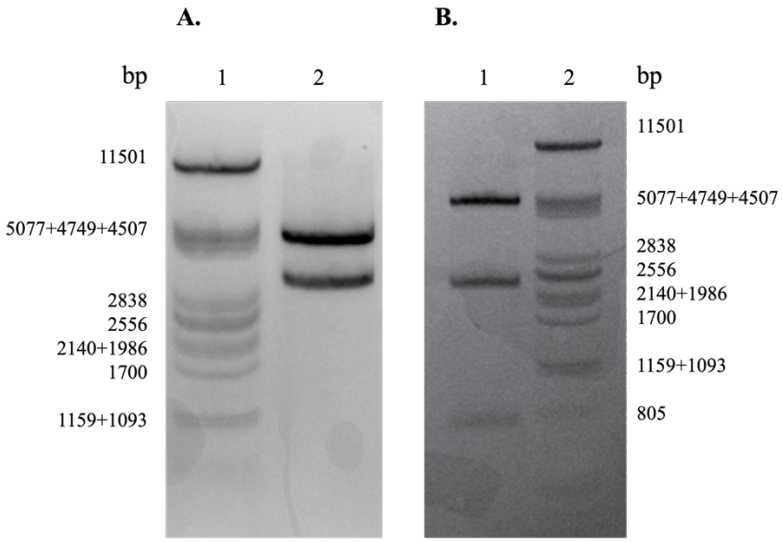

Figure 21: Gel electrophoresis of digested plasmid. **(A)** Lanes: 1) λ-DNA digested by PstI. 2) pSTH6, a ligation product of a PstI-NotI 6.7 kb fragment from pSTH1 and a SbfI-NotI 0.6 kb fragment of pSTH23. The plasmid was digested by SacI, DraIII and XbaI. A correct plasmid would result in two fragments (4.4 and 3 kb) whereas the parental plasmid pSTH1 would give rise to three fragments (4.4, 1.7 and 1.8 kb). **(B)** To doublecheck, in case SacI did not cut, pSTH6 was also digested by KpnI and DraI. Correct insert would give three fragments (4.5, 2.1 and 0.75 kb) whereas the parental plasmid pSTH1 would result in four fragments (4.5, 1.6, 1.0 and 0.75 kb). Lanes: 1) pSTH6, digested by KpnI and DraI. 2) λ-DNA digested by PstI.

3.1.2 Expression and purification of epimerases with His-tags

AcAlgE1, AcAlgE2 and AcAlgE3 with His-tags were encoded by pSTH3, pSTH5 and pSTH6, respectively. The gene expression was regulated by the LacI/P_{T7}*lac* regulator/promoter system, thus a T7 RNA polymerase was necessary. For this reason, the plasmids were transferred to *E. coli* SHuffle T7 Express. AcAlgE1-3 were expressed, harvested, sonicated and filtered before initial purification by IEC. The proteins were eluted at 0.34-0.44 M NaCl. The activity of AcAlgE1 was tested by a coupled epimerase/lyase assay. The activity of AcAlgE2 and AcAlgE3 was tested by a lyase assay, and the fractions with active enzyme were pooled and purified further.

Next, the proteins were attempted purified further by IMAC. Unfortunately, nearly all protein was eluted during the sample application (Appendix G: Chromatograms from protein purification). This was the case for all three enzymes and indicated that the His-tag attached to the C-terminus of the epimerases did not bind to the column. AcAlgE1 with His-tag was not used further, while AcAlgE2 and AcAlgE3 were purified further by a second round of IEC.

Next, AcAlgE2 and AcAlgE3 were tested by a lyase assay to identify the fractions with active enzymes. The protein concentration of AcAlgE2 and AcAlgE3 was measured (Table 7).

Table 7: Protein concentrations of crude extracts and fractions of purified AcAlgE2 and AcAlgE3.[1]

Enzyme	Sample	Protein concentration [mg/ml]	Total amount of protein [mg]
AcAlgE2	Crude extract	4.479	134
	Partially purified 1	0.411	16.4
	Partially purified 2	0.196	8.82
	Fraction 1B2	0.638	3.19
	Fraction 1B3	0.901	4.51
	Fraction 1B4	0.319	1.60
AcAlgE3	Crude extract	23.72	712
	Partially purified 1	1.422	64.0
	Fraction 1A8	0.716	3.58
	Fraction 1B1	3.015	15.1
	Fraction 1B2	2.563	12.8
	Fraction 1B3	1.479	7.40
	Fraction 1B4	0.712	3.56
	Fraction 1B5	1.427	7.14

Finally, the fractions with active enzyme of AcAlgE2 and AcAlgE3 were analysed by SDS-PAGE to check the molecular weight and the purity of the proteins (Figure 22).

[1] The protein concentration was measured with NanoDrop at 280 nm. The concentration of the crude extracts was measured based on the estimation that 1 Abs = 1mg/ml. The concentration of AcAlgE2 was measured for a molecular weight (Mw) of 90.60 kDa and an extinction coefficient (ε_M) of 57.19 $M^{-1}cm^{-1}$. The concentration of AcAlgE3 was measured for a Mw of 51.60 kDa and an ε_M of 33.81 $M^{-1}cm^{-1}$. The partially purified sample 1 had been purified trough one round of IEC, whereas partially purified sample 2 had been purified by one round of IEC and one round of IMAC. The 5 remaining fractions had been purified by two rounds of IEC.

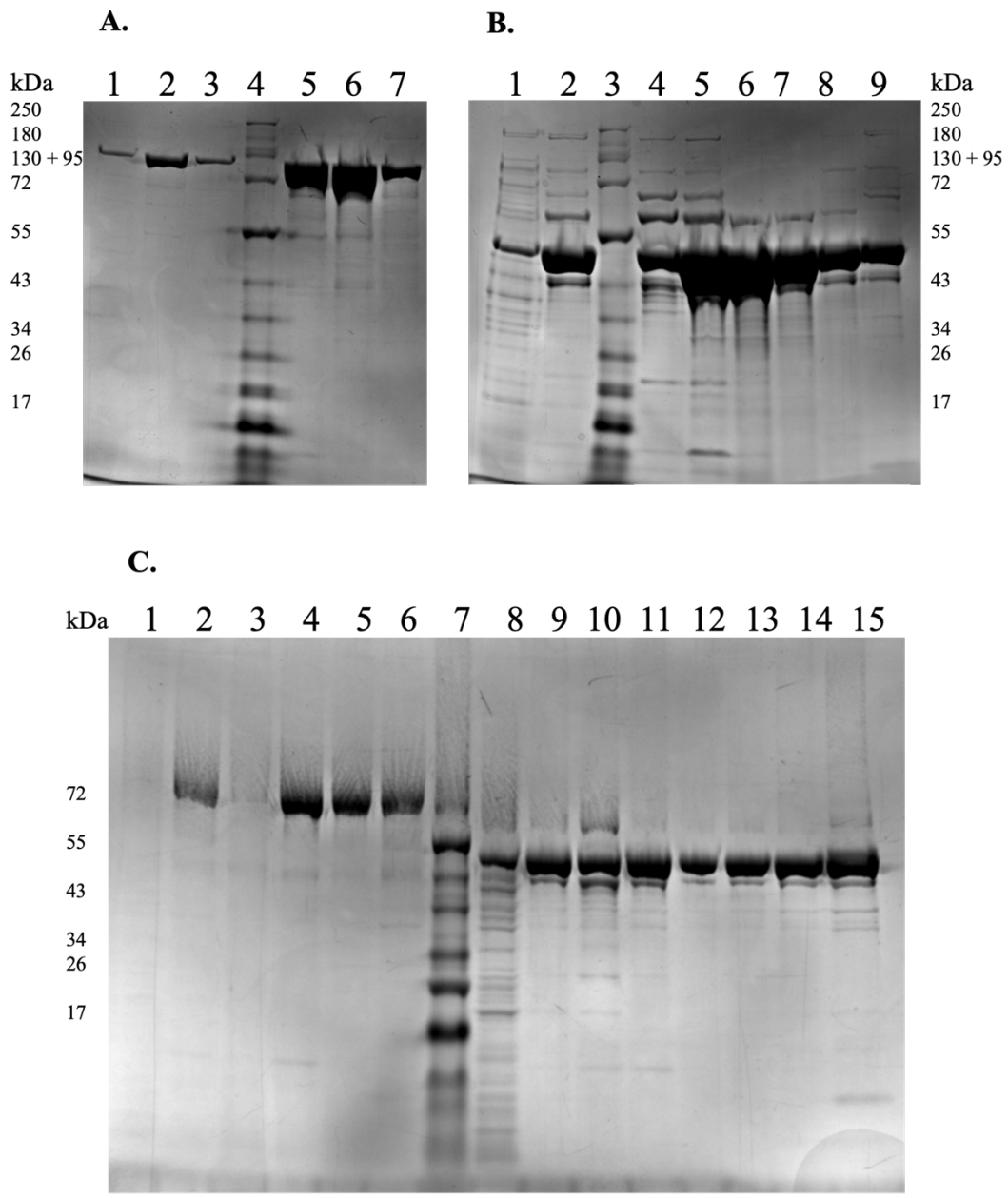

Figure 22: SDS-PAGE analysis of fractions collected during protein purification of AcAlgE2 and AcAlgE3 with His-tags. **(A)** Lanes: 1-3) AcAlgE2. Crude extract, sample after purification by one round of IEC, sample after one round of IEC and one round of IMAC. 4) Blue Prestained Protein Standard, Broad Range (NEB). 5-7) Fractions 1B2-1B4 of AcAlgE2 after two rounds of IEC. **(B)** Lanes: 1-2) AcAlgE3. Crude extract, sample after purification by one round of IEC. 3) Blue Prestained Protein Standard, Broad Range (NEB). 4-9) Fractions 1A8 and 1B1-1B5 of AcAlgE3 after two rounds of IEC. **(C)** The same results as a) and b) combined, but with less protein (maximum 6.7 ng) to make the bands more precise. The gel appears blurry due to leakage. Lanes: 1-3) AcAlgE2. Crude extract, sample after purification by one round of IEC, sample after one round of IEC and one round of IMAC. 4-6) AcAlgE2. Fractions 1B2-1B4 after two rounds of IEC. 7) Blue Prestained Protein Standard, Broad Range (NEB), 8-9) AcAlgE3. Crude extract, sample after purification by one round of IEC. 10-15) AcAlgE3. Fractions 1A8 and 1B1-1B5 after two rounds of IEC.

The SDS-PAGE analysis indicated that both AcAlgE2 and AcAlgE3 had been produced. There was strong band between 72 kb and 95 kb, indicating production of AcAlgE2 (90 624 kDa) (Figure 22A). There was also a strong band between 43 kb and 55 kb, indicating production of AcAlgE3 (51 567 kDa) (Figure 22B).

The crude extract of AcAlgE2 had few visible impurities, which indicate a strong expression and protein production. The crude extract of AcAlgE3 had more visible impurities, but this could be due to higher protein concentration in general (Table 7). By comparing the crude extract and sample after purification of AcAlgE3 by one round of IEC, it was observed that some impurities were removed by IEC. A second round of IEC did not appear to have any effect on the purity.

3.2 Effect of calcium and NaCl on lyase activity of AcAlgE2 and AcAlgE3

The fractions of AcAlgE2 and AcAlgE3 that showed activity and contained a high amount of relatively pure protein (Fractions 1B2-1B4) were pooled and desalted by gel filtration to remove salts and small molecules. The protein concentration of the desalted samples was 0.584 mg/ml and 1.472 mg/ml for AcAlgE2 and AcAlgE3, respectively.

Next, the effect of calcium and NaCl was tested by lyase assays at different $CaCl_2$ and NaCl concentrations.

3.2.1 NaCl dependency

Lyase assays were performed at different NaCl-concentrations (Table 12 in Appendix E: Calculated enzyme activity). The relative activity of AcAlgE2 and AcAlgE3 was plotted as a function of the NaCl concentration (Figure 23).

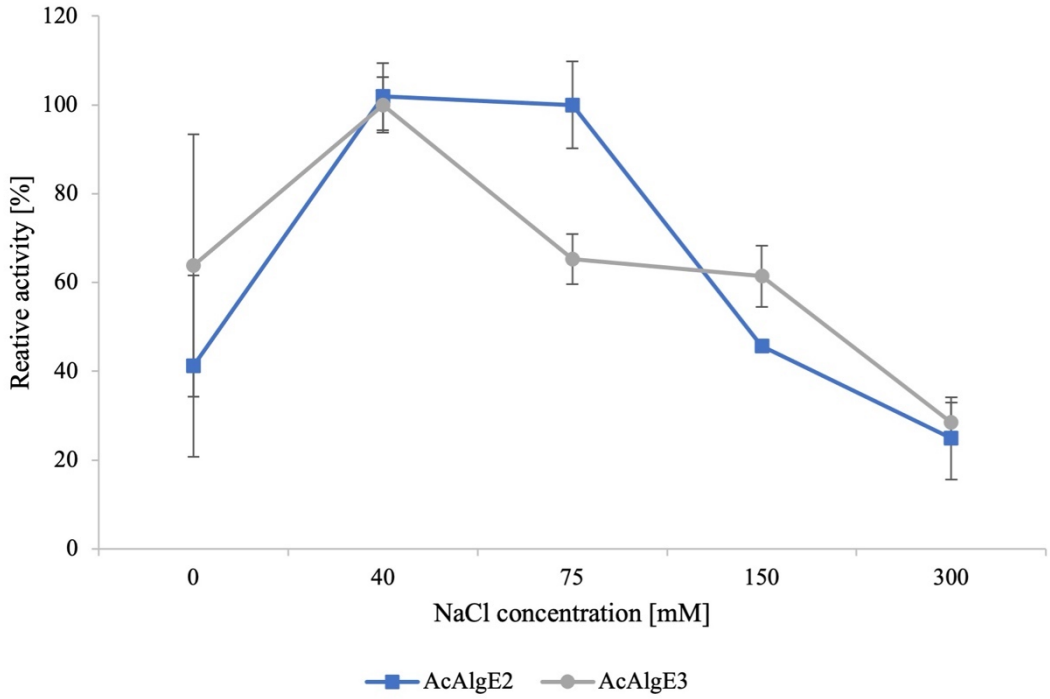

Figure 23: Relative activity of AcAlgE2 and AcAlgE3 at different NaCl-concentrations. For each enzyme, the highest measured activity was set as 100%. The substrate was 1 mM sodium alginate (Sigma V-90) in 50 mM MOPS, pH 6.9, 1 mM $CaCl_2$. The given activity is an average based on triplicates. The error bars indicate the standard deviation.

The assays indicated that the enzyme activity of both AcAlgE2 and AcAlgE3 was affected by the concentration of NaCl. The optimal NaCl concentration was 40 mM for both enzymes. Addition of 40 mM NaCl increased the activity of AcAlgE2 and AcAlgE3 by 147% and 57%, respectively. It was also observed that the activity of AcAlgE2 was approximately the same at 75 mM NaCl as at 40 mM NaCl, whereas the activity of AcAlgE3 was significantly reduced when the NaCl concentration was increased to 75 mM. These results indicate that AcAlgE2 has a higher optimal NaCl concentration compared to AcAlgE3.

3.2.2 Calcium dependency

Lyase assays of AcAlgE2 and AcAlgE3 were performed at different $CaCl_2$ concentrations (Table 13 in Appendix E: Calculated enzyme activity). The relative lyase activity was plotted as a function of the $CaCl_2$ concentration (Figure 24).

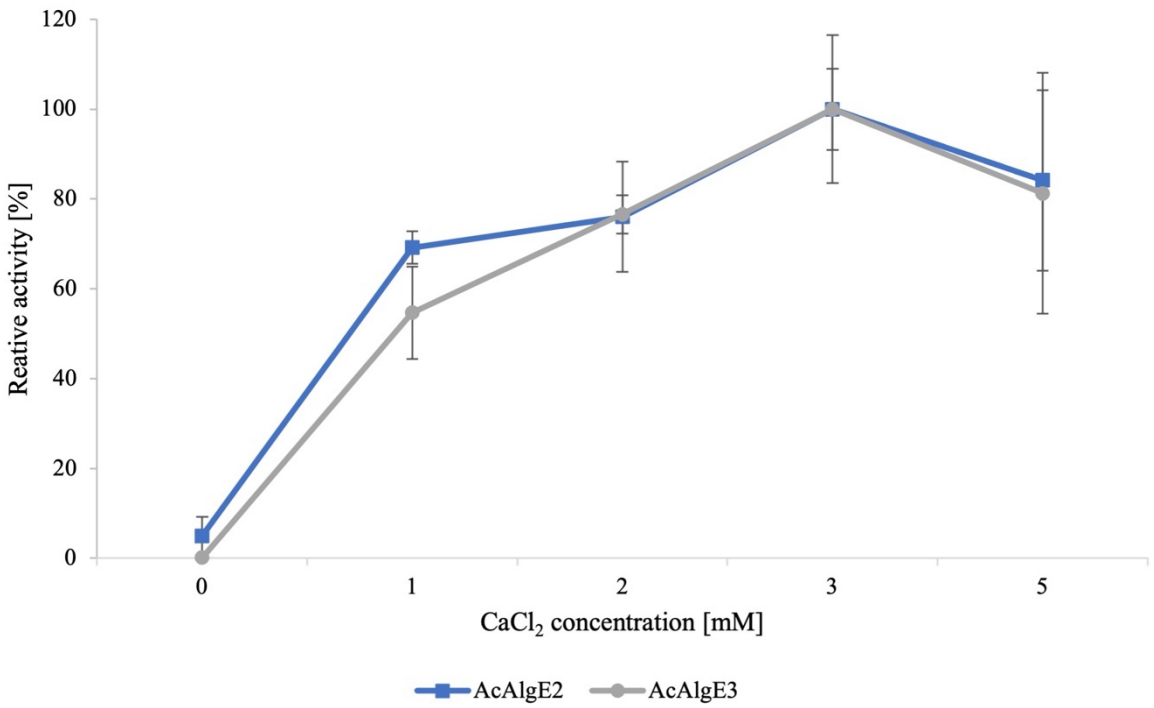

Figure 24: Relative activity of AcAlgE2 and AcAlgE3 at different $CaCl_2$ concentrations**.** For each enzyme, the highest measured activity was set as 100%. The substrate was 1 mM sodium alginate (Sigma V-90) in 50 mM MOPS, pH 6.9, 0 mM NaCl. The given activity is an average based on triplicates. The error bars indicate the standard deviation. It must be noted that there was 2 mM $CaCl_2$ present in the desalted protein samples since calcium is needed for structural stability of the epimerases, thus there was 0.05-0.2 mM $CaCl_2$ present in the 0 mM CaCl2-reactions.

The assay indicated that the enzyme activity of AcAlgE2 and AcAlgE3 was affected by the concentration of calcium. The optimal $CaCl_2$ concentration was 3 mM for both AcAlgE2 and AcAlgE3.

3.2.3 The effect of calcium on NaCl dependency

Next, another lyase assay was performed to test how the concentration of calcium influences the effect of NaCl. Three different $CaCl_2$ concentrations (1, 2 and 3 mM) and four different NaCl concentrations (0, 40, 75 and 150 mM) were used. These concentrations were used because 3 mM $CaCl_2$ and 40mM NaCl was found to be the optimal concentration for both AcAlgE2 and AcAlgE3. The lyase activity of AcAlgE2 and AcAlgE3 was measured (Appendix E: Calculated enzyme activity) and plotted (Figure 25).

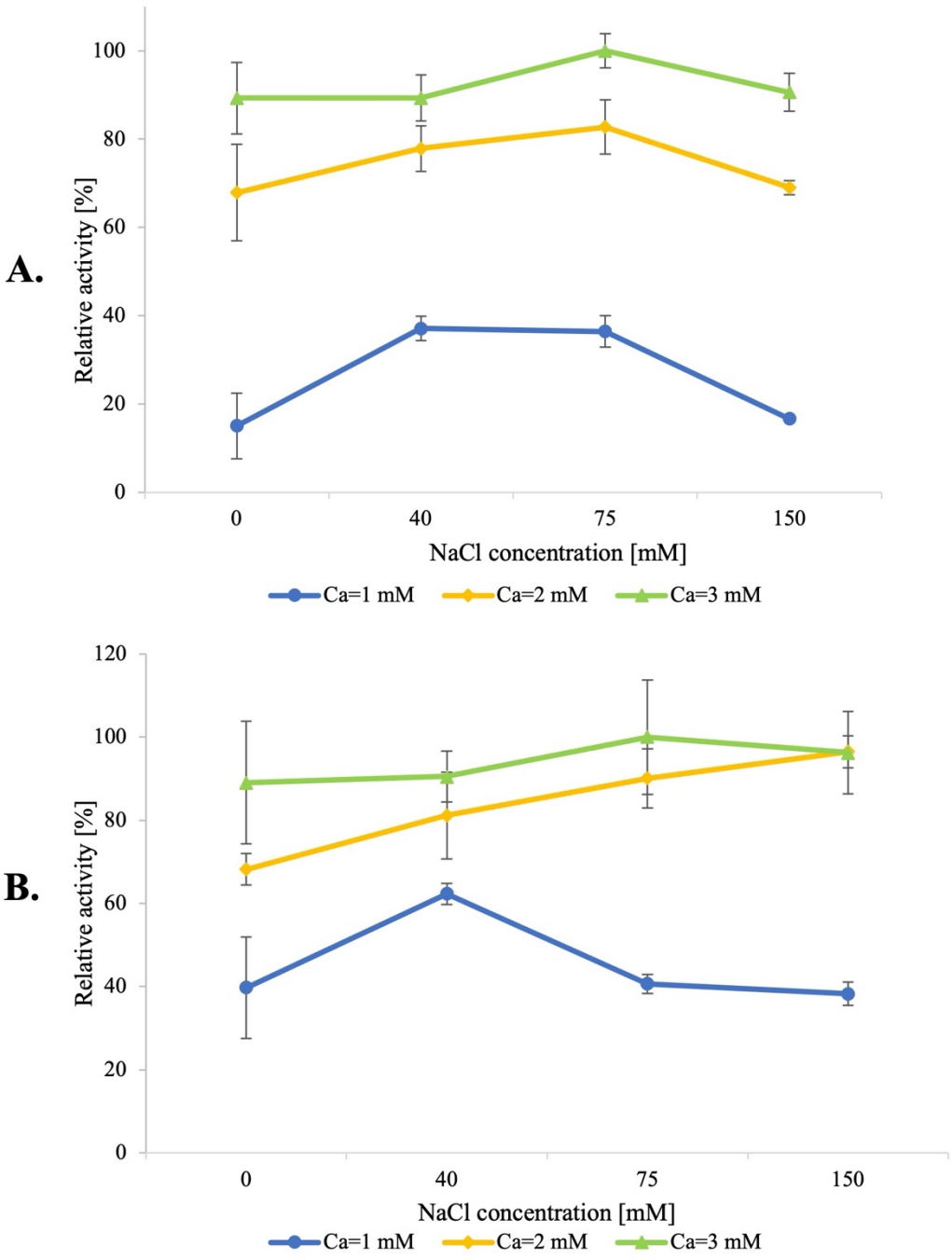

Figure 25: Relative lyase activity of AcAlgE2 **(A)** and AcAlgE3 **(B)** at different NaCl and $CaCl_2$ concentrations. The substrate was 1 mM sodium alginate (Sigma V-90) in 50 mM MOPS, pH 6.9. For each enzyme, the highest measured activity was set as 100%. The results and standard deviation are based on triplicates for all samples. The error bars show the standard deviation.

The enzyme assays indicate that increasing the calcium concentration reduce the negative effect of NaCl on both AcAlgE2 and AcAlgE3. Furthermore, the results also indicate that the optimal NaCl concentration was increased by increasing the calcium concentration.

3.3 Expression and purification of AcAlgE1-3 without His-tags

The His-tags attached to the C-terminal end of AcAlgE1-3 did not bind to the IMAC column and did therefore not contribute to increased purity. For this reason, AcAlgE1, AcAlgE2 and AcAlgE3 were also expressed without tags from the plasmids pAG550, pAG560 and pAG570, respectively (20). The gene expression was regulated by the XylS/P_m regulator/promoter system.

3.3.1 Protein production in *E. coli* RV308

Initially, the proteins were produced in *E. coli* RV308, similar to Gawin et. al (20). AcAlgE1-3 were harvested, sonicated and filtered before initial purification by IEC. The proteins were eluted at 0.37-0.46 M NaCl. The activity of AcAlgE2 and AcAlgE3 was tested with a lyase assay, whereas AcAlgE1 was tested with a coupled epimerase/lyase assay. Finally, crude extracts and the fractions with active enzyme were analysed by SDS-PAGE to check the molecular weight and the purity of the proteins (Figure 26).

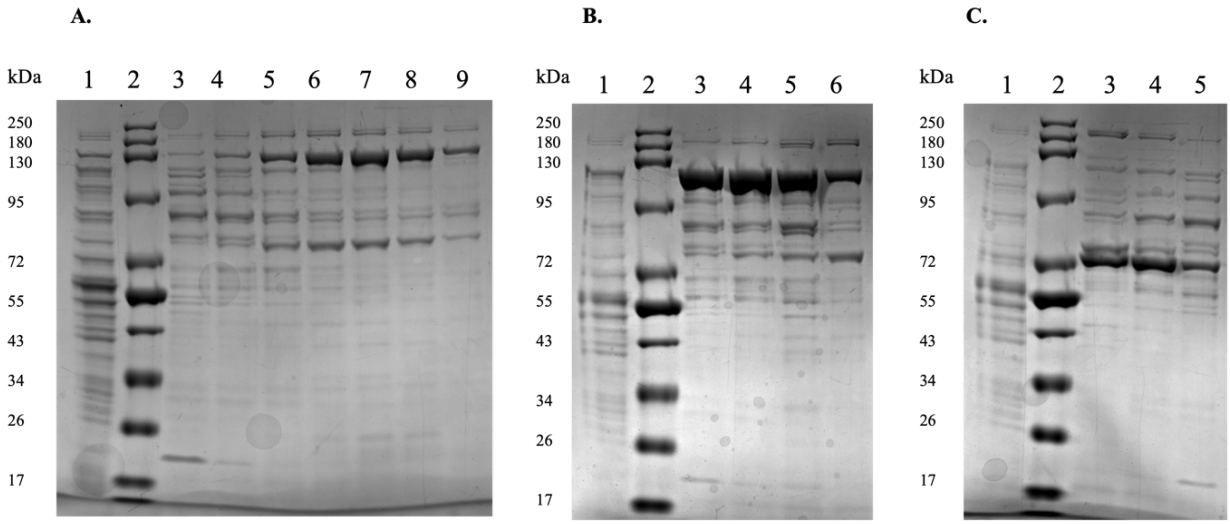

Figure 26: SDS-PAGE analysis of fractions collected during protein purification of AcAlgE1, AcAlgE2 and AcAlgE3. **(A)** AcAlgE1. Lanes: 1) Crude extract. 2) Blue Prestained Protein Standard, Broad Range (NEB). 3-9) Fractions 1B5, 1C1-1C5 and 2A1 after purification by IEC. **(B)** AcAlgE2. Lanes: 1) Crude extract. 2) Blue Prestained Protein Standard, Broad Range (NEB). 3-6) Fractions 1C1, 1C2/1C3, 1C4 and 1C5 after purification by IEC. **(C)** AcAlgE3. Lanes: 1) Crude extract. 2) Blue Prestained Protein Standard, Broad Range (NEB). 3-5) Fractions 1C1-1C3 after purification by IEC.

The SDS-PAGE analysis indicated that AcAlgE1, AcAlgE2 and AcAlgE3 were produced. There was a relatively strong band around 130 kb (Figure 26A), which corresponds to a higher molecular mass larger than expected for AcAlgE1 (104 kDa). The same trend was also found for AcAlgE2 (91 kDa), with a strong band between 95 and 130 kDa, and AcAlgE3 (52 kDa), with a strong band around 72 kDa (Figure 26B and C, respectively). This tendency has been reported for AcAlgE1-3 and other AlgE-type mannuronan C-5-epimerases in previous studies (3, 20). It is therefore reasonable to assume that AcAlgE1-3 were produced, although not in abundance compared to other proteins, which is seen by analysing the crude extracts. Purification by IEC resulted in an increased purity, but there were still impurities in all fractions.

3.3.2 Large scale protein production by fermentation

To obtain large amounts of protein, AcAlgE1-3 were produced in *E. coli* RV308 by fermentation. The cells were harvested when OD_{600} reached 160-180. 4.5-6.3 g cell pellet was dissolved in Buffer A and sonicated. The crude extract was filtered and purified by IEC. The crude extract and the fractions eluted at 0.37-0.45 M NaCl were analysed by SDS-PAGE to investigate the molecular weight and purity of the proteins (Figure 27).

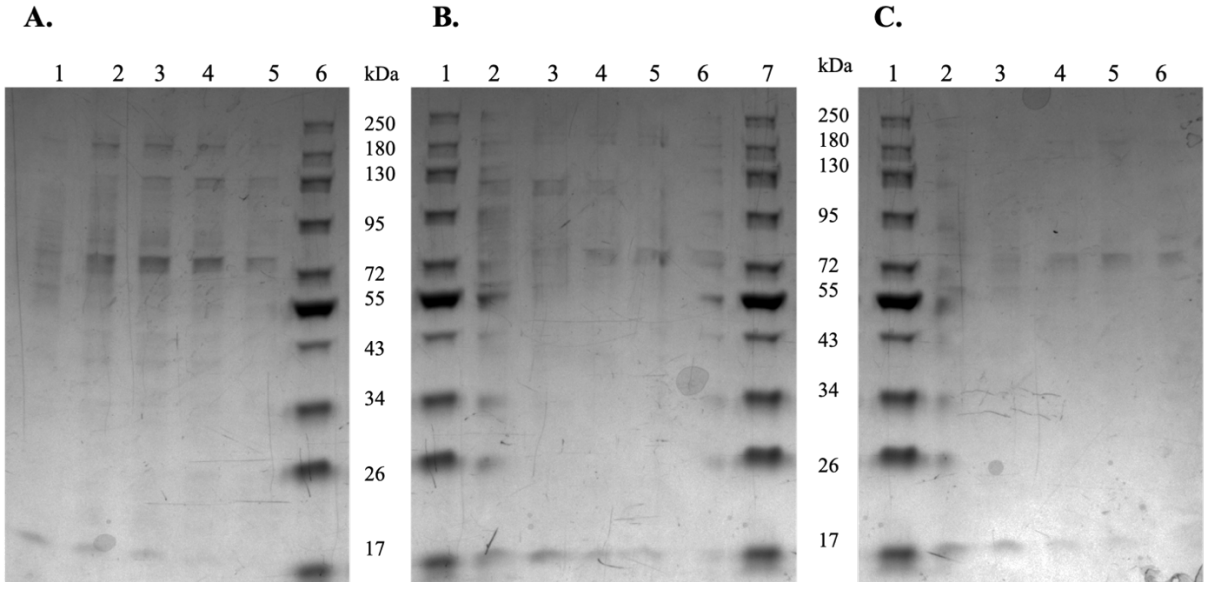

Figure 27: SDS-PAGE analysis of fractions collected during protein purification of AcAlgE1-3. **(A)** AcAlgE1. Lanes: 1-5) Fractions 1C2-1C5 and 2A1 after purification by IEC. 6) Blue Prestained Protein Standard, Broad Range (NEB). **(B)** AcAlgE2. Lanes: 1 and 7) Blue Prestained Protein Standard, Broad Range (NEB). 2-6) Fractions 1C1-1C5 after purification by IEC **(C)** AcAlgE3. Lanes: 1) Blue Prestained Protein Standard, Broad Range (NEB). 2-6) Fractions 1C1-1C5 after purification by IEC.

There was not a significant epimerase production by fermentation. The production was better in flasks (Figure 26) and appeared to be greater when the proteins were expressed in *E. coli* SHuffle T7 Express (Figure 22). The plasmids were therefore transferred to this strain.

3.3.3 Protein production in *E. coli* SHuffle T7 Express

To increase the protein production, *acalgE1, acalgE2 and acalgE3* were expressed in *E. coli* SHuffle T7 Express, using the XylS/P_m regulator/promoter system. AcAlgE1-3 were harvested, sonicated and filtered before initial purification by IEC. The proteins were eluted at 0.37-0.45 M NaCl and analysed by SDS-PAGE (Figure 28).

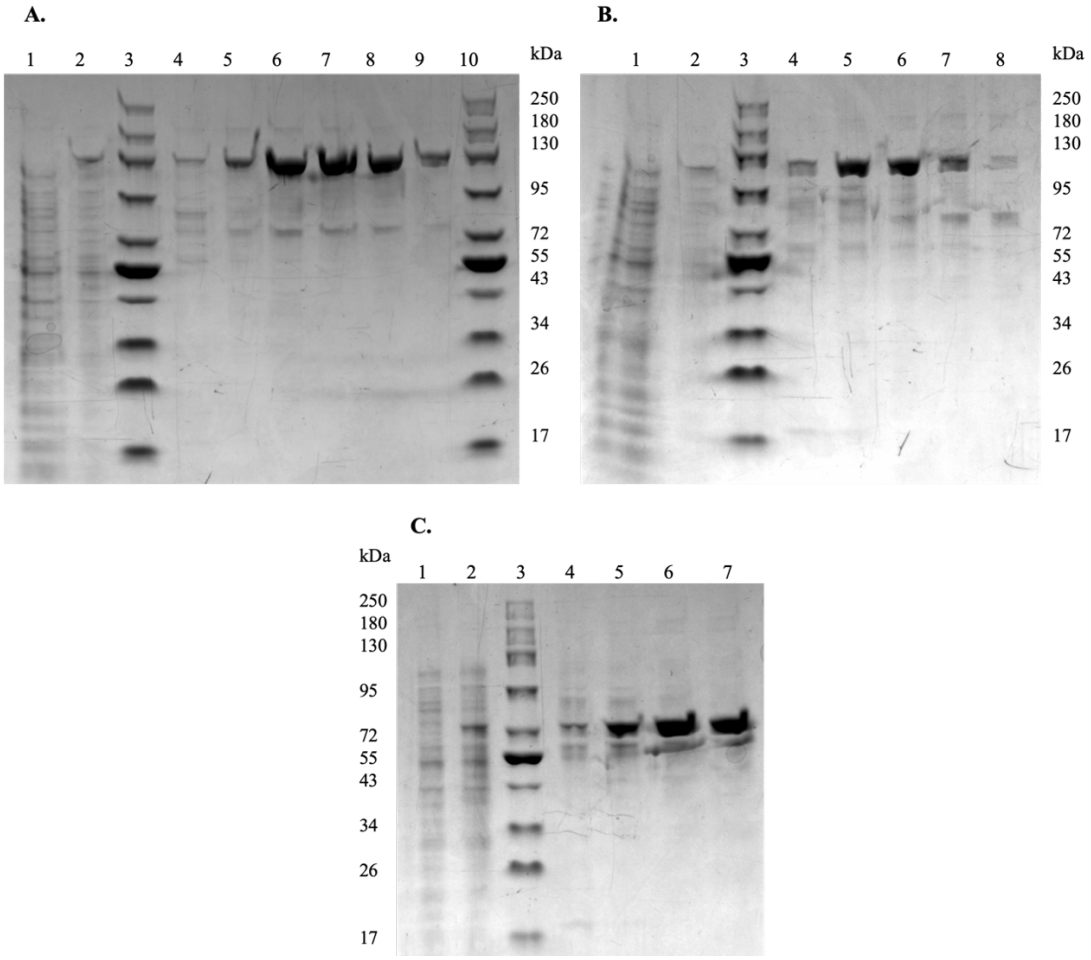

Figure 28: SDS-PAGE analysis of fractions collected during protein purification of AcAlgE1-3. **(A)** AcAlgE1. Lanes: 1) Uninduced protein sample. 2) Crude extract. 3 and 10) Blue Prestained Protein Standard, Broad Range (NEB). 4-9) Fractions 1C1-1C5 and 2A1 after purification by IEC. **(B)** AcAlgE2. Lanes: 1) Uninduced protein sample. 2) Crude extract. 3) Blue Prestained Protein Standard, Broad Range (NEB). 4-8) Fractions 1B5 and 1C1-1C4 after purification by IEC. **(C)** AcAlgE3. Lanes: 1) Uninduced protein sample. 2) Crude extract. 3) Blue Prestained Protein Standard, Broad Range (NEB). 4-9) Fractions 1B5 and 1C1-1C3 after purification by IEC.

The SDS-PAGE analysis indicated that the protein production was improved by changing the bacterial strain. Fractions 1C1-1C5 and 2A1 with AcAlgE1 were pooled. As was fractions 1C1-1C3 with AcAlgE2 and fractions 1C1-1C3 with AcAlgE3. The proteins were purified further by SEC. Interesting fractions were analysed by SDS-PAGE (Figure 29).

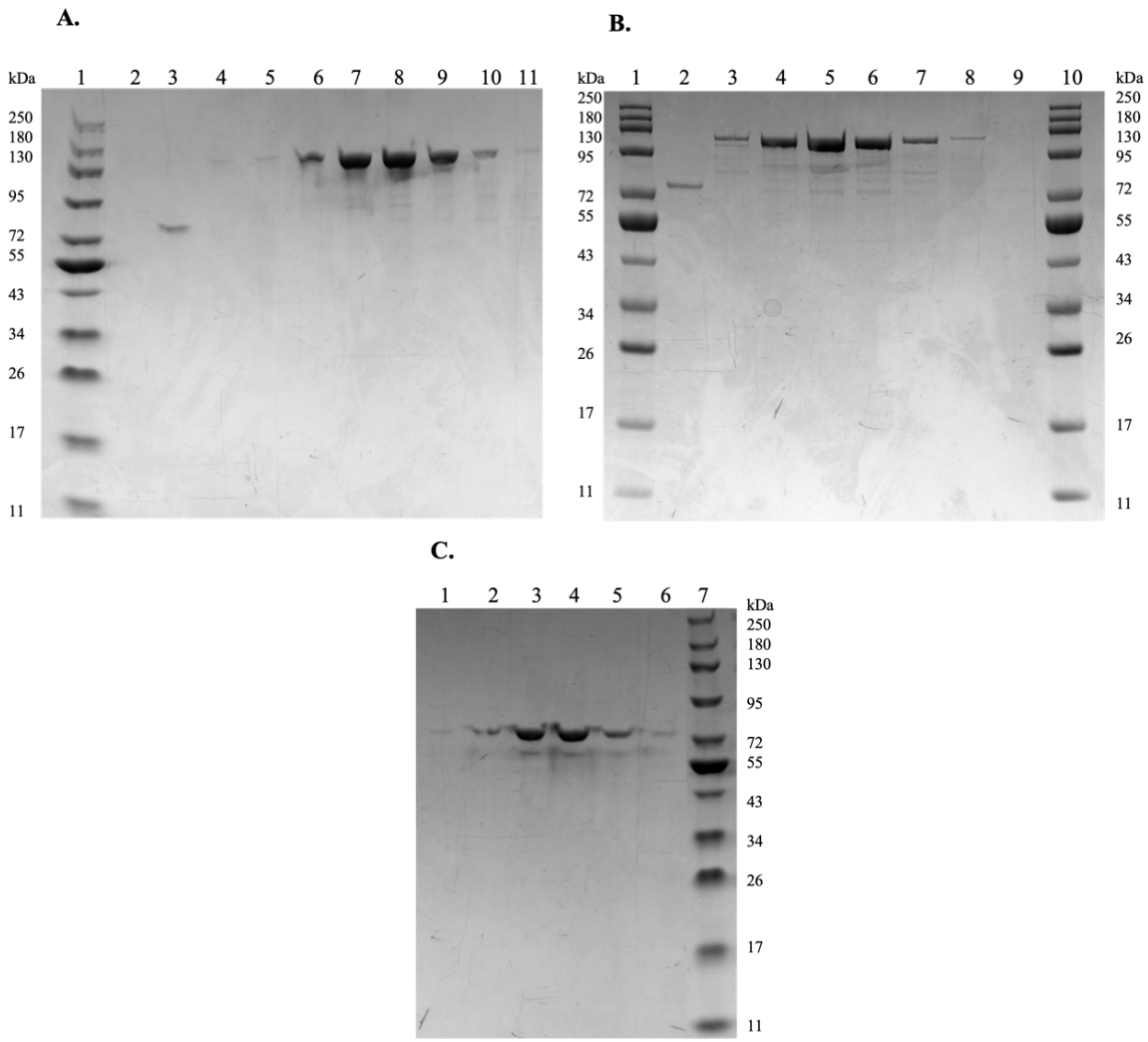

Figure 29: SDS-PAGE analysis of fractions collected during protein purification of AcAlgE1-3. The proteins were purified by IEC and SEC. **(A)** AcAlgE1. Lanes: 1) Blue Prestained Protein Standard, Broad Range (NEB). 2-11) Fractions 1B1, 1C1, 2A2, 2B1-2B5 and 2C1 after purification by SEC. **(B)** AcAlgE2. Lanes: 1 and 10) Blue Prestained Protein Standard, Broad Range (NEB). 2-9) Fractions 2A4, 2C3-2C5, 1A1, 3A2, 3A3 and 5B1 after purification by SEC. **(C)** AcAlgE3. Lanes: 1-6) Fractions 2A3-2A5 and 2B1-2B3 after purification by SEC. 7) Blue Prestained Protein Standard, Broad Range (NEB).

Based on the results from SDS-PAGE (Figure 29), the proteins were relatively pure, and were considered suitable to be used further in studies of enzyme kinetics and for NMR-spectroscopy. First, the final protein concentrations was measured (Table 8).

Table 8: Protein concentrations of pooled fractions of AcAlgE1-3 after purification by SEC.[2]

Enzyme	Fractions	Protein concentration [mg/ml]	Total amount of protein [mg]
AcAlgE1	2B2, 2B3, 2B4	0.462	6.93
AcAlgE2	2C4, 2C5, 3A1	0.184	2.76
AcAlgE3	2A5, 2B1	0.230	2.30

3.4 Enzyme kinetics of AcAlgE2 and AcAlgE3

AcAlgE2 and AcAlgE3 are bifunctional mannuronan C-5-epimerases and alginate lyases. To get an understanding of the activity of these enzymes, it is interesting to study and compare their enzyme kinetics. For this purpose, the lyase activity of AcAlgE2 and AcAlgE3 was measured at different substrate concentrations. The enzymes were working on sodium alginate (Sigma V-90) in 50 mM MOPS, pH 6.9, 1.5 mM $CaCl_2$, 25 mM NaCl. ΔAbs_{230} was measured for 20 min, and V_0 was found for each substrate concentration according to the equations in Section 2.21.4. V_0 was plotted as a function of [S] in Figure 30.

[2] The concentration was measured with NanoDrop at 280 nm. The concentration of AcAlgE1 was measured for a molecular weight (Mw) of 103.6 kDa and an extinction coefficient (ε_M) of 68 650 $M^{-1}cm^{-1}$. The concentration of AcAlgE2 was measured for a Mw of 90.60 kDa and an ε_M of 57.19 $M^{-1}cm^{-1}$. The concentration of AcAlgE3 was measured for a Mw of 51.60 kDa and an ε_M of 33.81 $M^{-1}cm^{-1}$.

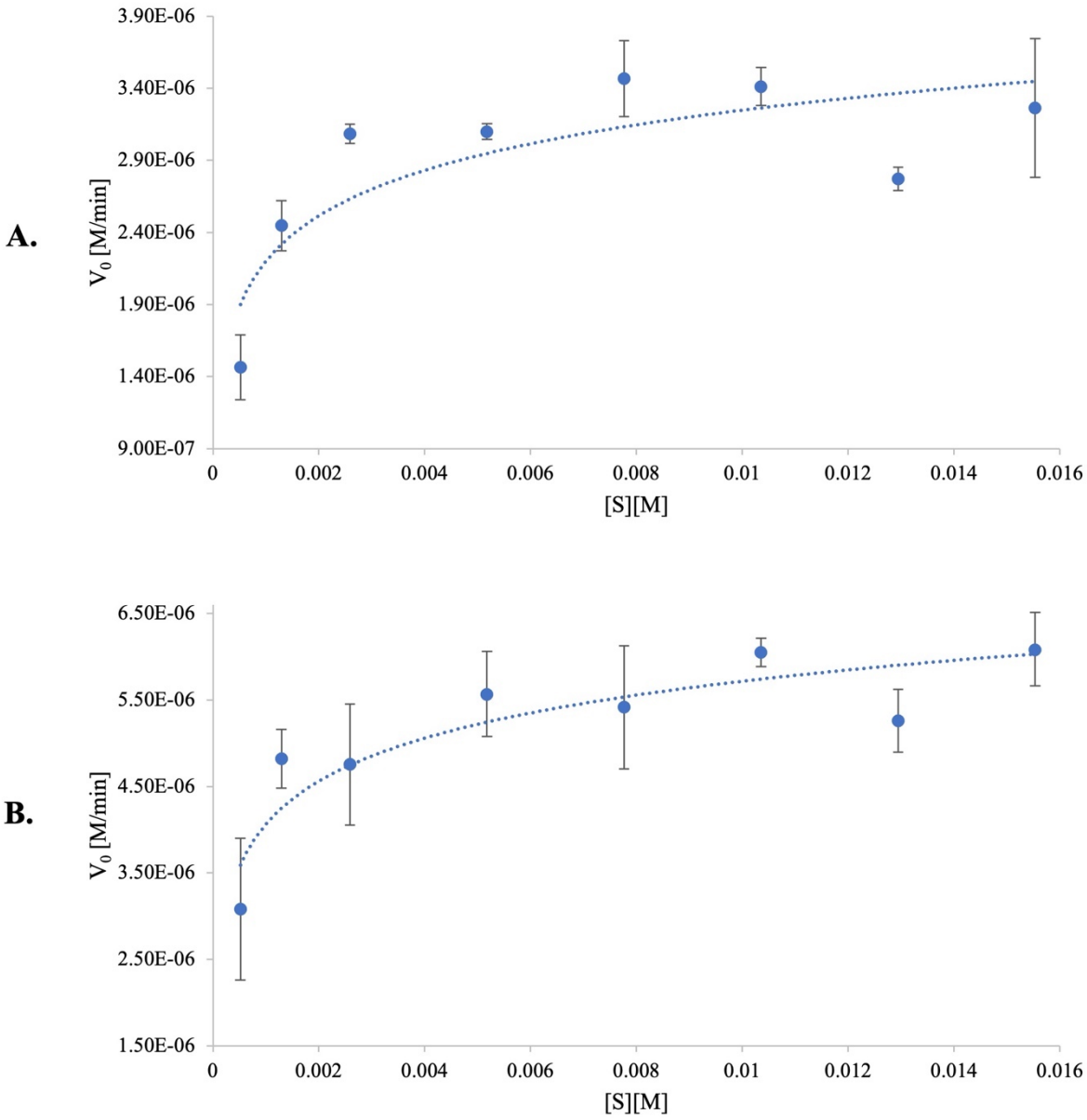

Figure 30: Michaelis-Menten plot of the lyase activity of AcAlgE2 (A) and AcAlgE3 (B). The initial turnover rate of the enzymes (V_0) measured in M/min is plotted as a function of the substrate concentration [S] measured in M. (V_0) is estimated from lyase assays at different [S].

The activity of both AcAlgE2 and AcAlgE3 increased along with the substrate concentration and showed a tendency of approaching a maximum level. The inverse velocity was plotted as a function of the inverse of the substrate concentration in a Lineweaver Burk-plot (Appendix F: Lineweaver Burk-plot). A linear regression was fitted in Excel to estimate V_{max}, K_m and k_{cat}, resulting in the trendlines $y = 198x + 2.83 \times 10^5$ and $y = 78.3x + 1.67 \times 10^5$ for AcAlgE2 and AcAlgE3 respectively. V_{max}, K_m and k_{cat} were estimated (Table 9) according to the equations in Section 2.21.4.

Table 9: Enzyme kinetics of AcAlgE2 and AcAlgE3.

Enzyme	V_{max} [min^{-1}]	K_m [M]	k_{cat} [min^{-1}]
AcAlgE2	3.53 x 10^{-6}	7.01 x 10^{-4}	1.74
AcAlgE3	5.97 x 10^{-6}	4.67 x 10^{-4}	1.34

3.5 Comparison of AcAlgE1 and AvAlgE1

3.5.1 Mode of action on mannuronan over time of AcAlgE1 and AlgE1

To elucidate the epimerization pattern of AcAlgE1, the mode of action of AcAlgE1 and AlgE1 on mannuronan was studied and compared. AlgE1 is an epimerase with two A-modules; A_1 which catalyse production of G-blocks and A_2 which introduce single G residues (96). AcAlgE1 has one A-module, homologous to AlgE1A_2, and has been shown to introduce a high G-content (20). The mode of action on ^{13}C1-labled mannuronan was studied using time-resolved ^{13}C-NMR spectroscopy. Firstly, the purified AcAlgE1 sample was up concentrated to 4.7 mg/ml. A sample of AlgE1 with similar molar concentration was also prepared for time-resolve NMR-spectroscopy (Figure 31).

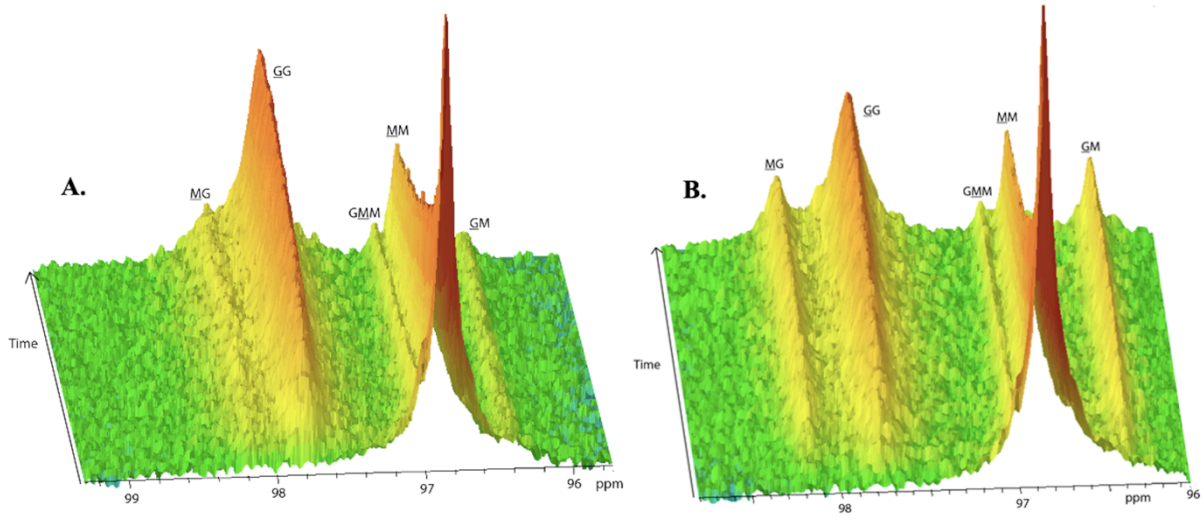

Figure 31: Time-resolved ^{13}C-NMR-spectra (800 mHz) of 5 µM AcAlgE1 (A) and AlgE1 (B) working on 9 mg/ml ^{13}C1-labeled mannuronan in 5 mM MOPS pH 6.9, 2,5 mM $CaCl_2$, 75 mM NaCl in 99.9% D_2O. The reaction was measured every 10 min for 16 hours.

The time- resolved ^{13}C-NMR-specra (Figure 31) were integrated (Figure 32).

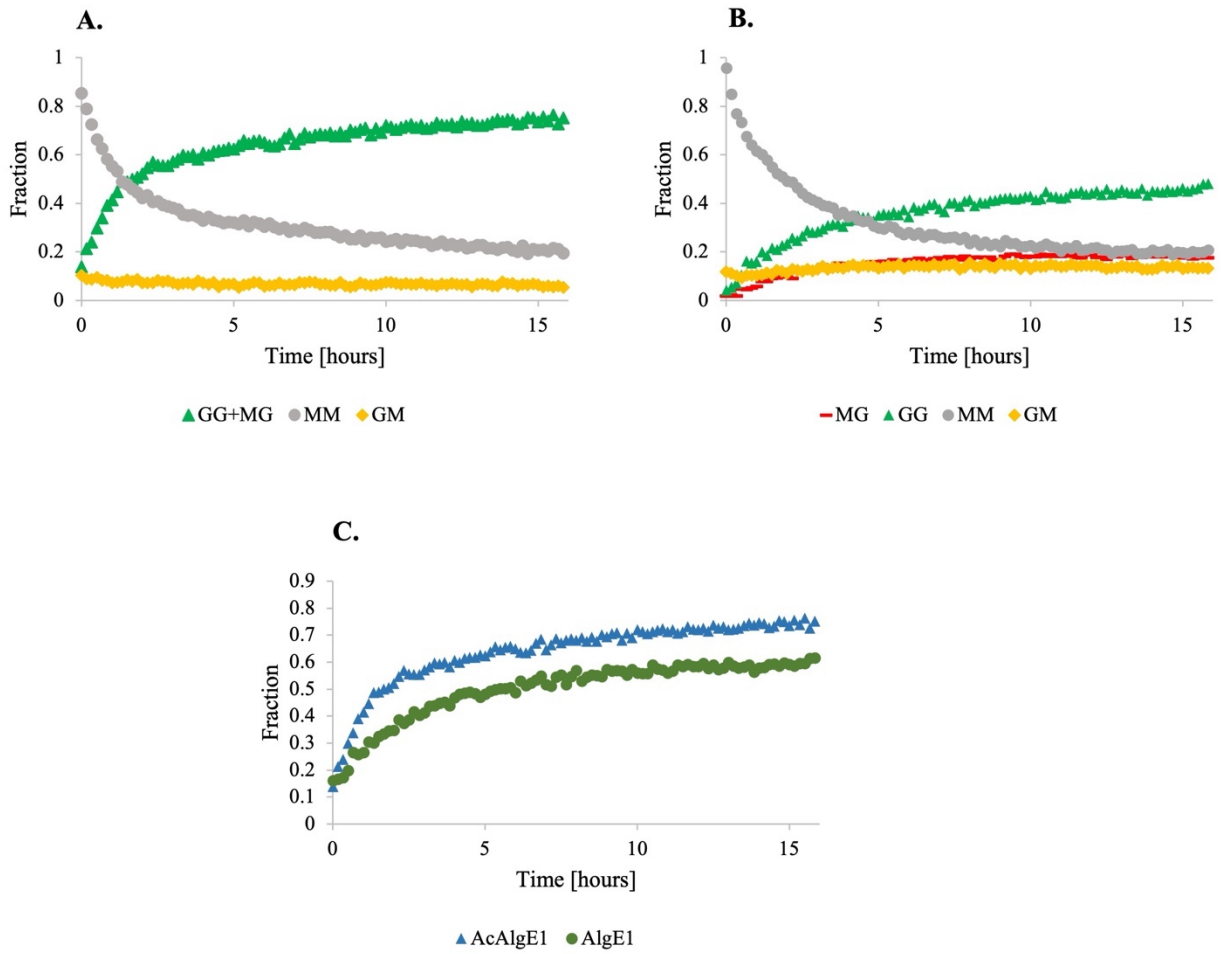

Figure 32: Integrated peaks from ^{13}C-NMR peaks every 10 min for 16 hours. The integrals are converted to fraction of each block-type. 5 µM AcAlgE1 (A) and AlgE1 (B) were working on 9 mg/ml ^{13}C1-labeled mannuronan in 5 mM MOPS pH 6.9, 2,5 mM $CaCl_2$, 75 mM NaCl in 99.9% D_2O. The MG- and GG-signals for AcAlgE1 could not be integrated separately and are therefore shown combined. (C) The MG+GG signal for AcAlgE1 and AlgE1.

The integrated peaks indicate that both AlgE1 and AcAlgE1 introduce a high degree of G residues. There was a strong increase in GG+MG-signal the first two hours when AcAlgE1 was working on mannuronan (Figure 32A). The increase was steeper and higher for AcAlgE1 compared to AlgE1 (Figure 32C), indicating that AcAlgE1 epimerize at a higher rate and produce a higher G-content than AlgE1.

3.5.2 Sequential parameters of AcAlgE1 and AlgE1

High molecular weight mannuronan was epimerized by AcAlgE1 and AlgE1. Samples were taken after 24 and 48 hours, and the alginate was analysed by endpoint ^{1}H-NMR (Figure 33).

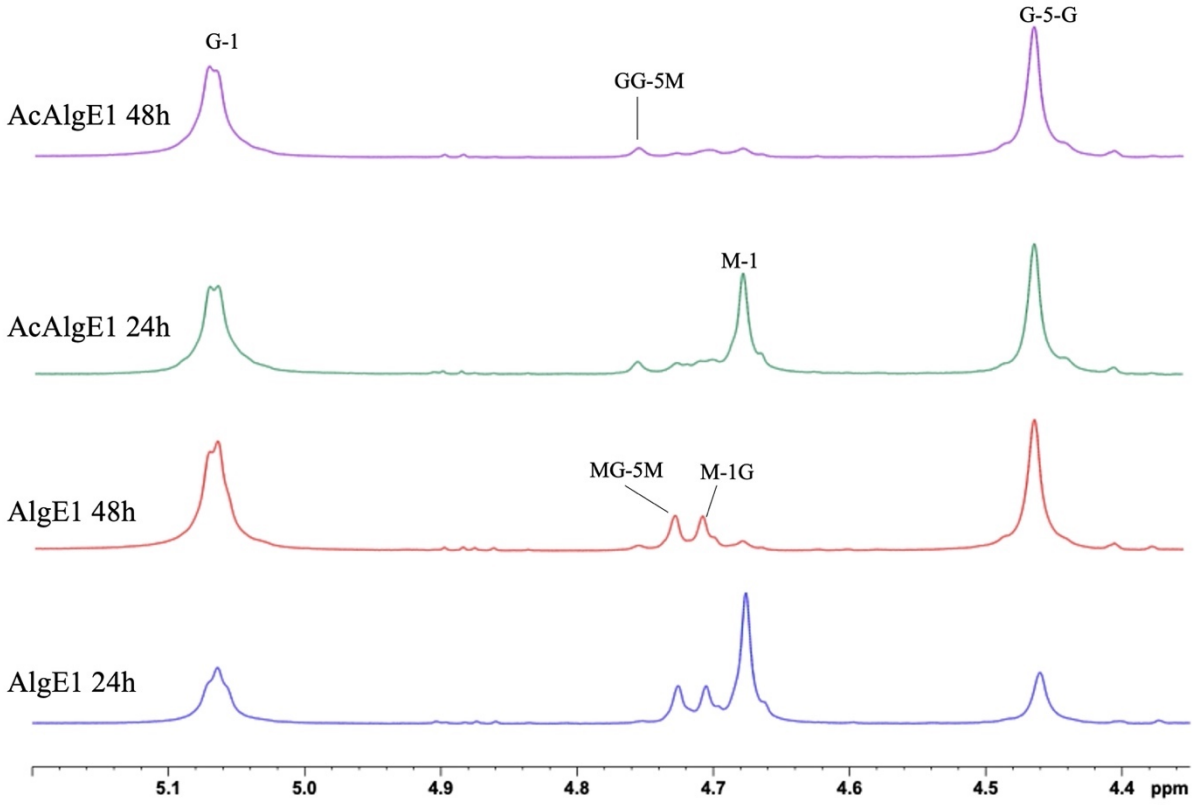

Figure 33: ^{1}H-NMR spectra after epimerization of long chain mannuronan. 0.9 µM AcAlgE1 and AlgE1 were working on 5 mg/ml long chained mannuronan in 5 mM MOPS pH 6.9, 2,5 mM $CaCl_2$, 75 mM NaCl in 99.9% D_2O for 24 and 48 hours. The G-1, GG-5M, G-5-G, M-1, MG-5M and M-1G signals are indicated in the spectra.

The spectra clearly show that both AcAlgE1 and AlgE1 produce a product with high G-content, especially after 48 hours. It was also found that AlgE1 produce more MG-blocks than AcAlgE1.

The signals were integrated, and the sequential parameters were calculated (Table 10) according to Appendix C: Calculation of sequential parameters.

Table 10: Sequential parameters of alginate epimerized by AlgE1 and AcAlgE1.[3]

Sample	F_G	F_M	F_{GG}	$F_{GM/MG}$	F_{MM}	$F_{GGM/MGG}$	F_{MGM}	F_{GGG}	$N_{G>1}$
AlgE1 24h	0.39	0.61	0.25	0.13	0.48	0.01	0.12	0.24	26
AlgE1 48h	0.83	0.17	0.71	0.12	0.05	0.02	0.11	0.65	43
AcAlgE1 24h	0.59	0.41	0.52	0.07	0.34	0.03	0.04	0.47	16
AcAlgE1 48h	0.89	0.11	0.83	0.06	0.06	0.04	0.02	0.76	23

It was found that AcAlgE1 introduce a higher degree of G residues than AlgE1, but the average G-block was longer with AlgE1.

3.6 Optimalization of the epimerase assay

A coupled epimerase/lyase assay has been used in several studies to measure epimerase activity (20, 85, 97). This method is an endpoint analysis, and the epimerase reaction may have stopped any time during the incubation. Fractions with AlgE6, AlgE6-Ca and AlgE6-G148R/L172K were tested with this epimerase assay, and activity was successfully observed for all enzymes. However, ΔAbs_{230} was very similar for all enzymes (3.5, 3.5 and 3.6) and it was consequently not possible to use this assay to compare activity. Therefore, the coupled epimerase/lyase assay was optimized to achieve a quantitative assay. This was done by adding the G-specific lyase and the epimerase enzyme solution simultaneously before measuring ΔAbs_{230}. A challenge with this approach was that the epimerases and lyase have different optimal NaCl-concentrations. The G-specific lyase was originally working at 200 mM NaCl, whereas the epimerase reactions in this project were performed at lower concentrations, typically 75 mM NaCl. For this reason, the activity of the G-specific lyase was tested at both 200 and 75 mM NaCl (Figure 34).

[3] 0.9 µM AcAlgE1 and AlgE1 were working on 5 mg/ml mannuronan in 5 mM MOPS pH 6.9, 2,5 mM $CaCl_2$, 75 mM NaCl in 99.9% D_2O for 24 and 48 hours. F_G denotes the fraction of G. F_M denotes the fraction of M. The fraction of different diads is indicated with two letters, and the fraction of the different triads are denoted with three letters. $N_{G>1}$ is the calculated average G-block length.

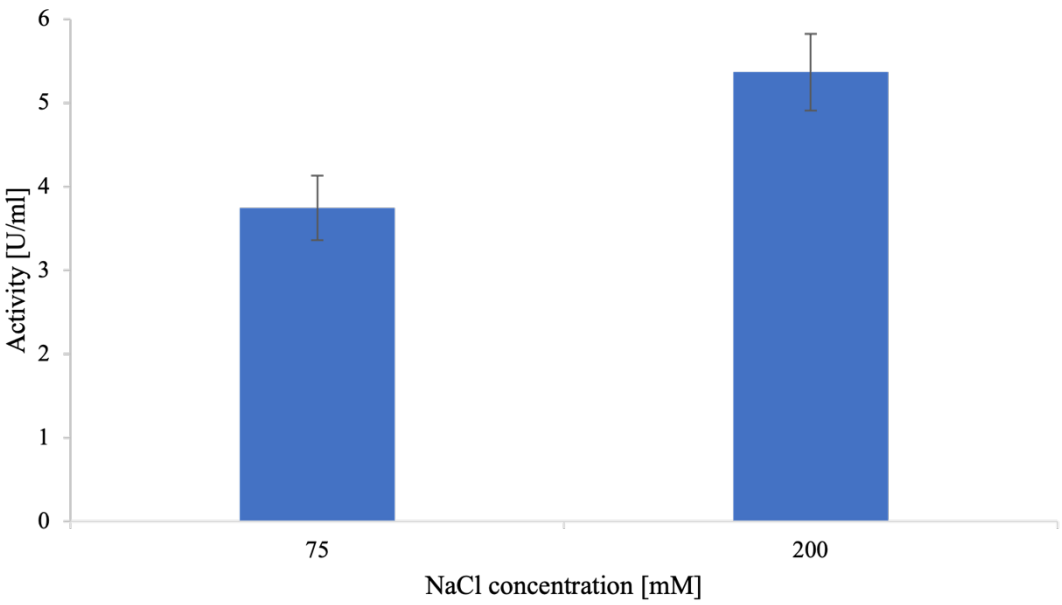

Figure 34: Activity of a G-specific lyase working on sodium alginate (Sigma V-90) at two different NaCl-concentrations in 50 mM MOPS, pH 6.9, 1.5 mM $CaCl_2$.

It was found that the activity of the G-specific lyase was highest at 200 mM NaCl with 5.4 ± 0.21 U/ml compared to 3.7 ± 0.17 U/ml at 75 mM NaCl. Lowering the NaCl-concentration reduced the activity by 31%, but it was still sufficient, and this concentration was therefore used as a compromise between the epimerase and lyase.

AlgE6 was used to test the optimized epimerase assay. The protein was encoded by pSTS1 and was produced in *E. coli* SHuffle T7 Express using the LacI/P_{T7}*lac* regulator/promoter system. AlgE6 was partially purified by IEC, giving a protein concentration of 2.6 mg/ml, assuming a pure protein sample. Finally, the activity of AlgE6 was tested using the optimized epimerase assay (Figure 35).

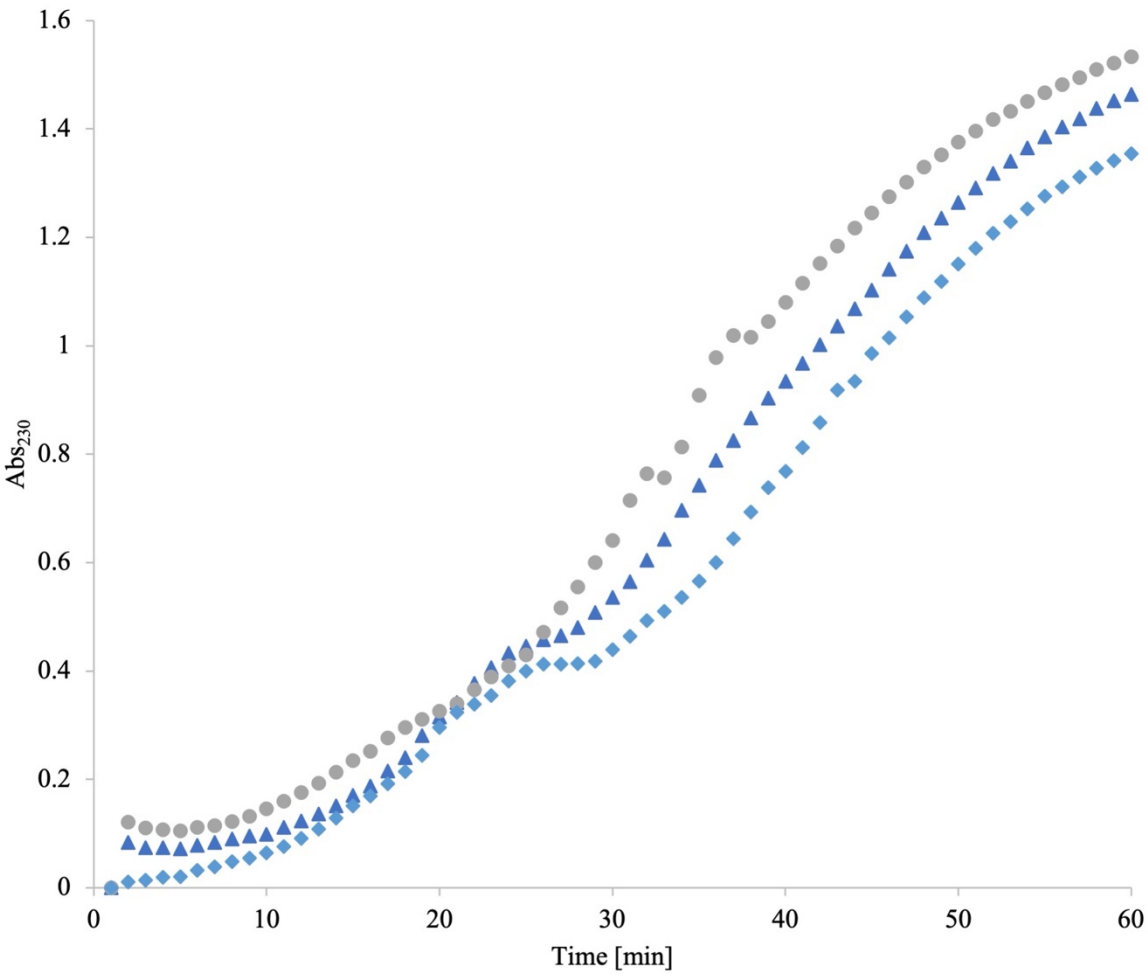

Figure 35: Abs_{230} during an optimized epimerase assay of partially purified AlgE6. The reaction mix contained 1 mg/ml mannuronan, 50 mM MOPS buffer with 75 mM NaCl and 1.5 mM $CaCl_2$, to which 8 µl G-specific lyase and 8 µl enzyme sample was added. Abs_{230} was measured every min for an hour. Three parallels were measured and are indicated with different symbols.

The increase in absorbance was not linear throughout the entire time-period, but the trend was generally the same for all triplicates. A relatively linear area of the graph with similar slope for all three parallels was seen from 30-45 min. Based on ΔAbs_{230} during this time-period, the average activity was 2.178 ± 0.06 U/ml. Assuming a pure protein sample, the average enzyme activity of AlgE6 was $7.49 \times 10^7 \pm 2.03 \times 10^6$ U/mole.

3.7 Evaluation of AlgE6/AlgE7 hybrids

In a previous study, several AlgE6/AlgE7 hybrids were constructed (56). One of them was an *algE6-G148R/L172K* double mutant with two point-mutations in the A-module of AlgE6. Two amino acids from AlgE6 were replaced by the amino acids at the same position of the A-modules of AlgE7. By sequence alignment of AlgE1-7 and AcAlgE1-3, it was found that the amino acids at position 148 and 172 are conserved as Gly148 and Leu172 in epimerases and as Arg148 and Lys172 in lyases (20).

Additionally, *algE6-Ca* was constructed by introducing a sequence from *algE7* (56). The first 136 amino acids in the A-module of AlgE6 were replaced by the first 136 amino acids in the A-module of AlgE7. The sequence was a proposed calcium binding site and was positioned by several lyase specific residues (56).

AlgE6-G148R/L172K showed indication of lyase activity in the previous study (56). The results were inconclusive, and this mutant was therefore tested again. AlgE6-Ca was also tested again for lyase activity.

3.7.1 Expression of wild type AlgE6 and two AlgE6 mutants

algE6, *algE6-G148R/L172K* and *algE6-Ca* were expressed in *E. coli* SHuffle T7 Express using the plasmids pSTS1, pSTS5 and pSTS10 respectively. The proteins were partially purified by IEC and eluted at 0.27-0.37 M NaCl. The purity and molecular weight of the proteins were analysed by SDS-PAGE (Figure 36).

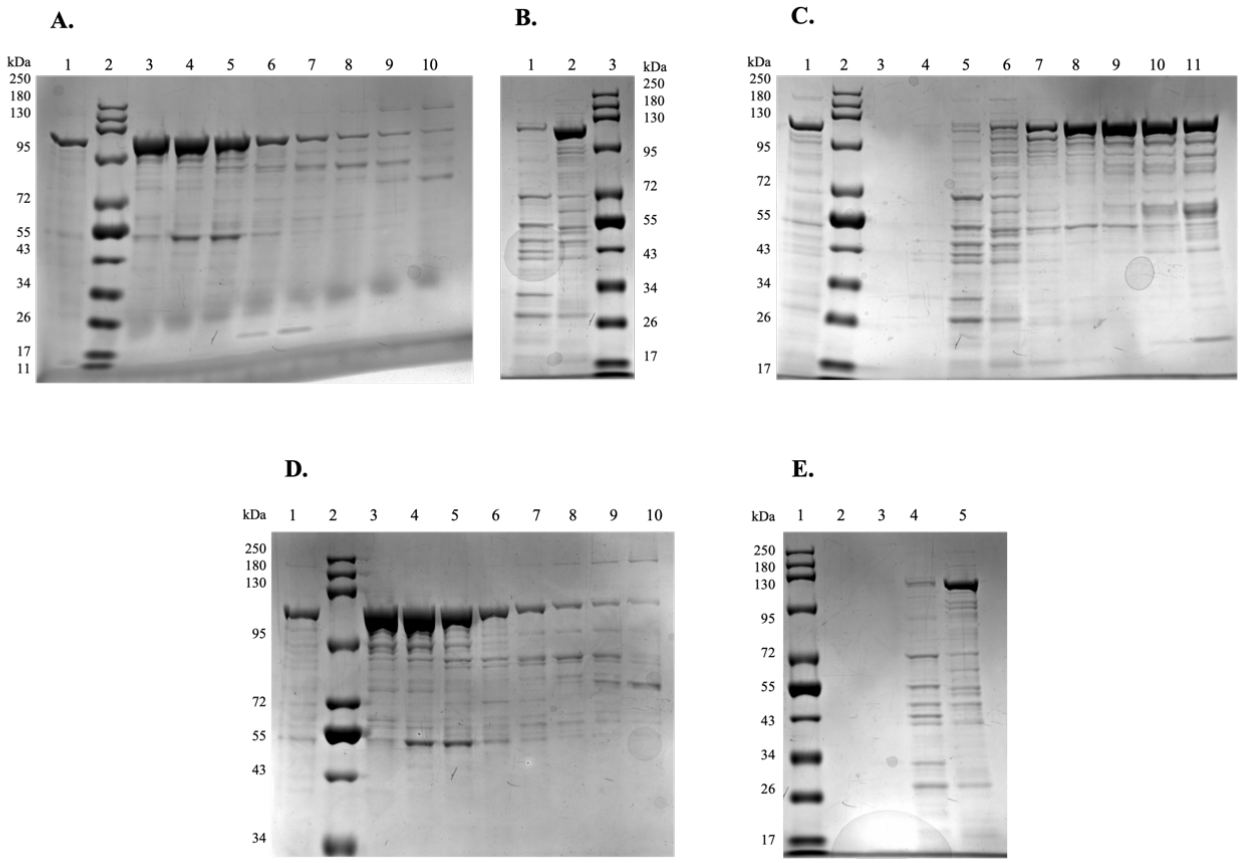

Figure 36: SDS-PAGE analysis of fractions collected during protein purification of AlgE6, AlgE6-G148R/L172K and AlgE6-Ca by IEC. **(A)** AlgE6. Lanes: 1) Crude extract. 2) Blue Prestained Protein Standard, Broad Range (NEB). 3-10) Fractions 1B1-1B5 and 1C1-1C3 after purification by IEC. **(B)** AlgE6. Lanes: 1-2) Fractions 1A4 and 1A5. 3) Blue Prestained Protein Standard, Broad Range (NEB). **C)** AlgE6-Ca. Lanes: 1) Crude extract. 2) Blue Prestained Protein Standard, Broad Range (NEB). 3-11) Fractions 1A2,-1A5 and 1B1-1B5. **(D)** AlgE6-G148R/L172K. Lanes: 1) Crude extract. 2) Blue Prestained Protein Standard, Broad Range (NEB). 3-10) Fractions 1B1-1B5 and 1C1-1C3. **E)** AlgE6-G148R/L172K. Lanes: 1) Blue Prestained Protein Standard, Broad Range (NEB). 2-5) Fraction 1A2-1A5.

The SDS-PAGE analysis of AlgE6, AlgE6-G148R/L172K and AlgE6-Ca resulted in a strong band between 95 and 130 kDa. The theoretical molecular weight of AlgE6 is 90 kDa, but because AlgE-type mannuronan C-5-epimerases have been shown to migrate shorter than expected, it is reasonable to assume that AlgE6, AlgE6-G148R/L172K and AlgE6-Ca were produced. The fractions were pooled, and the protein concentration was measured, assuming a pure protein sample (Table 11).

Table 11: Protein concentration of pooled fractions of AlgE6, AlgE6 G148R/L172K and AlgE6-Ca.[4]

Enzyme	Fractions	Protein concentration [mg/ml]	Total amount of protein [mg]
AlgE6	1A5, 1B1, 1B2, 1B3	2.6	52
AlgE6-G148R/L172K	1A5, 1B1, 1B2, 1B3	2.8	56
AlgE6-Ca	1B2, 1B3, 1B4, 1B5	2.3	46

3.7.2 Lyase activity of two AlgE6 mutants

A lyase assay was performed to test if AlgE6-G148R/L172K and AlgE6-Ca exhibited lyase activity (Figure 37).

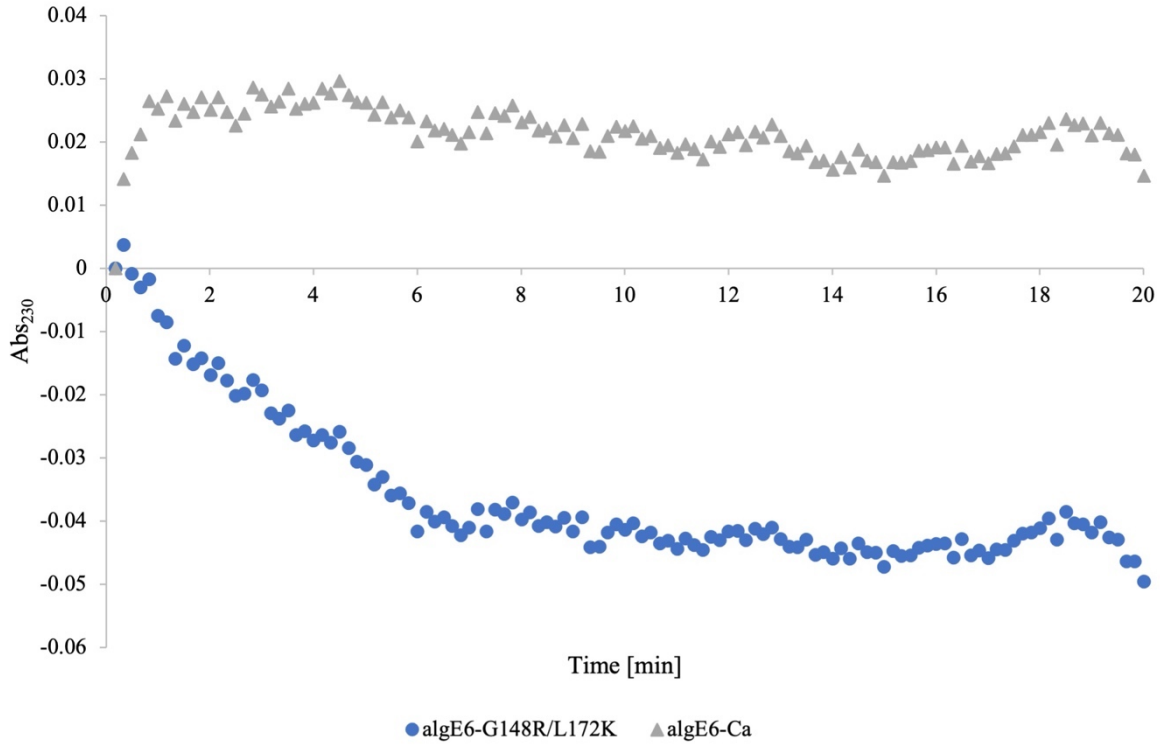

Figure 37: Abs_{230} measured every 10 sec for 20 min. Partially purified AlgE6-G148/L172K and AlgE6-Ca were working on 1 mg/ml sodium alginate (Sigma V-90) in 50 mM MOPS buffer, 75 mM NaCl and 1.5 mM $CaCl_2$. The values are averages of triplicates and are corrected by a blank sample without enzyme.

[4] The concentration was measured with NanoDrop at 280 nm. The concentration was measured for a molecular weight (Mw) of 90.1 kDa and an extinction coefficient (ε_M) of 50 610 $M^{-1}cm^{-1}$ cm.

Neither algE6-G148R/L172K nor algE6-Ca showed any sign of lyase activity.

3.7.3 Calcium dependency of an AlgE6 mutant compared to wild-type AlgE6

The epimerase activity of AlgE6-Ca was compared to AlgE6 at different $CaCl_2$ concentrations to test if introducing the proposed calcium binding site from AlgE7 would affect the calcium dependency of the epimerase. The optimized epimerase assay was used to measure the activity of AlgE6 and AlgE6-Ca at four different Ca^{2+} concentrations (Table 15 in Appendix E: Calculated enzyme activity). The relative activity of AlgE6 and AlgE6-Ca was plotted as a function of calcium concentration in Figure 38.

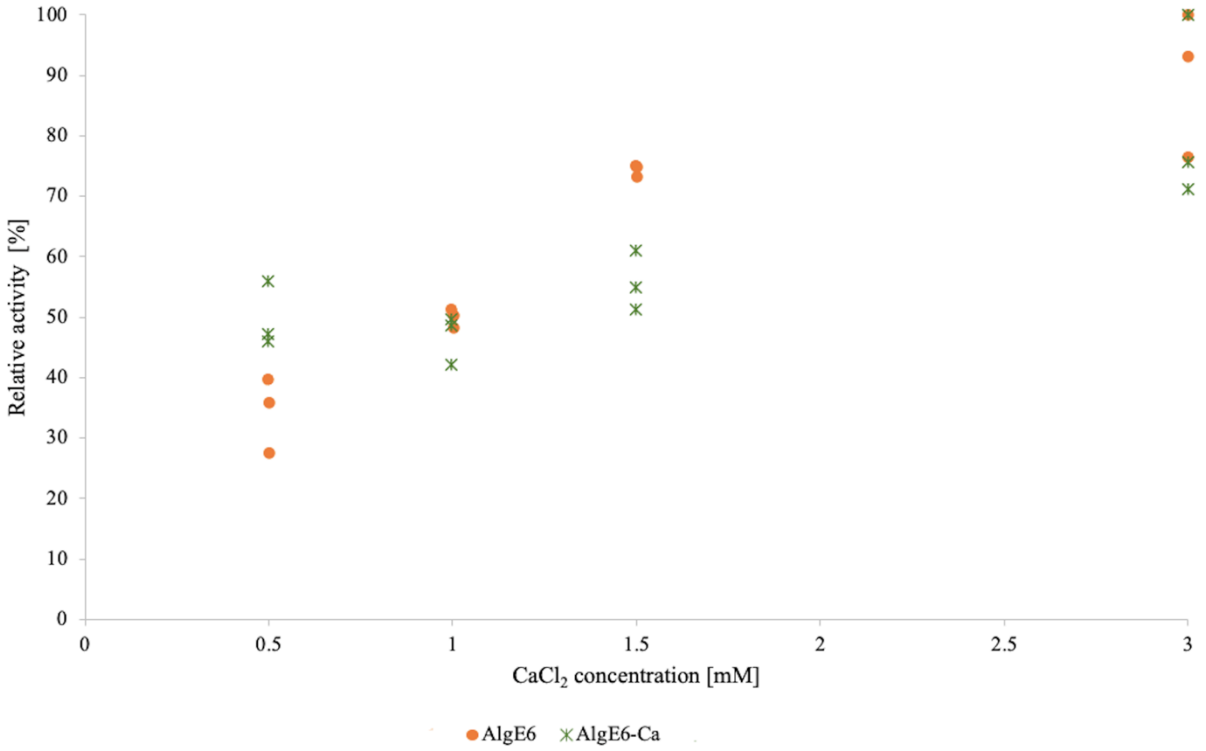

Figure 38: Relative epimerase activity of AlgE6 and AlgE6-Ca at different $CaCl_2$ concentrations, measured by an optimized epimerase assay. The highest measured activity was set as 100% for each enzyme. The substrate was 1 mM mannuronan in 50 mM MOPS, pH 6.9, 75 mM NaCl. The triplicates are shown with the same indicators for each enzyme.

The activity of both AlgE6 and AlgE6-Ca increased with increasing $CaCl_2$ concentration, but the positive effect of Ca^{2+} from 0.5 mM to 1.5 mM $CaCl_2$ was only observed for the wild type.

3.7.4 Construction of an AlgE6 mutant with a calcium binding site from AlgE7

The construction of another AlgE6/AlgE7 hybrid that had been started in an earlier study (56) was continued in this work. Two proposed calcium binding sites from AlgE7 were to replace the amino acid sequences at the same position in AlgE6. Therefore, two fragments from *algE7* were to be inserted within *algE6*. Two PCR products were constructed and named Ca1-3 and Ca1-4 by Sønsteby (56). In this work, these PCR products were cloned into TOPO-vectors and transformed to *E. coli* DH5α. To test if the PCR products had been inserted correctly, the plasmids were digested by restriction enzymes. The gel electrophoresis indicated correct plasmids (Figure 39). The plasmids with the PCR products Ca1-4 and Ca1-3 were named pSTH7 and pSTH8 respectively. The inserts were verified by sequencing (Appendix B: Sequencing of TOPO-vectors).

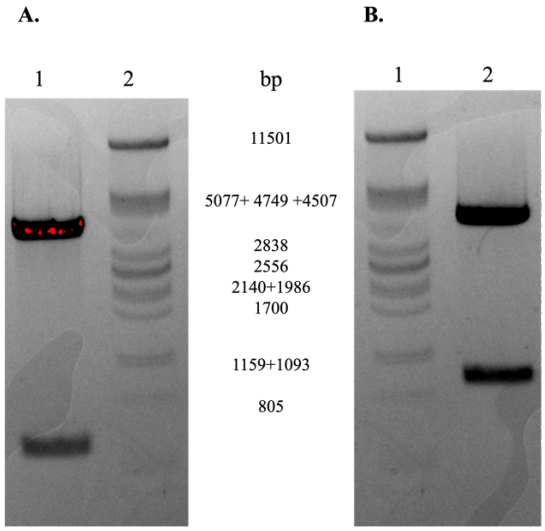

Figure 39: Gel electrophoresis of digested plasmid. **(A)** Lanes: 1) pSTH7, a TOPO-vector with a 526 bp PCR product named Ca1-4 (56). The plasmid was digested by BamHI and PstI. Correct insert would result in the two fragments (3.4 kb and 526 bp). 2) λ-DNA digested by PstI. **(B)** Lanes: 1) λ-DNA digested by PstI. 2) pSTH8, TOPO-vector with a 866 bp PCR product named Ca1-3 (56). The plasmid was digested by BamHI and XhoI. Correct insert would result in the two fragments (3.4 kb and 866 bp).

Ca1-4 and Ca1-3 were used to construct a final fragment containing the two fragments from *algE7* that were to be inserted within *algE6*. This was done by overlap-PCR using the same approach as in a previous study (56). This approach was not successful in this project either and the construction of the mutant was terminated. pSTH7 and pSTH8 were stored at -20ºC for further work. If the construction of this mutant is continued, a different cloning approach should be used.

4 Discussion

In this study, AlgE-type mannuronan C-5-epimerases from *A. chroococcum* and *A. vinelandii* were studied to get a better understanding of the functional characteristics of these enzymes. Firstly, different methods were tested to produce pure and active AlgE epimerases. AcAlgE1 was compared to AlgE1 based on their mode of action on mannuronan. The enzyme kinetics and salt dependency of AcAlgE2 and AcAlgE3 was studied by lyase assays. In addition, two AlgE6 mutants were tested for lyase activity. One of the mutants was compared to wild type AlgE6 at different concentrations of $CaCl_2$. This was done by a coupled epimerase assay, which was optimized and tested in this work.

4.1 Expression and purification approach for AcAlgE1-3

In this project, different methods were tested for purification of AcAlgE1-3. Initially, a C-terminal His-tag was tested for purification by IMAC. This approach was tested because a previously used Intein Mediated Purification resulted in very low enzyme activity (56). In a study of AlgE4, His-tags were successfully used for purification of the A- and R-modules of AlgE4 by IMAC (98). It was therefore reason to believe that this could be a good approach. The proteins were partially purified by IEC before purification by IMAC. Unfortunately, nearly all protein was eluted during sample application. A possible explanation could have been that the initial imidazole concentration was too high, but this is an unlikely explanation since no imidazole was added to the samples and the binding buffer contained only 20 mM imidazole, which is the lowest recommended concentration according to GE Healthcare (53).

The reason why the proteins did not bind could also be inaccessibility of the His-tag to the immobilized metal in the column (52). The protein folding might have led to an occlusion of the tag. The SDS-PAGE analysis indicate that this might be true. When AcAlgE2 and AcAlgE3 with His-tags were analysed, a strong band was seen at the expected sizes (Figure 22). When the same proteins without His-tags were analysed, the bands indicated a larger molecular weight (Figure 29). The reason why epimerases often give rise to bands that correspond to a higher molecular weight than expected could possibly be the elongated shape of the epimerases which make them migrate slower through the polyacrylamide gel than other proteins (99, 100). The epimerases are negatively charged whereas the His-tag is positively charged at pH 6.9, which

was used in this work. It is therefore possible that the positively charged His-tag has folded in towards some of the negatively charged residues of the enzymes. This would lead to a more globular shape, which could be the reason why they migrate faster than epimerases without tags. It is therefore reasonable to assume that protein folding probably led to occlusion of the His-tag.
Nevertheless, the enzymes were still active. It is possible that the His-tag had folded in towards the R-modules, and that the catalytic site in the A-modules was not affected. In a study of AlgE4, the active site of the A-modules was found in a binding groove involved in substrate binding (100). This substrate binding site contain positively charged amino acid residues that are assumed to control the binding of the negatively charged alginate substrate. It is thus more likely that the His-tag has folded in towards other regions of the protein than the active site.

Carrying out the purification at denaturing conditions could possibly resolve the problem with occlusion of the tag, but because the proteins were to be used in enzyme assays it was necessary to keep them active. The denaturation and refolding of the proteins could likely affect the yield and activity of the protein (101, 102), and was therefore not done in this work. In future studies, a different tag should be used instead, preferably without a positive charge. The FLAG-tag, consisting of the amino acid sequence DYKDDDK, could for instance be tested for purification by affinity chromatography.

AcAlgE1-3 with His-tags were expressed using the LacI/P_{T7}*lac* promoter system in *E. coli* SHuffle T7 express. This expression system was selected because it has resulted in high protein expression is a previous study of AcAlgE1, AcAlgE2 and AcAlgE3 (56) as well as for other proteins (43, 103). AcAlgE1-3 were also expressed without tags, since the His-tag did not contribute to increased purification. This was done using the XylS/P_m regulator/promoter system in *E. coli* RV308, which had been used for expression of these enzymes in a recent study (20). It was seen by SDS-PAGE and enzyme assays that the proteins were produced, but that the production appeared to be greater with the LacI/P_{T7}*lac* promoter system in *E. coli* SHuffle T7 express. This was found by cultivation of *E. coli* RV308 both in flaks and by HCDC (Figure 26 and Figure 27, respectively). When the same plasmids were transferred to *E. coli* SHuffle T7 express, an SDS-PAGE analysis indicated that the protein expression was improved (Figure 28). This implies that the protein expression of AcAlgE1-3 was better in *E. coli* SHuffle T7 express than in *E. coli* RV308. A potential reason for this could be that this strain lacks the proteases Lon and OmpT, unlike *E. coli* RV308 (61, 104). It is also possible that the B strain

of *E. coli* is better for protein production than the K-12 strain. It has for instance been found that the B strain has greater capacity for amino acid biosynthesis and fewer proteases (105).

In this work, the enzyme activity was measured in U/mole to compare the enzymes. This is a simplification based on the assumption that the protein samples were pure. Based on the final SDS-PAGE analysis after purification by IEC and SEC, there were still some impurities in the final fractions (Figure 29). The measured activity in U/mole is therefore not accurate. In future studies, the purification should be improved to achieve more accurate measures of the activity.

4.2 Comparison of AcAlgE1 and AlgE1

Time-resolved NMR was used to compare the mode of action of AcAlgE1 and AlgE1 on mannuronan. A high protein purity was needed to reduce noise, and AcAlgE1 was therefore purified by IEC followed by SEC. The GG-signal of the NMR spectra for AcAlgE1 could not be quantified without including the MG-signal because the peaks were overlapping and could therefore not be integrated alone. Nevertheless, it was clear from studying the NMR spectra (Figure 31) that the GG + MG-signal was strongly dominated by GG, thus it was a useful measure of the G-block formation in this work. It was found that AcAlgE1 form G-blocks faster and in a higher degree than AlgE1. AcAlgE1 has also been shown to be an efficient epimerase for G-block formation in other studies (20, 56). Regarding the reaction rates, it was shown in a previous study, that AlgE1-1, the catalytic site which catalyse formation of G-blocks, has a relatively low specific activity, compared to AlgE1-2 and AlgE1, which could be a reason why AlgE1 epimerize at a slower rate than AcAlgE1 (27).

On the other hand, it was found by endpoint NMR that the average G-block was longer with AlgE1 than AcAlgE1 (Table 10). These findings are also supported by a previous study (20). It could be hypothesised that the cooperation of the two catalytic sites of AlgE1 is a factor for production of long G-blocks. The two catalytic domains cooperate in a way that make them contribute approximately equally to epimerization of alginate (27). The epimerase AlgE6 also produce long G-blocks, although not equally long as AlgE1 and with a broader size distribution (21, 106). Analogous to AcAlgE1, AlgE6 only has one A-module, but neither the A-module nor the R-modules of AcAlgE1 show strong sequence homology to AlgE6 (Figure 3). The sequence of AcAlgE1 resembles AlgE2 and AlgE5 more (Figure 3), which both mainly

introduce short G-blocks (21, 23). However, it has been found that AcAlgE1 have a similar epimerization pattern to AlgE6 and produce both higher G content and longer G-blocks than AlgE2 (18, 20, 57, 107). In future studies, it could therefore be interesting to compare AcAlgE1 and AlgE6 and their epimerization pattern and mechanism further.

Accordingly, AcAlgE1 is an effective epimerase, yielding a high G-block content, but AlgE1 remains more effective at forming longer G-blocks. This could result in a stronger gel-formation by AlgE1, compared to AcAlgE1. It has been shown that alginate with the same G-content, but shorter G-blocks, form less stiff hydrogels (107). After epimerization, it was in fact seen visually that the samples with AlgE1 appeared to have a stronger gel formation than the samples with AcAlgE1. The long G-blocks probably lead to the strong gel formation, but it is also possible that MG-blocks have contributed to gel-formation because the junctions between M and G can bind Ca^{2+} similarly. Although the results indicate that AlgE1 form longer G-blocks than AcAlgE1, it is important to note that NMR only gives a statistical distribution of the G and M residues and that $N_{G>1}$ only is an average block length. It is therefore possible that AcAlgE1 also produce some equally long G-blocks as AlgE1.

4.3 Enzyme kinetics of AcAlgE2 and AcAlgE3

To measure enzyme kinetics, a high protein purity was needed, hence the proteins were purified by IEC followed by SEC. AcAlgE1-3 without His-tags were used for this purpose. The Michaelis-Menten constants V_{max}, K_m and k_{cat} were estimated as if classical Michaelis-Menten kinetics did apply, to compare the lyase activity of AcAlgE2 and AcAlgE3.

It was found that AcAlgE2 had a higher K_m than AcAlgE3 (Table 9). These results indicate that AcAlgE3 had a higher substrate affinity than AcAlgE2 and that AcAlgE2 thus need a higher substrate concentration to reach V_{max}. It is possible that the substrate affinity of AcAlgE3 appeared to be higher due to MG-blocks in the substrate, which only AcAlgE3 seem to utilize (20). In this work, it was found that the turnover rate of AcAlgE2 was higher than for AcAlgE3 (Table 9). None of the enzymes were found to have high activity compared to for instance AlgL from *A. vinelandii*, which was found to have a k_{cat} of 63.8 min^{-1} (108).

A problem with the approach that was used to study enzyme kinetics in this project is that the enzymes are bifunctional and are therefore per definition not Michaelis-Menten enzymes (34). The epimerase activity was not taken under consideration during the enzyme assays, where only the lyase activity was measured. Due to epimerization and cleavage of alginate, the substrate also changes throughout the reaction. In a previous study, it was found that poly-M appeared to be the optimal substrate for lyase reaction catalysed by AcAlgE2 and AcAlgE3 (20). It was also found that neither AcAlgE2 nor AcAlgE3 cleave poly G, and that probably only AcAlgE3 cleave MG, which made it impossible to select a substrate that would not be affected by the epimerase activity. Furthermore, the substrate can also be seen as the number of bonds, although this too is a simplification since it is known that maximum every other bond is cleaved. The final products are typically dimers, trimers, tetramers or pentamers (6). Due to the bifunctionality of AcAlgE2 and AcAlgE3 and the modification of the substrate throughout the reaction, the estimation of V_{max}, K_m and k_{cat} is only a simplification. More research is thus needed to understand the enzyme kinetics of AcAlgE2 and AcAlgE3. It remains a challenge to measure the activity of the bifunctional mannuronan C-5-epimerases and alginate lyases.

4.4 Salt dependency of AcAlgE2 and AcAlgE3

AcAlgE2 and AcAlgE3 are Ca^{2+}-dependent mannuronan C-5-epimerases. In this work, it was found that the lyase activity increased with increasing calcium concentration and that the optimal concentration was 3 mM $CaCl_2$ for both AcAlgE2 and AcAlgE3 (Figure 24). Increasing the concentration further to 5 mM $CaCl_2$ reduced the activity. These results are in accordance with the results of similar studies, where it was found that Ca^{2+} enhanced the activity of AcAlgE2 and AcAlgE3 (20).

It was found that 40 mM NaCl was the optimal concentration for both AcAlgE2 and AcAlgE3 (Figure 23). To get a more accurate measure, additional concentrations below and above 40 mM NaCl should be tested. This positive effect of NaCl has also been shown for AlgE1 (27) and AlgL from *A. vinelandii* (109). The reason for this could be that Na^+ and Cl^- stabilize the enzyme. In a study of alginate lyases from brown algae, it was for instance found that NaCl stabilized conformational fluctuations of loops involved in their catalytic reaction (110).

In a recent study of the bifunctional alginate lyase/epimerase AlgE7, it was observed that increasing the NaCl concentration reduced the lyase activity (29). In this work, a similar effect was observed, and the activity of AcAlgE2 and AcAlgE3 was reduced after addition of 150 and 75 mM NaCl, respectively. The reason for this effect could be that Na^+ and Cl^- shield the charges on the epimerases and the alginate that are necessary for binding (29). These results also indicate that the lyase activity of AcAlgE3 is more sensitive to an increase in NaCl than AcAlgE2.

Moreover, it was found that increasing the $CaCl_2$ concentration decreased the negative effect of NaCl. At 3 mM $CaCl_2$, 75 mM NaCl was the optimal concentration for lyase activity of both AcAlgE2 and AcAlgE3 (Figure 25). These findings are supported by the study of AlgE7, where the same effect was observed (29).

It should be noted that the salt dependency of AcAlgE2 and AcAlgE3 was tested on enzymes with C-terminal His-tag in this project. As previously mentioned, the tag probably led to a conformational change of the enzymes, and it is therefore possible that the effect of calcium and NaCl would be different for AcAlgE2 and AcAlgE3 without tags. This should consequently be studied further.

In future studies, the effect of NaCl and calcium concentration should also be measured by time-resolved NMR to study the effect on epimerase activity, and how the buffer influences the bifunctionality of the enzymes. This was done in a previous study, but the results were somewhat inconclusive (56). In a study of AlgE7, it was discovered that high NaCl concentrations reduced lyase activity, but increased epimerase activity (29), and it would be interesting to test if AcAlgE2 and AcAlgE3 show the same tendency.

4.5 Development and testing of an optimized epimerase assay

A coupled epimerase/lyase assay (85) is useful to identify epimerase activity. A drawback with this assay is that it is an endpoint analysis, and the epimerase reaction may have stopped at any time during the incubation. To avoid this, the amount of enzyme or the incubation time should be altered. It is also possible to inactivate the epimerase, by addition of chemicals or by heating. A problem with this approach is that heat-inactivation could lead to an increase in enzyme

activity before the enzyme is inactivated, which could result in an overestimation of the activity. Chemical inactivation can also be problematic if it affects the subsequential lyase reaction.

When the coupled epimerase/lyase assay was used to identify the fractions with enzyme activity for AlgE6, AlgE6-Ca and AlgE6-G148R/L172K, approximately the same ΔAbs_{230} was measured for all enzymes (3.5, 3.5 and 3.6). For this reason, this assay was not used to compare enzyme activity in this work, only to identify fractions with epimerase activity. The coupled epimerase/lyase assay was therefore optimized to achieve a quantitative measurement of epimerase activity. This was done by adding the epimerase sample and the G-specific lyase simultaneously.

A challenge with this assay compared to the lyase assay was to select the linear area of the graph when Abs_{230} was plotted as a function of time. The graph was not linear throughout the whole hour but had a sigmoid shape in several cases. This made it possible to find several linear regions with different slopes at different parts of the graph. The incline in Abs_{230} was typically gentle in the beginning, which could be due to the epimerase reaction that needs to happen before the lyase can cleave the alginate. The increase was steepest in the middle and ceased in the end for the samples with high activity. The steepest linear region that lasted over at least 10 min was considered most likely to be the area that represented the epimerase activity best and was therefore selected. For some of the samples, the graph was not linear, but had a rather uneven increase. The reason for the uneven increase in Abs_{230} could be the interplay of the two enzymes in the reaction. This makes it especially important to have several replicates, since it was easier to locate the steepest linear area when the replicates were overlayed. Even though several replicates had an uneven increase, it was possible to find a general trend for all assays performed in this work.

Although there were some challenges in relation to this optimalization of the epimerase assay, it made it possible to qualitatively measure epimerase activity and compare different enzymes. This gives the method a great potential for further use and development in future studies.

The optimized epimerase assay was used to measure the activity of AlgE6-Ca and wild type AlgE6 at different calcium concentrations. It was seen that the activity of AlgE6 increased more by addition of calcium than AlgE6-Ca. This supports that the first 136 amino acids of the A-module may be involved in calcium binding (56) and indicate that the calcium dependency is

different for AlgE6 and AlgE7. The epimerase activity of AlgE6 has also been shown to be dependent of calcium in a previous study, where it was found that the highest degree of epimerisation was achieved at 2 mM calcium (85). Due to the bifunctionality of AlgE7, it is difficult to determine whether the calcium dependency of the AlgE6/AlgE7 hybrid resembles AlgE7 or AlgE6 the most. However, it has been found that the lyase activity of AlgE7 was reduced whereas the epimerase activity of AlgE6 increased when the calcium concentration was increased from 1 to 3 mM, which indicates that the calcium dependency of the enzymes might be different (29, 85). It has also been observed that calcium inhibited the formation of consecutive G residues by AlgE7 (29). Based on the results in this study, it appears as if the calcium binding site from the A-module of AlgE7 is less dependent on calcium, hence it was found that the activity of the AlgE6/AlgE7 hybrid was approximately the same at 0.5 and 1.5 mM calcium. This should be tested further and could be used in future studies to construct a less calcium-dependent epimerase than wild type AlgE6. An epimerase with reduced calcium dependency can be useful for production of G-blocks, since crosslinking with calcium lead to gelation, resulting in inaccessibility of the substrate.

5 Conclusion and Further work

The aim of this work was to improve the understanding of the function of some AlgE-type mannuronan C-5-epimerases from *Azotobacter* and how their enzyme activity can be altered. In this study, it was found that AcAlgE1-3 cannot be purified using a C-terminal His-tag. Finding an optimal purification method remains a challenge and should be investigated further in future studies of these enzymes. Additionally, it was demonstrated that the production of AcAlgE1-3 was better in *E. coli* SHuffle T7 express than in *E. coli* RV308. The use of *E. coli* SHuffle T7 express should therefore be continued for protein production in future studies.

Moreover, it was confirmed that AcAlgE1 is an effective epimerase, rapidly producing higher G-content than AlgE1, although the average G-block length was shorter. The studies of the reaction mechanisms of AcAlgE1 should be continued to get a better understanding of the structural properties of the epimerases that lead to formation of G-blocks of different lengths. This knowledge can be used to select and design epimerases for production of long and pure G-blocks. In future studies it might also be interesting to compare AcAlgE1 to AcAlgE6 since both enzymes show similar epimerization patterns and only have one catalytic site.

The lyase activity of AcAlgE2 and AcAlgE3 was found to be dependent on calcium and was affected by the NaCl concentration. It was also found that calcium reduced the negative effect of NaCl, similar to the tendency observed for AlgE7. Furthermore, it was found that the lyase activity of AcAlgE2 was higher than AcAlgE3 per time unit, but that AcAlgE3 had higher substrate specificity working on sodium alginate (SigmaV-90).

The mechanism of bifunctional mannuronan C-5-epimerases/alginate lyases is still unknown and the amino acids that are responsible for the lyase activity of these enzymes are yet to be discovered. In this work, it was indicated that introducing a proposed calcium binding site from AlgE7 lowered the calcium dependency of AlgE6. Especially from 0.5-1.5 mM $CaCl_2$, the effect of calcium was greater for wild type AlgE6. The epimerase assay that was developed for this purpose was successful and can be used in future studies to quantitatively measure and compare epimerase activity.

6 References

1. Eltaweil AS, Abd El-Monaem EM, Elshishini HM, El-Aqapa HG, Hosny M, Abdelfatah AM, et al. Recent developments in alginate-based adsorbents for removing phosphate ions from wastewater: a review. RSC Adv. 2022;12(13):8228-48.
2. Gheorghita Puscaselu R, Lobiuc A, Dimian M, Covasa M. Alginate: from food industry to biomedical applications and management of metabolic disorders. Polymers. (Basel). 2020;12(10):2417.
3. Høidal HK, Ertesvåg H, Skjåk-Bræk G, Stokke BT, Valla S. The recombinant *Azotobacter vinelandii* mannuronan C-5-epimerase AlgE4 epimerizes alginate by a nonrandom attack mechanism. J Biol Chem. 1999;274(18):12316-22.
4. Niculescu A-G, Grumezescu AM. Applications of chitosan-alginate-based nanoparticles;an up-to-date review. J. Nanomater. 2022;12(2):186.
5. Cheng D, Jiang C, Xu J, Liu Z, Mao X. Characteristics and applications of alginate lyases: A review. Int. J. Biol. Macromol. 2020;164:1304-20.
6. Ertesvåg H. Alginate-modifying enzymes: biological roles and biotechnological uses. Front. Microbiol. 2015;6:523-.
7. Wong TY, Preston LA, Schiller NL. Alginate lyase: review of major sources and enzyme characteristics, structure-function analysis, biological roles, and applications. Annu. Rev. Microbiol. 2000;54(1):289-340.
8. Aarstad O, Heggset EB, Pedersen IS, Bjørnøy SH, Syverud K, Strand BL. Mechanical properties of composite hydrogels of alginate and cellulose nanofibrils. Polymers. (Basel). 2017;9(8):378.
9. Davis TA, Llanes F, Volesky B, Diaz-Pulido G, McCook L, Mucci A. 1H-NMR study of Na alginates extracted from *Sargassum* spp. in relation to metal biosorption. Appl. Biochem. Biotechnol. 2003;110(2):75-90.
10. Espevik T, Otterlei M, Skjåk-Bræk G, Ryan L, Wright SD, Sundan A. The involvement of CD14 in stimulation of cytokine production by uronic acid polymers. Eur. J. Immunol. 1993;23(1):255-61.
11. Zhu B, Yin H. Alginate lyase: Review of major sources and classification, properties, structure-function analysis and applications. Bioengineered. 2015;6(3):125-31.
12. Bakkevig K, Sletta H, Gimmestad M, Aune R, Ertesvåg H, Degnes K, et al. Role of the *Pseudomonas fluorescens* alginate lyase (AlgL) in clearing the periplasm of

alginates not exported to the extracellular environment. J. Bacteriol. 2005;187(24):8375-84.

13. Jain S, Ohman DE. Role of an alginate lyase for alginate transport in mucoid *Pseudomonas aeruginosa*. Infect. Immun. 2005;73(10):6429-36.
14. Hashimoto W, Kawai S, Murata K. Bacterial supersystem for alginate import/metabolism and its environmental and bioenergy applications. Bioeng. Bugs. 2010;1(2):97-109.
15. Ci F, Jiang H, Zhang Z, Mao X. Properties and potential applications of mannuronan C5-epimerase: A biotechnological tool for modifying alginate. Int. Biolymers. Macromol. 2021;168:663-75.
16. Lee KY, Mooney DJ. Alginate: properties and biomedical applications. Prog. Polym. Sci. 2012;37(1):106-26.
17. Gimmestad M, Steigedal M, Ertesvåg H, Moreno S, Christensen BE, Espín G, et al. Identification and characterization of an *Azotobacter vinelandii* type I secretion system responsible for export of the AlgE-type mannuronan C-5-epimerases. J. Bacteriol. 2006;188(15):5551-60.
18. Ertesvåg H, Høidal HK, Schjerven H, Svanem BIG, Valla S. Mannuronan C-5-epimerases and their application for *in vitro* and *in vivo* design of new alginates useful in biotechnology. Metab. Eng. 1999;1(3):262-9.
19. Høidal HK, Glærum Svanem BI, Gimmestad M, Valla S. Mannuronan C-5 epimerases and cellular differentiation of *Azotobacter vinelandii*. Environ. Microbiol. 2000;2(1):27-38.
20. Gawin A, Tietze L, Aarstad OA, Aachmann FL, Brautaset T, Ertesvåg H. Functional characterization of three *Azotobacter chroococcum* alginate-modifying enzymes related to the *Azotobacter vinelandii* AlgE mannuronan C-5-epimerase family. Sci. Rep. 2020;10(1):12470.
21. Holtan S, Bruheim P, Skjåk-Bræk G. Mode of action and subsite studies of the guluronan block-forming mannuronan C-5 epimerases AlgE1 and AlgE6. Biochem J. 2006;395(2):319-29.
22. Hartmann M, Holm OB, Johansen GA, Skjåk-Bræk G, Stokke BT. Mode of action of recombinant *Azotobacter vinelandii* mannuronan C-5 epimerases AlgE2 and AlgE4. Biopolymers. 2002;63(2):77-88.

23. Ramstad MV, Ellingsen TE, Josefsen KD, Høidal HK, Valla S, Skjåk-Bræk G, et al. Properties and action pattern of the recombinant mannuronan C-5-epimerase AlgE2. Enzyme Microb. Technol. 1999;24(10):636-46.
24. Park C, Raines RT. Quantitative Analysis of the Effect of Salt Concentration on Enzymatic Catalysis. J. Am. Chem. Soc. 2001;123(46):11472-9.
25. Aachmann FL, Svanem BIG, Güntert P, Petersen SB, Valla S, Wimmer R. NMR Structure of the R-module: A parallel β-roll subunit from an *Azotobacter vinelandii* mannuronan C-5 epimerase. J. Biol. Chem. 2006;281(11):7350-6.
26. Wolfram F, Kitova EN, Robinson H, Walvoort MTC, Codée JDC, Klassen JS, et al. Catalytic mechanism and mode of action of the periplasmic alginate epimerase AlgG. J. Biol. Chem. 2014;289(9):6006-19.
27. Ertesvåg H, Høidal HK, Skjåk-Bræk G, Valla S. The *Azotobacter vinelandii* mannuronan C-5-epimerase AlgE1 consists of two separate catalytic domains. J. Biol. Chem. 1998;273(47):30927-32.
28. Boyd J, Turvey JR. Isolation of a poly-α-l-guluronate lyase from *Klebsiella aerogenes*. Carbohydr. Res. 1977;57:163-71.
29. Gaardløs M, Heggeset TMB, Tøndervik A, Tezé D, Svensson B, Ertesvåg H, et al. Mechanistic basis for understanding the dual activities of the bifunctional *Azotobacter vinelandii* mannuronan C-5-epimerase and alginate lyase AlgE7. Appl. Environ. Microbiol. 2022;88(3):e0183621-e.
30. LeRoux MA, Guilak F, Setton LA. Compressive and shear properties of alginate gel: effects of sodium ions and alginate concentration. J. Biomed. Mater. Res. 1999;47(1):46-53.
31. Uribe S, Sampedro JG. Measuring solution viscosity and its effect on enzyme activity. Biol. Proced. Online. 2003;5(1):108-15.
32. Xie XS. Enzyme kinetics, past and present. Science. 2013;342(6165):1457-9.
33. Robinson PK. Enzymes: principles and biotechnological applications. Essays Biochem. 2015;59:1-41.
34. Punekar NS. Enzymes: catalysis, kinetics and mechanisms. 1 ed: Springer Singapore; 2018.
35. Friedrich Birger Anspach JB, Alessandre Bossi, Laura Castelletti, J. P. Chervet, Tomaz Dylag, Rolf Ekman, Andras Guttman, et. al. Chromatography. Fundamentals and applications of chromatography and related differential migration methods. 6th ed: Heftmann E: Elsevier; 2004.

36. Eisenthal R, Danson MJ, Hough DW. Catalytic efficiency and k_{cat}/K_M: a useful comparator? Trends Biotechnol. 2007;25(6):247-9.
37. Michael T. Madigan KSB, Daniel H. Buckley, W. Matthew Sattley, David A. Stahl. Brock Biology of Microorganisms. 15 ed: Pearson; 2019.
38. Mathieu K, Javed W, Vallet S, Lesterlin C, Candusso M-P, Ding F, et al. Functionality of membrane proteins overexpressed and purified from *E. coli* is highly dependent upon the strain. Sci. Rep. 2019;9(1):2654.
39. Bruce Alberts AJ, Julian Morgan, Martin Raff, Keith Roberts, Peter Walter. Molecular Biology of the cell. 6 ed. New York: Garland Science; 2015.
40. Anton BP, Raleigh EA. Complete Genome Sequence of NEB 5-alpha, a derivative of *Escherichia coli* K-12 DH5α. Genome Announc. 2016;4(6):e01245-16.
41. Kostylev M, Otwell AE, Richardson RE, Suzuki Y. Cloning should be simple: *Escherichia coli* DH5α-mediated assembly of multiple DNA fragments with short end homologies. PLoS One. 2015;10(9):e0137466-e.
42. Marisch K, Bayer K, Scharl T, Mairhofer J, Krempl PM, Hummel K, et al. A comparative analysis of industrial *Escherichia coli* K-12 and B strains in high-glucose batch cultivations on process-, transcriptome- and proteome level. PLoS One. 2013;8(8):e70516-e.
43. Lobstein J, Emrich CA, Jeans C, Faulkner M, Riggs P, Berkmen M. SHuffle, a novel *Escherichia coli* protein expression strain capable of correctly folding disulfide bonded proteins in its cytoplasm. Microb. Cell Fact. 2012;11:56-.
44. Yu TC, Liu WL, Brinck MS, Davis JE, Shek J, Bower G, et al. Multiplexed characterization of rationally designed promoter architectures deconstructs combinatorial logic for IPTG-inducible systems. Nat. Commun. 2021;12(1):325.
45. Gawin A, Valla S, Brautaset T. The XylS/P_m regulator/promoter system and its use in fundamental studies of bacterial gene expression, recombinant protein production and metabolic engineering. Microb. Biotechnol. 2017;10(4):702-18.
46. Inouye S, Nakazawa A, Nakazawa T. Molecular cloning of gene *xylS* of the TOL plasmid: evidence for positive regulation of the xylDEGF operon by *xylS*. J Bacteriol. 1981;148(2):413-8.
47. González-Pérez MM, Marqués S, Domínguez-Cuevas P, Ramos JL. XylS activator and RNA polymerase binding sites at the P_m promoter overlap. FEBS Lett. 2002;519(1-3):117-22.

48. Pontis HG. Chapter 3 - Protein and carbohydrate separation and purification. In: Pontis HG, editor. Methods for analysis of carbohydrate metabolism in photosynthetic organisms. Boston: AP; 2017. p. 45-63.
49. Gottschalk U. Industrial biotechnology and commodity products: ion exchange chromatography. In: Moo-Young M, editor. Comprehensive Biotechnology. 3 ed. Oxford: Pergamon; 2019. p. 698-711.
50. GE Healthcare [Internet]. HiTrap Q HP. Instructions 71-7149-00 AP. [cited 11. 01.2021]. Avaliable from: https://at.vwr.com/assetsvc/asset/de_AT/id/17888504/contents
51. Schmidt M, Hafner M, Frech C. Modeling of salt and pH gradient elution in ion-exchange chromatography. J Sep Sci. 2014;37(1-2):5-13.
52. Bornhorst JA, Falke JJ. Purification of proteins using polyhistidine affinity tags. Methods Enzymol. 2000;326:245-54.
53. GE Healthcare [Internet]. HisTrap HP. Instructions 71-5027-68 AK. [cited 10.01.2021]. Avaliavble from: http://wwwuser.gwdg.de/~jgrossh/protocols/protein-purification/HisTrap.pdf
54. Yip T-T, Hutchens TW. Immobilized metal ion affinity chromatography. In: Kenney A, Fowell S, editors. Practical protein chromatography. Totowa, NJ: Humana Press; 1992. p. 17-31.
55. Lee JJ, Bruley DF, Kang KA, editors. Effect of pH and imidazole on protein C purification from Cohn Ffaction IV-1 by IMAC. 2008; Boston, MA: Springer US.
56. Sønsteby ST. A structural and functional study of AlgE mannuronan C5-epimerases and lyases from *Azotobacter vinelandii* and *Azotobacter chroococcum* [Master's thesis]. Trondheim: NTNU; 2021.
57. Aarstad OA, Stanisci A, Sætrom GI, Tøndervik A, Sletta H, Aachmann FL, et al. Biosynthesis and function of long guluronic acid-blocks in alginate produced by *Azotobacter vinelandii*. Biomacromolecules. 2019;20(4):1613-22.
58. New England Biolabs [Internet]. Reagents For the Life Science Industry. [cited 14.10.2021]. Avaliable from: https://international.neb.com/
59. Zymo Research Plasmid Miniprep™ -Classic [Internet]. Source: Zymo Research. [cited 15.11.2021]. Avaliable from: https://www.zymoresearch.com/products/zymopure-ii-plasmid-miniprep-kit
60. Life Technologies. Zero Blunt® TOPO® PCR Cloning Kit. [cited 14.10.2021]. Avaliable from: Invitrogen by life Technologies.

61. Krempl PM, Mairhofer J, Striedner G, Thallinger GG. Finished genome sequence of the laboratory strain *Escherichia coli* K-12 RV308 (ATCC 31608). Genome Announc. 2014;2(6):e00971-14.
62. Jakobsen ME. ATP-dependent citrate lyase and glycerol 3 phosphate hehydrogenase in *Aurantiochytrium* T66: an attempted *in vivo* analysis and heterologous expression [Master's thesis]. Trondheim: NTNU; 2019.
63. Moghaddam SS. Secreted mannuronan C-5 epimerases from *Azotobacter chroococcum* [Specialization Project]. Trondheim: NTNU; 2016.
64. Gibbs RA. DNA amplification by the polymerase chain reaction. Anal. Chem. 1990;62(13):1202-14.
65. Garibyan L, Avashia N. Polymerase chain reaction. J. Invest Dermatol. 2013;133(3):1-4.
66. Lorenz TC. Polymerase chain reaction: basic protocol plus troubleshooting and optimization strategies. J. Vis. Exp.: 2012(63):e3998-e.
67. Davis LG, Dibner MD, Battey JF. Basic methods in molecular biology. New York: Elsevier; 1986.
68. Lee PY, Costumbrado J, Hsu C-Y, Kim YH. Agarose gel electrophoresis for the separation of DNA fragments. J. Vis. Exp: 2012(62):3923.
69. Tóth E, Huszár K, Bencsura P, Kulcsár PI, Vodicska B, Nyeste A, et al. Restriction enzyme body doubles and PCR cloning: on the general use of type IIs restriction enzymes for cloning. PLoS One. 2014;9(3):e90896-e.
70. Loenen WAM, Dryden DTF, Raleigh EA, Wilson GG, Murray NE. Highlights of the DNA cutters: a short history of the restriction enzymes. Nucleic Acids Res. Spec. Publ. 2014;42(1):3-19.
71. Lehman IR. DNA ligase: structure, mechanism, and function. Science. 1974;186(4166):790-7.
72. Shintani M, Sanchez ZK, Kimbara K. Genomics of microbial plasmids: classification and identification based on replication and transfer systems and host taxonomy. Front. Microbiol. 2015;6.
73. Low KB. Conjugation. In: Brenner S, Miller JH, editors. Encyclopedia of genetics. New York: A.P.; 2001. p. 449-53.
74. Smillie C, Garcillán-Barcia MP, Francia MV, Rocha Eduardo PC, de la Cruz F. Mobility of plasmids. Microbiol. Mol. 2010;74(3):434-52.

75. Germer TA, Zwinkels JC, Tsai BK. Chapter 1 - Introduction. In: Germer TA, Zwinkels JC, Tsai BK, editors. Experimental Methods in the Physical Sciences. 46: A.P.; 2014. p. 1-9.
76. Stevenson K, McVey AF, Clark IBN, Swain PS, Pilizota T. General calibration of microbial growth in microplate readers. Sci. Rep. 2016;6(1):38828.
77. Pace CN, Vajdos F, Fee L, Grimsley G, Gray T. How to measure and predict the molar absorption coefficient of a protein. Protein Sci. 1995;4(11):2411-23.
78. Tang X, Nakata Y, Li HO, Zhang M, Gao H, Fujita A, et al. The optimization of preparations of competent cells for transformation of *E. coli*. Nucleic Acids Res. Spec. Publ. 1994;22(14):2857-8.
79. Mandel M, Higa A. Calcium-dependent bacteriophage DNA infection. J. Mol. Biol. 1970;53(1):159-62.
80. Asif A, Mohsin H, Tanvir R, Rehman Y. Revisiting the mechanisms involved in calcium chloride induced bacterial transformation. Front. Microbiol. 2017;8:2169-.
81. Froger A, Hall JE. Transformation of plasmid DNA into *E. coli* using the heat shock method. J. Vis. Exp. 2007(6):253-.
82. Panja S, Saha S, Jana B, Basu T. Role of membrane potential on artificial transformation of *E. coli* with plasmid DNA. J. Biotechnol. 2006;127(1):14-20.
83. Thermo Fisher Scientific. The technology behind TOPO cloning. Retrieved from: ThermoFisher Scientific [30.11.2021].
84. Østgaard K. Determination of alginate composition by a simple enzymatic assay. Hydrobiologia. 1993;260(1):513-20.
85. Stanisci A, Aarstad OA, Tøndervik A, Sletta H, Dypås LB, Skjåk-Bræk G, et al. Overall size of mannuronan C5-epimerases influences their ability to epimerize modified alginates and alginate gels. Carbohydr. Polym. 2018;180:256-63.
86. Matsushima R, Watanabe R, Tsuda M, Suzuki T. Analysis of extracellular alginate lyase (alyA) expression and its regulatory region in a marine bacterial strain, Pseudoalteromonas atlantica AR06, using a gfp gene reporter system. Mar. Biotechnol. (NY). 2013;15(3):349-56.
87. Shevchik VE, Condemine G, Robert-Baudouy J, Hugouvieux-Cotte-Pattat N. The exopolygalacturonate lyase PelW and the oligogalacturonate lyase Ogl, two cytoplasmic enzymes of pectin catabolism in *Erwinia chrysanthemi* 3937. J Bacteriol. 1999;181(13):3912-9.

88. Hobbs JK, Lee SM, Robb M, Hof F, Barr C, Abe KT, et al. KdgF, the missing link in the microbial metabolism of uronate sugars from pectin and alginate. Proc. Natl. Acad. Sci. U.S.A. 2016;113(22):6188-93.
89. GenScript. eStain® L1 Protein Staining System user manual [User manual]. Retrieved from: GenScript [24.04.2022].
90. Riesenberg D, Guthke R. High-cell-density cultivation of microorganisms. Appl. Microbiol. Biotechnol. 1999;51(4):422-30.
91. Sletta H, Nedal A, Aune TEV, Hellebust H, Hakvåg S, Aune R, et al. Broad-host-range plasmid pJB658 can be used for industrial-level production of a secreted host-toxic single-chain antibody fragment in *Escherichia coli*. Appl Environ. Microbiol. 2004;70(12):7033-9.
92. Dunkel R, Wu X. Identification of organic molecules from a structure database using proton and carbon NMR analysis results. J Magn. Reson. 2007;188(1):97-110.
93. Silverstein RM, Webster FX, Kiemle D. Spectrometric identification of organic compounds, 7th Edition: Wiley; 2005.
94. Gołowicz D, Kasprzak P, Orekhov V, Kazimierczuk K. Fast time-resolved NMR with non-uniform sampling. Prog. Nucl. Magn. Reson. Spectrosc. 2020;116:40-55.
95. ASTM [Internet]. Standard test method for determining the chemical composition and sequence in alginate by proton nuclear magnetic resonance (^{1}H NMR) spectroscopy. [cited 25.04.2022]. Avaliable from: ASTM https://www.astm.org/standards/f2259
96. Ertesvåg H, Valla S. The A modules of the *Azotobacter vinelandii* mannuronan C-5-epimerase AlgE1 are sufficient for both epimerization and binding of Ca^{2+}. J Bacteriol. 1999;181(10):3033-8.
97. Tøndervik A, Klinkenberg G, Aachmann FL, Svanem BI, Ertesvåg H, Ellingsen TE, et al. Mannuronan C-5 epimerases suited for tailoring of specific alginate structures obtained by high-throughput screening of an epimerase mutant library. Biomacromolecules. 2013;14(8):2657-66.
98. Buchinger E, Aachmann FL, Aranko AS, Valla S, Skjåk-Bræk G, Iwaï H, et al. Use of protein trans-splicing to produce active and segmentally (2)H, (15)N labeled mannuronan C5-epimerase AlgE4. Protein Sci. 2010;19(8):1534-43.
99. Buchinger E, Knudsen DH, Behrens MA, Pedersen JS, Aarstad OA, Tøndervik A, et al. Structural and functional characterization of the R-modules in alginate C-5 epimerases AlgE4 and AlgE6 from *Azotobacter vinelandii*. J. Biol. Chem. 2014;289(45):31382-96.

100. Gaardløs M, Samsonov SA, Sletmoen M, Hjørnevik M, Sætrom GI, Tøndervik A, et al. Insights into the roles of charged residues in substrate binding and mode of action of mannuronan C-5 epimerase AlgE4. Glycobiology. 2021;31(12):1616-35.
101. Yamaguchi H, Miyazaki M. Refolding techniques for recovering biologically active recombinant proteins from inclusion bodies. Biomolecules. 2014;4(1):235-51.
102. Zhu S, Gong C, Ren L, Li X, Song D, Zheng G. A simple and effective strategy for solving the problem of inclusion bodies in recombinant protein technology: His-tag deletions enhance soluble expression. Appl. Microbiol. Biotechnol. 2013;97(2):837-45.
103. Angius F, Ilioaia O, Amrani A, Suisse A, Rosset L, Legrand A, et al. A novel regulation mechanism of the T7 RNA polymerase based expression system improves overproduction and folding of membrane proteins. Sci. Rep. 2018;8(1):8572.
104. Fathi-Roudsari M, Akhavian-Tehrani A, Maghsoudi N. Comparison of three *Escherichia coli* strains in recombinant production of reteplase. Avicenna J. Med. Biotechnol. 2016;8(1):16-22.
105. Yoon SH, Han M-J, Jeong H, Lee CH, Xia X-X, Lee D-H, et al. Comparative multi-omics systems analysis of *Escherichia coli* strains B and K-12. Genome Biol. 2012;13(5):R37-R.
106. Tøndervik A, Aarstad OA, Aune R, Maleki S, Rye PD, Dessen A, et al. Exploiting mannuronan C-5 epimerases in commercial alginate production. Mar. Drugs. 2020;18(11).
107. Aarstad O, Strand BL, Klepp-Andersen LM, Skjåk-Bræk G. Analysis of G-block distributions and their impact on gel properties of *in vitro* epimerized mannuronan. Biomacromolecules. 2013;14(10):3409-16.
108. Jang C, Piao Y, Huang X, Yoon E, Park S, Lee K, et al. Modeling and re-engineering of *Azotobacter vinelandii* alginate lyase to enhance its catalytic efficiency for accelerating biofilm degradation. PLoS One. 2016;11:e0156197.
109. Ertesvåg H, Erlien F, Skjåk-Bræk G, Rehm BH, Valla S. Biochemical properties and substrate specificities of a recombinantly produced *Azotobacter vinelandii* alginate lyase. J Bacteriol. 1998;180(15):3779-84.
110. Zhang Y-H, Shao Y, Jiao C, Yang Q-M, Weng H-F, Xiao A-F. Characterization and application of an alginate lyase, Aly1281 from marine bacterium *Pseudoalteromonas carrageenovora* ASY5. Mar. Drugs. 2020;18(2):95.

111. MacDonald L, Berger B. A polysaccharide lyase from *Stenotrophomonas maltophilia* with a unique, pH-regulated substrate specificity. J. Biol. Chem. 2013;289.

Appendix A: DNA and protein standards

In this project, a protein standard (Figure 40A) and two DNA standards were used (Figure 40B and C).

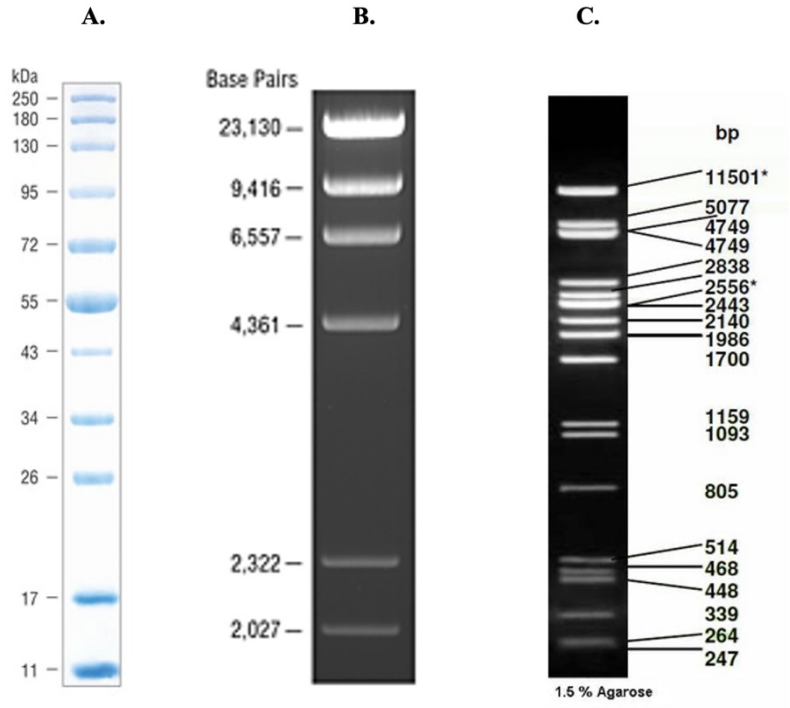

Figure 40: (A) Blue Prestained Protein Standard, Broad Range (NEB). **(B)** λ-DNA digested by HindIII. **(C)** λ-DNA digested by PstI.

Appendix B: Sequencing of TOPO-vectors

The TOPO-vectors pSTH7, pSTH8, pSTH18, pSTH21, pSTH22 and pSTH23 were sequenced by Sanger sequencing. The primers that were used for sequencing were M13F, M13R, Ac550F2 and AcAlgE3sjekk, which are described in Section 2.6. The sequencing alignments are shown below, where mismatches are marked in red.

pSTH7

```
            2461                                                                    2542
pSTH7       TGAGCGGATAACAATTTCACACAGGAAACAGCTATGACCATGATTACGCCAAGCTATTTAGGTGACACTATAGAATACTCAA
EWY756_33... TGAGCGGATAACAATTTCACACAGGAAACAGCTATGACCATGATTACGCCAAGCTATTTAGGTGACACTATAGAATACTCAA

            2543                                                                    2624
pSTH7       GCTATGCATCAAGCTTGGTACCGAGCTCGGATCCACTAGTAACGGCCGCCAGTGTGCTGGAATTCGCCCTTCCGCGCCATTC
EWY756_33... GCTATGCATCAAGCTTGGTACCGAGCTCGGATCCACTAGTAACGGCCGCCAGTGTGCTGGAATTCGCCCTTCCGCGCCATTC

            2625                                                                    2706
pSTH7       TTGCCGGGAATATAGCCGGTTGAACCAGCCGTCGACCTTGTCGACGGTGTTGGCGCGGTTGCCGTCCAGGGTCAGGTCGCGC
EWY756_33... TTGCCGGGAATATAGCCGGTTGAACCAGCCGTCGACCTTGTCGACGGTGTTGGCGCGGTTGCCGTCCAGGGTCAGGTCGCGC
```

```
            2707                                                                    2788
pSTH7       ATGCCGTAATCATGGGTTTTCTCGCCGTTGGCCGAGCGGACTATGCCGGTGATCTTCTGGGCCGAGCCGTCGACCAGTTTGA
EWY756_33... ATGCCGTAATCATGGGTTTTCTCGCCGTTGGCCGAGCGGACTATGCCGGTGATCTTCTGGGCCGAGCCGTCGACCAGTTTGA

            2789                                                                    2870
pSTH7       TCACCGTCTGGCCCATGCCGGCGCCGGCCAGGTAGACGTTGTCCCTGAGCGTCAGGCAGCCGTCGGAAGGTTCCCCGGCGGC
EWY756_33... TCACCGTCTGGCCCATGCCGGCGCCGGCCAGGTAGACGTTGTCCCTGAGCGTCAGGCAGCCGTCGGAAGGTTCCCCGGCGGC

            2871                                                                    2952
pSTH7       GCTGACCCGGTATTCGCCGGGCGGCAGGTAGACGGTACCGCCGCCCGCGGCGTGAGCGGCGTCGATCGCCGCCTGGATGGCG
EWY756_33... GCTGACCCGGTATTCGCCGGGCGGCAGGTAGACGGTACCGCCGCCCGCGGCGTGAGCGGCGTCGATCGCCGCCTGGATGGCG

            2953                                                                    3034
pSTH7       ACCCGGTCGTCGCTGACGCCGTCGCCCAGTGCTCCGAAATCCTTGACGTTGTAATCCATATGTATATCTCCTTCTTAAAGTT
EWY756_33... ACCCGGTCGTCGCTGACGCCGTCGCCCAGTGCTCCGAAATCCTTGACGTTGTAATCCATATGTATATCTCCTTCTTAAAGTT

            3035                                                                    3116
pSTH7       AAACAAAATTATTTCTAGAGGGGAATTGTTATCCGCTCACAATTCCCAAGGGCGAATTCTGCAGATATCCATCACACTGGCG
EWY756_33... AAACAAAATTATTTCTAGAGGGGAATTGTTATCCGCTCACAATTCCCAAGGGCGAATTCTGCAGATATCCATCACACTGGCG
```

pSTH8

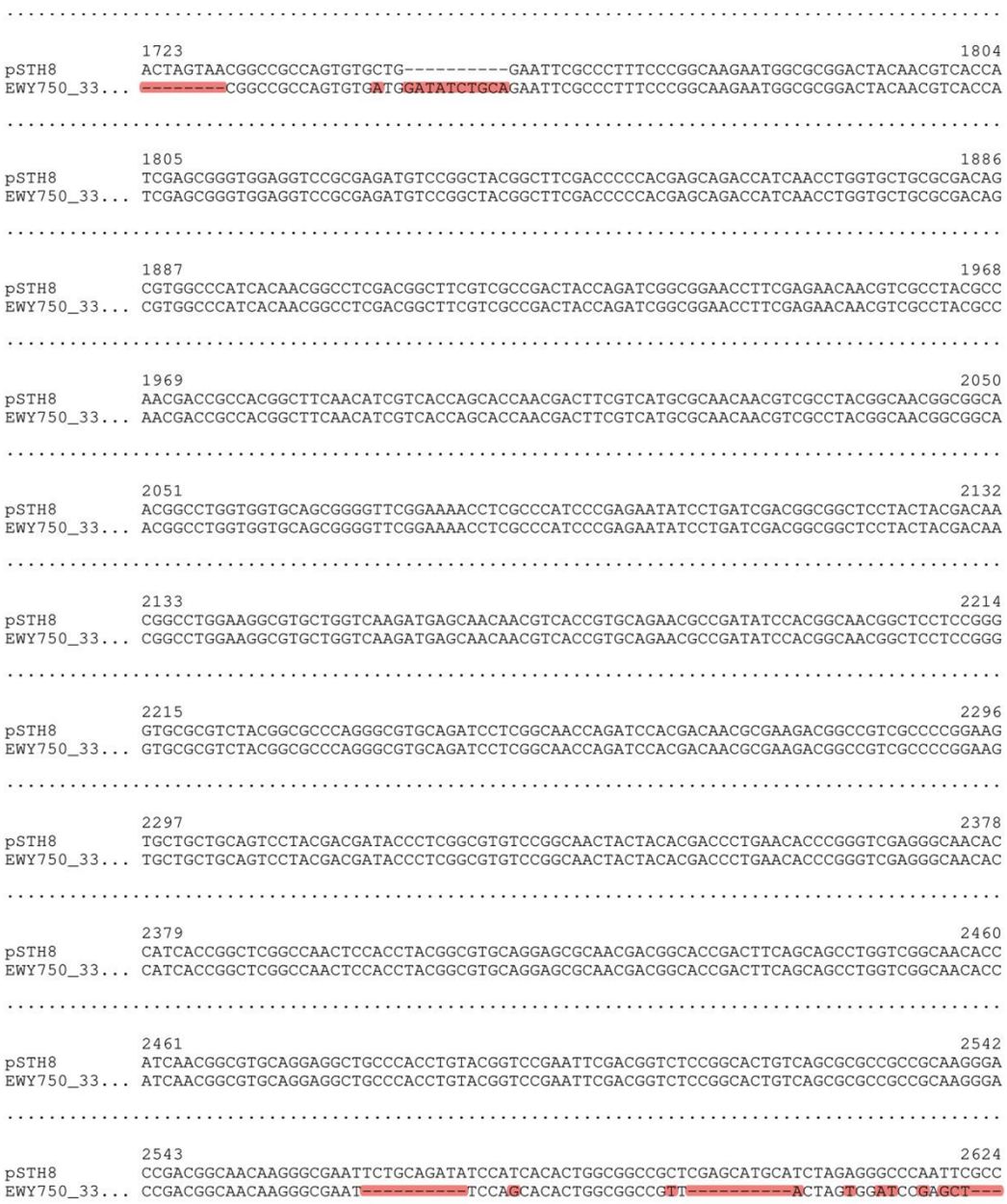
1723 1804
pSTH8 ACTAGTAACGGCCGCCAGTGTGCTG----------GAATTCGCCCTTTCCCGGCAAGAATGGCGCGGACTACAACGTCACCA
EWY750_33... --------CGGCCGCCAGTGTGATGGATATCTGCAGAATTCGCCCTTTCCCGGCAAGAATGGCGCGGACTACAACGTCACCA
1805 1886
pSTH8 TCGAGCGGGTGGAGGTCCGCGAGATGTCCGGCTACGGCTTCGACCCCCACGAGCAGACCATCAACCTGGTGCTGCGCGACAG
EWY750_33... TCGAGCGGGTGGAGGTCCGCGAGATGTCCGGCTACGGCTTCGACCCCCACGAGCAGACCATCAACCTGGTGCTGCGCGACAG
1887 1968
pSTH8 CGTGGCCCATCACAACGGCCTCGACGGCTTCGTCGCCGACTACCAGATCGGCGGAACCTTCGAGAACAACGTCGCCTACGCC
EWY750_33... CGTGGCCCATCACAACGGCCTCGACGGCTTCGTCGCCGACTACCAGATCGGCGGAACCTTCGAGAACAACGTCGCCTACGCC
1969 2050
pSTH8 AACGACCGCCACGGCTTCAACATCGTCACCAGCACCAACGACTTCGTCATGCGCAACAACGTCGCCTACGGCAACGGCGGCA
EWY750_33... AACGACCGCCACGGCTTCAACATCGTCACCAGCACCAACGACTTCGTCATGCGCAACAACGTCGCCTACGGCAACGGCGGCA
2051 2132
pSTH8 ACGGCCTGGTGGTGCAGCGGGGTTCGGAAAACCTCGCCCATCCCGAGAATATCCTGATCGACGGCGGCTCCTACTACGACAA
EWY750_33... ACGGCCTGGTGGTGCAGCGGGGTTCGGAAAACCTCGCCCATCCCGAGAATATCCTGATCGACGGCGGCTCCTACTACGACAA
2133 2214
pSTH8 CGGCCTGGAAGGCGTGCTGGTCAAGATGAGCAACAACGTCACCGTGCAGAACGCCGATATCCACGGCAACGGCTCCTCCGGG
EWY750_33... CGGCCTGGAAGGCGTGCTGGTCAAGATGAGCAACAACGTCACCGTGCAGAACGCCGATATCCACGGCAACGGCTCCTCCGGG
2215 2296
pSTH8 GTGCGCGTCTACGGCGCCCAGGGCGTGCAGATCCTCGGCAACCAGATCCACGACAACGCGAAGACGGCCGTCGCCCCGGAAG
EWY750_33... GTGCGCGTCTACGGCGCCCAGGGCGTGCAGATCCTCGGCAACCAGATCCACGACAACGCGAAGACGGCCGTCGCCCCGGAAG
2297 2378
pSTH8 TGCTGCTGCAGTCCTACGACGATACCCTCGGCGTGTCCGGCAACTACTACACGACCCTGAACACCCGGGTCGAGGGCAACAC
EWY750_33... TGCTGCTGCAGTCCTACGACGATACCCTCGGCGTGTCCGGCAACTACTACACGACCCTGAACACCCGGGTCGAGGGCAACAC
2379 2460
pSTH8 CATCACCGGCTCGGCCAACTCCACCTACGGCGTGCAGGAGCGCAACGACGGCACCGACTTCAGCAGCCTGGTCGGCAACACC
EWY750_33... CATCACCGGCTCGGCCAACTCCACCTACGGCGTGCAGGAGCGCAACGACGGCACCGACTTCAGCAGCCTGGTCGGCAACACC
2461 2542
pSTH8 ATCAACGGCGTGCAGGAGGCTGCCCACCTGTACGGTCCGAATTCGACGGTCTCCGGCACTGTCAGCGCGCCGCCGCAAGGGA
EWY750_33... ATCAACGGCGTGCAGGAGGCTGCCCACCTGTACGGTCCGAATTCGACGGTCTCCGGCACTGTCAGCGCGCCGCCGCAAGGGA
2543 2624
pSTH8 CCGACGGCAACAAGGGCGAATTCTGCAGATATCCATCACACTGGCGGCCGCTCGAGCATGCATCTAGAGGGCCCAATTCGCC
EWY750_33... CCGACGGCAACAAGGGCGAAT----------TCCAGCACACTGGCGGCCGTT----------ACTAGTGGATCCGAGCT---

pSTH18

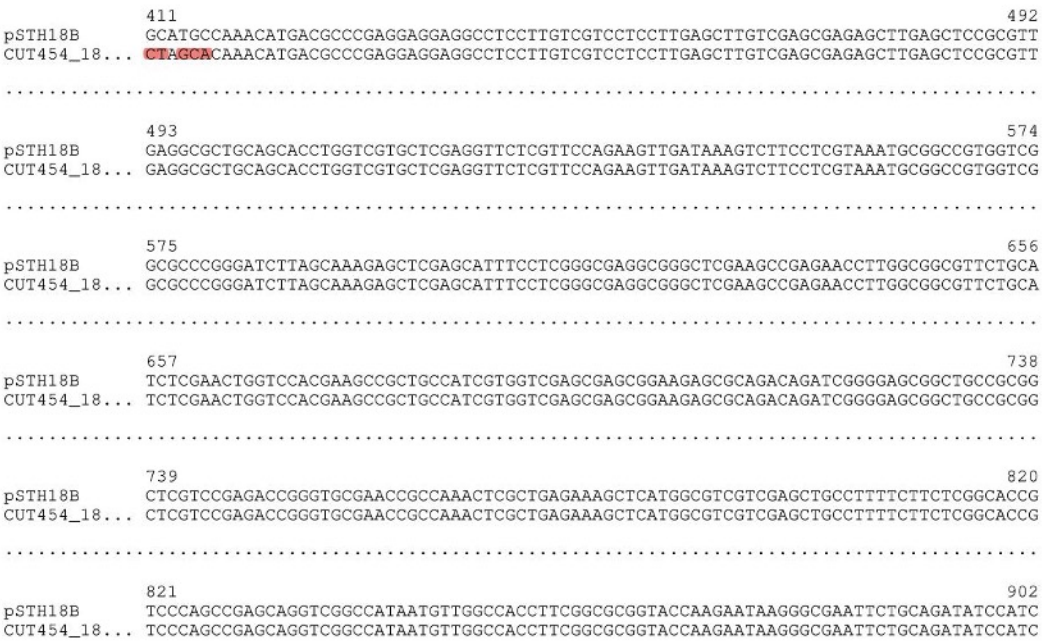
411
492
pSTH18B GCATGCCAAACATGACGCCCGAGGAGGAGGCCTCCTTGTCGTCCTCCTTGAGCTTGTCGAGCGAGAGCTTGAGCTCCGCGTT
CUT454_18... CTAGCACAAACATGACGCCCGAGGAGGAGGCCTCCTTGTCGTCCTCCTTGAGCTTGTCGAGCGAGAGCTTGAGCTCCGCGTT
493
574
pSTH18B GAGGCGCTGCAGCACCTGGTCGTGCTCGAGGTTCTCGTTCCAGAAGTTGATAAAGTCTTCCTCGTAAATGCGGCCGTGGTCG
CUT454_18... GAGGCGCTGCAGCACCTGGTCGTGCTCGAGGTTCTCGTTCCAGAAGTTGATAAAGTCTTCCTCGTAAATGCGGCCGTGGTCG
575
656
pSTH18B GCGCCCGGGATCTTAGCAAAGAGCTCGAGCATTTCCTCGGGCGAGGCGGGCTCGAAGCCGAGAACCTTGGCGGCGTTCTGCA
CUT454_18... GCGCCCGGGATCTTAGCAAAGAGCTCGAGCATTTCCTCGGGCGAGGCGGGCTCGAAGCCGAGAACCTTGGCGGCGTTCTGCA
657
738
pSTH18B TCTCGAACTGGTCCACGAAGCCGCTGCCATCGTGGTCGAGCGAGCGGAAGAGCGCAGACAGATCGGGGAGCGGCTGCCGCGG
CUT454_18... TCTCGAACTGGTCCACGAAGCCGCTGCCATCGTGGTCGAGCGAGCGGAAGAGCGCAGACAGATCGGGGAGCGGCTGCCGCGG
739
820
pSTH18B CTCGTCCGAGACCGGGTGCGAACCGCCAAACTCGCTGAGAAAGCTCATGGCGTCGTCGAGCTGCCTTTTCTTCTCGGCACCG
CUT454_18... CTCGTCCGAGACCGGGTGCGAACCGCCAAACTCGCTGAGAAAGCTCATGGCGTCGTCGAGCTGCCTTTTCTTCTCGGCACCG
821
902
pSTH18B TCCCAGCCGAGCAGGTCGGCCATAATGTTGGCCACCTTCGGCGCGGTACCAAGAATAAGGGCGAATTCTGCAGATATCCATC
CUT454_18... TCCCAGCCGAGCAGGTCGGCCATAATGTTGGCCACCTTCGGCGCGGTACCAAGAATAAGGGCGAATTCTGCAGATATCCATC

pSTH21

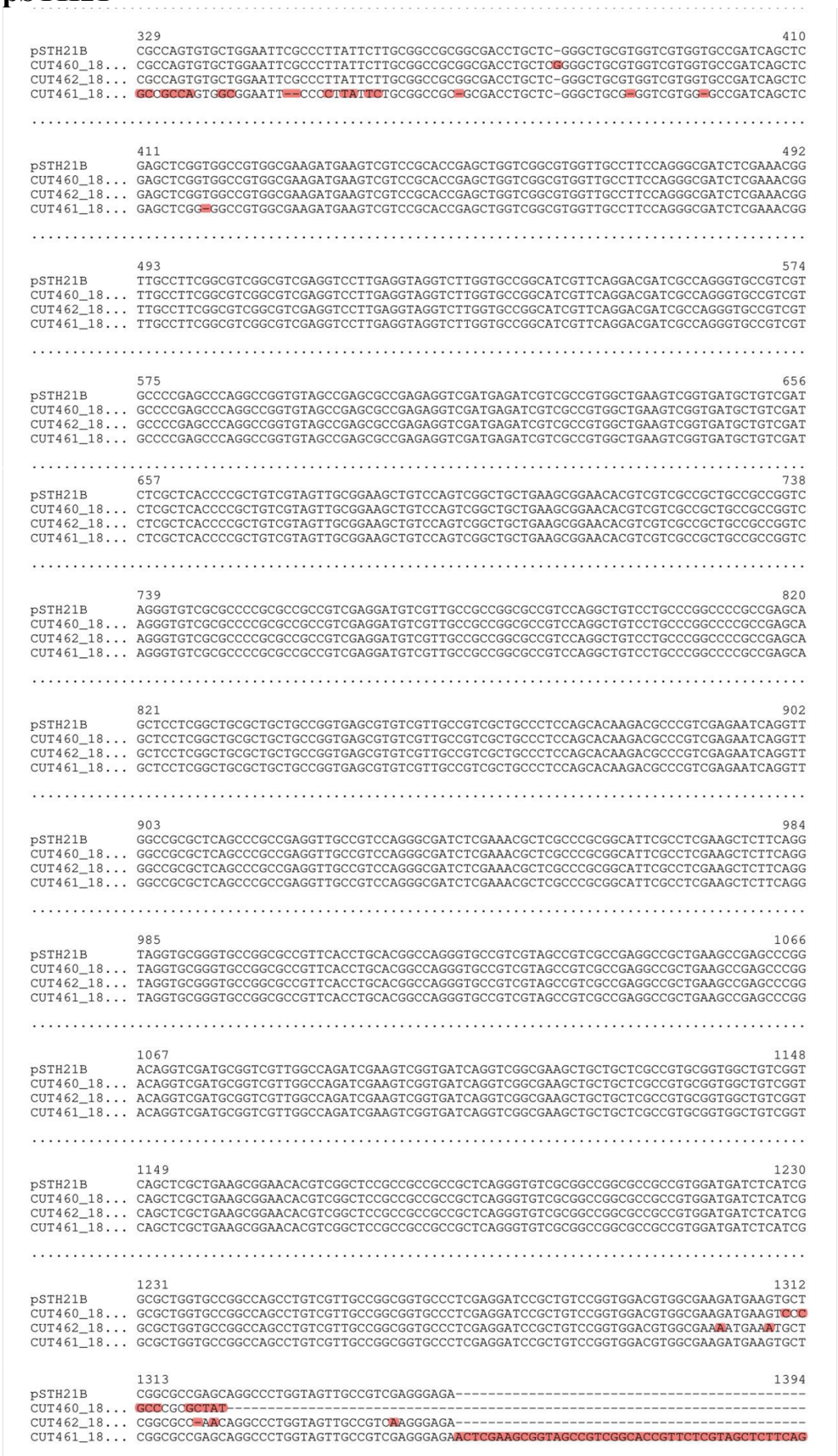
329 410
pSTH21B CGCCAGTGTGCTGGAATTCGCCCTTATTCTTGCGGCCGCGGCGACCTGCTC-GGGCTGCGTGGTCGTGGTGCCGATCAGCTC
CUT460_18... CGCCAGTGTGCTGGAATTCGCCCTTATTCTTGCGGCCGCGGCGACCTGCTCGGGGCTGCGTGGTCGTGGTGCCGATCAGCTC
CUT462_18... CGCCAGTGTGCTGGAATTCGCCCTTATTCTTGCGGCCGCGGCGACCTGCTC-GGGCTGCGTGGTCGTGGTGCCGATCAGCTC
CUT461_18... GCCGCCAGTGGCGGAATT--CCCGTTATTCTGCGGCCGC-GCGACCTGCTC-GGGCTGCG-GGTCGTGG-GCCGATCAGCTC
411 492
pSTH21B GAGCTCGGTGGCCGTGGCGAAGATGAAGTCGTCCGCACCGAGCTGGTCGGCGTGGTTGCCTTCCAGGGCGATCTCGAAACGG
CUT460_18... GAGCTCGGTGGCCGTGGCGAAGATGAAGTCGTCCGCACCGAGCTGGTCGGCGTGGTTGCCTTCCAGGGCGATCTCGAAACGG
CUT462_18... GAGCTCGGTGGCCGTGGCGAAGATGAAGTCGTCCGCACCGAGCTGGTCGGCGTGGTTGCCTTCCAGGGCGATCTCGAAACGG
CUT461_18... GAGCTCGG-GGCCGTGGCGAAGATGAAGTCGTCCGCACCGAGCTGGTCGGCGTGGTTGCCTTCCAGGGCGATCTCGAAACGG
493 574
pSTH21B TTGCCTTCGGCGTCGGCGTCGAGGTCCTTGAGGTAGGTCTTGGTGCCGGCATCGTTCAGGACGATCGCCAGGGTGCCGTCGT
CUT460_18... TTGCCTTCGGCGTCGGCGTCGAGGTCCTTGAGGTAGGTCTTGGTGCCGGCATCGTTCAGGACGATCGCCAGGGTGCCGTCGT
CUT462_18... TTGCCTTCGGCGTCGGCGTCGAGGTCCTTGAGGTAGGTCTTGGTGCCGGCATCGTTCAGGACGATCGCCAGGGTGCCGTCGT
CUT461_18... TTGCCTTCGGCGTCGGCGTCGAGGTCCTTGAGGTAGGTCTTGGTGCCGGCATCGTTCAGGACGATCGCCAGGGTGCCGTCGT
575 656
pSTH21B GCCCCGAGCCCAGGCCGGTGTAGCCGAGCGCCGAGAGGTCGATGAGATCGTCGCCGTGGCTGAAGTCGGTGATGCTGTCGAT
CUT460_18... GCCCCGAGCCCAGGCCGGTGTAGCCGAGCGCCGAGAGGTCGATGAGATCGTCGCCGTGGCTGAAGTCGGTGATGCTGTCGAT
CUT462_18... GCCCCGAGCCCAGGCCGGTGTAGCCGAGCGCCGAGAGGTCGATGAGATCGTCGCCGTGGCTGAAGTCGGTGATGCTGTCGAT
CUT461_18... GCCCCGAGCCCAGGCCGGTGTAGCCGAGCGCCGAGAGGTCGATGAGATCGTCGCCGTGGCTGAAGTCGGTGATGCTGTCGAT
657 738
pSTH21B CTCGCTCACCCCGCTGTCGTAGTTGCGGAAGCTGTCCAGTCGGCTGCTGAAGCGGAACACGTCGTCGCCGCTGCCGCCGGTC
CUT460_18... CTCGCTCACCCCGCTGTCGTAGTTGCGGAAGCTGTCCAGTCGGCTGCTGAAGCGGAACACGTCGTCGCCGCTGCCGCCGGTC
CUT462_18... CTCGCTCACCCCGCTGTCGTAGTTGCGGAAGCTGTCCAGTCGGCTGCTGAAGCGGAACACGTCGTCGCCGCTGCCGCCGGTC
CUT461_18... CTCGCTCACCCCGCTGTCGTAGTTGCGGAAGCTGTCCAGTCGGCTGCTGAAGCGGAACACGTCGTCGCCGCTGCCGCCGGTC
739 820
pSTH21B AGGGTGTCGCGCCCCGCGCCGCCGTCGAGGATGTCGTTGCCGCCGGCGCCGTCCAGGCTGTCCTGCCCGGCCCCGCCGAGCA
CUT460_18... AGGGTGTCGCGCCCCGCGCCGCCGTCGAGGATGTCGTTGCCGCCGGCGCCGTCCAGGCTGTCCTGCCCGGCCCCGCCGAGCA
CUT462_18... AGGGTGTCGCGCCCCGCGCCGCCGTCGAGGATGTCGTTGCCGCCGGCGCCGTCCAGGCTGTCCTGCCCGGCCCCGCCGAGCA
CUT461_18... AGGGTGTCGCGCCCCGCGCCGCCGTCGAGGATGTCGTTGCCGCCGGCGCCGTCCAGGCTGTCCTGCCCGGCCCCGCCGAGCA
821 902
pSTH21B GCTCCTCGGCTGCGCTGCTGCCGGTGAGCGTGTCGTTGCCGTCGCTGCCCTCCAGCACAAGACGCCCGTCGAGAATCAGGTT
CUT460_18... GCTCCTCGGCTGCGCTGCTGCCGGTGAGCGTGTCGTTGCCGTCGCTGCCCTCCAGCACAAGACGCCCGTCGAGAATCAGGTT
CUT462_18... GCTCCTCGGCTGCGCTGCTGCCGGTGAGCGTGTCGTTGCCGTCGCTGCCCTCCAGCACAAGACGCCCGTCGAGAATCAGGTT
CUT461_18... GCTCCTCGGCTGCGCTGCTGCCGGTGAGCGTGTCGTTGCCGTCGCTGCCCTCCAGCACAAGACGCCCGTCGAGAATCAGGTT
903 984
pSTH21B GGCCGCGCTCAGCCCGCCGAGGTTGCCGTCCAGGGCGATCTCGAAACGCTCGCCCGCGGCATTCGCCTCGAAGCTCTTCAGG
CUT460_18... GGCCGCGCTCAGCCCGCCGAGGTTGCCGTCCAGGGCGATCTCGAAACGCTCGCCCGCGGCATTCGCCTCGAAGCTCTTCAGG
CUT462_18... GGCCGCGCTCAGCCCGCCGAGGTTGCCGTCCAGGGCGATCTCGAAACGCTCGCCCGCGGCATTCGCCTCGAAGCTCTTCAGG
CUT461_18... GGCCGCGCTCAGCCCGCCGAGGTTGCCGTCCAGGGCGATCTCGAAACGCTCGCCCGCGGCATTCGCCTCGAAGCTCTTCAGG
985 1066
pSTH21B TAGGTGCGGGTGCCGGCGCCGTTCACCTGCACGGCCAGGGTGCCGTCGTAGCCGTCGCCGAGGCCGCTGAAGCCGAGCCCGG
CUT460_18... TAGGTGCGGGTGCCGGCGCCGTTCACCTGCACGGCCAGGGTGCCGTCGTAGCCGTCGCCGAGGCCGCTGAAGCCGAGCCCGG
CUT462_18... TAGGTGCGGGTGCCGGCGCCGTTCACCTGCACGGCCAGGGTGCCGTCGTAGCCGTCGCCGAGGCCGCTGAAGCCGAGCCCGG
CUT461_18... TAGGTGCGGGTGCCGGCGCCGTTCACCTGCACGGCCAGGGTGCCGTCGTAGCCGTCGCCGAGGCCGCTGAAGCCGAGCCCGG
1067 1148
pSTH21B ACAGGTCGATGCGGTCGTTGGCCAGATCGAAGTCGGTGATCAGGTCGGCGAAGCTGCTGCTCGCCGTGCGGTGGCTGTCGGT
CUT460_18... ACAGGTCGATGCGGTCGTTGGCCAGATCGAAGTCGGTGATCAGGTCGGCGAAGCTGCTGCTCGCCGTGCGGTGGCTGTCGGT
CUT462_18... ACAGGTCGATGCGGTCGTTGGCCAGATCGAAGTCGGTGATCAGGTCGGCGAAGCTGCTGCTCGCCGTGCGGTGGCTGTCGGT
CUT461_18... ACAGGTCGATGCGGTCGTTGGCCAGATCGAAGTCGGTGATCAGGTCGGCGAAGCTGCTGCTCGCCGTGCGGTGGCTGTCGGT
1149 1230
pSTH21B CAGCTCGCTGAAGCGGAACACGTCGGCTCCGCCGCCGCCGCTCAGGGTGTCGCGGCCGGCGCCGCCGTGGATGATCTCATCG
CUT460_18... CAGCTCGCTGAAGCGGAACACGTCGGCTCCGCCGCCGCCGCTCAGGGTGTCGCGGCCGGCGCCGCCGTGGATGATCTCATCG
CUT462_18... CAGCTCGCTGAAGCGGAACACGTCGGCTCCGCCGCCGCCGCTCAGGGTGTCGCGGCCGGCGCCGCCGTGGATGATCTCATCG
CUT461_18... CAGCTCGCTGAAGCGGAACACGTCGGCTCCGCCGCCGCCGCTCAGGGTGTCGCGGCCGGCGCCGCCGTGGATGATCTCATCG
1231 1312
pSTH21B GCGCTGGTGCCGGCCAGCCTGTCGTTGCCGGCGGTGCCCTCGAGGATCCGCTGTCCGGTGGACGTGGCGAAGATGAAGTGCT
CUT460_18... GCGCTGGTGCCGGCCAGCCTGTCGTTGCCGGCGGTGCCCTCGAGGATCCGCTGTCCGGTGGACGTGGCGAAGATGAAGTCCC
CUT462_18... GCGCTGGTGCCGGCCAGCCTGTCGTTGCCGGCGGTGCCCTCGAGGATCCGCTGTCCGGTGGACGTGGCGAAAATGAAATGCT
CUT461_18... GCGCTGGTGCCGGCCAGCCTGTCGTTGCCGGCGGTGCCCTCGAGGATCCGCTGTCCGGTGGACGTGGCGAAGATGAAGTGCT
1313 1394
pSTH21B CGGCGCCGAGCAGGCCCTGGTAGTTGCCGTCGAGGGAGA----------
CUT460_18... GCCCGGCGCTAT----------
CUT462_18... CGGCGCC-AACAGGCCCTGGTAGTTGCCGTCAAGGGAGA----------
CUT461_18... CGGCGCCGAGCAGGCCCTGGTAGTTGCCGTCGAGGGAGAACTCGAAGCGGTAGCCGTCGGCACCGTTCTCGTAGCTCTTCAG

pSTH22

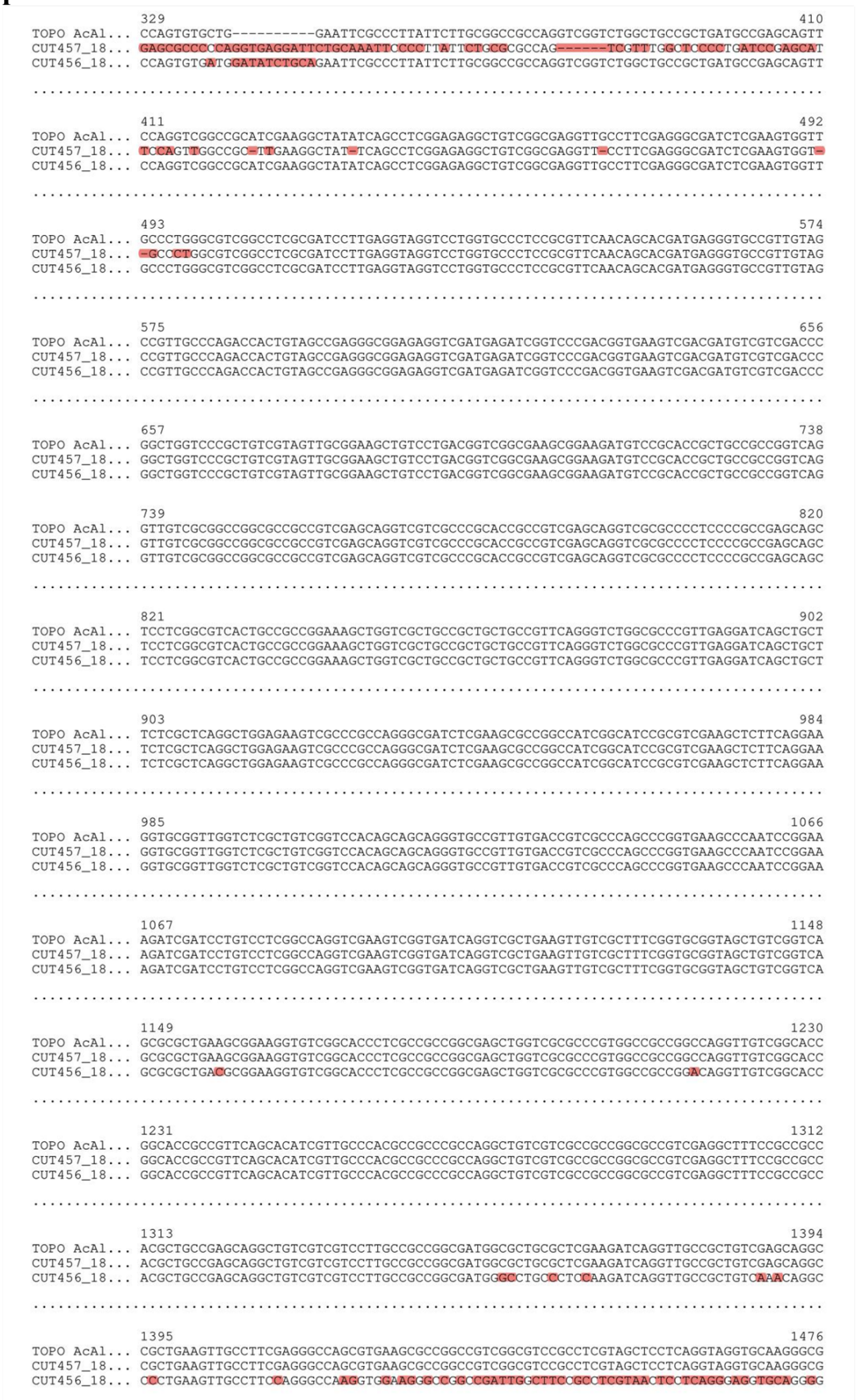
329 410
TOPO AcAl... CCAGTGTGCTG----------GAATTCGCCCTTATTCTTGCGGCCGCCAGGTCGGTCTGGCTGCCGCTGATGCCGAGCAGTT
CUT457_18... GAGCGCCCCCAGGTGAGGATTCTGCAAATTCCCCTTATTCTCGCGCGCCAG------TCGTTTGGCTCCCCTGATCCGAGCAT
CUT456_18... CCAGTGTGATGGATATCTGCAGAATTCGCCCTTATTCTTGCGGCCGCCAGGTCGGTCTGGCTGCCGCTGATGCCGAGCAGTT
411 492
TOPO AcAl... CCAGGTCGGCCGCATCGAAGGCTATATCAGCCTCGGAGAGGCTGTCGGCGAGGTTGCCTTCGAGGGCGATCTCGAAGTGGTT
CUT457_18... TCCAGTTGGCCGC-TTGAAGGCTAT-TCAGCCTCGGAGAGGCTGTCGGCGAGGTT-CCTTCGAGGGCGATCTCGAAGTGGT-
CUT456_18... CCAGGTCGGCCGCATCGAAGGCTATATCAGCCTCGGAGAGGCTGTCGGCGAGGTTGCCTTCGAGGGCGATCTCGAAGTGGTT
493 574
TOPO AcAl... GCCCTGGGCGTCGGCCTCGCGATCCTTGAGGTAGGTCCTGGTGCCCTCCGCGTTCAACAGCACGATGAGGGTGCCGTTGTAG
CUT457_18... -GCCCTGGCGTCGGCCTCGCGATCCTTGAGGTAGGTCCTGGTGCCCTCCGCGTTCAACAGCACGATGAGGGTGCCGTTGTAG
CUT456_18... GCCCTGGGCGTCGGCCTCGCGATCCTTGAGGTAGGTCCTGGTGCCCTCCGCGTTCAACAGCACGATGAGGGTGCCGTTGTAG
575 656
TOPO AcAl... CCGTTGCCCAGACCACTGTAGCCGAGGGCGGAGAGGTCGATGAGATCGGTCCCGACGGTGAAGTCGACGATGTCGTCGACCC
CUT457_18... CCGTTGCCCAGACCACTGTAGCCGAGGGCGGAGAGGTCGATGAGATCGGTCCCGACGGTGAAGTCGACGATGTCGTCGACCC
CUT456_18... CCGTTGCCCAGACCACTGTAGCCGAGGGCGGAGAGGTCGATGAGATCGGTCCCGACGGTGAAGTCGACGATGTCGTCGACCC
657 738
TOPO AcAl... GGCTGGTCCCGCTGTCGTAGTTGCGGAAGCTGTCCTGACGGTCGGCGAAGCGGAAGATGTCCGCACCGCTGCCGCCGGTCAG
CUT457_18... GGCTGGTCCCGCTGTCGTAGTTGCGGAAGCTGTCCTGACGGTCGGCGAAGCGGAAGATGTCCGCACCGCTGCCGCCGGTCAG
CUT456_18... GGCTGGTCCCGCTGTCGTAGTTGCGGAAGCTGTCCTGACGGTCGGCGAAGCGGAAGATGTCCGCACCGCTGCCGCCGGTCAG
739 820
TOPO AcAl... GTTGTCGCGGCCGGCGCCGCCGTCGAGCAGGTCGTCGCCCGCACCGCCGTCGAGCAGGTCGCGCCCCTCCCCGCCGAGCAGC
CUT457_18... GTTGTCGCGGCCGGCGCCGCCGTCGAGCAGGTCGTCGCCCGCACCGCCGTCGAGCAGGTCGCGCCCCTCCCCGCCGAGCAGC
CUT456_18... GTTGTCGCGGCCGGCGCCGCCGTCGAGCAGGTCGTCGCCCGCACCGCCGTCGAGCAGGTCGCGCCCCTCCCCGCCGAGCAGC
821 902
TOPO AcAl... TCCTCGGCGTCACTGCCGCCGGAAAGCTGGTCGCTGCCGCTGCTGCCGTTCAGGGTCTGGCGCCCGTTGAGGATCAGCTGCT
CUT457_18... TCCTCGGCGTCACTGCCGCCGGAAAGCTGGTCGCTGCCGCTGCTGCCGTTCAGGGTCTGGCGCCCGTTGAGGATCAGCTGCT
CUT456_18... TCCTCGGCGTCACTGCCGCCGGAAAGCTGGTCGCTGCCGCTGCTGCCGTTCAGGGTCTGGCGCCCGTTGAGGATCAGCTGCT
903 984
TOPO AcAl... TCTCGCTCAGGCTGGAGAAGTCGCCCGCCAGGGCGATCTCGAAGCGCCGGCCATCGGCATCCGCGTCGAAGCTCTTCAGGAA
CUT457_18... TCTCGCTCAGGCTGGAGAAGTCGCCCGCCAGGGCGATCTCGAAGCGCCGGCCATCGGCATCCGCGTCGAAGCTCTTCAGGAA
CUT456_18... TCTCGCTCAGGCTGGAGAAGTCGCCCGCCAGGGCGATCTCGAAGCGCCGGCCATCGGCATCCGCGTCGAAGCTCTTCAGGAA
985 1066
TOPO AcAl... GGTGCGGTTGGTCTCGCTGTCGGTCCACAGCAGCAGGGTGCCGTTGTGACCGTCGCCCAGCCCGGTGAAGCCCAATCCGGAA
CUT457_18... GGTGCGGTTGGTCTCGCTGTCGGTCCACAGCAGCAGGGTGCCGTTGTGACCGTCGCCCAGCCCGGTGAAGCCCAATCCGGAA
CUT456_18... GGTGCGGTTGGTCTCGCTGTCGGTCCACAGCAGCAGGGTGCCGTTGTGACCGTCGCCCAGCCCGGTGAAGCCCAATCCGGAA
1067 1148
TOPO AcAl... AGATCGATCCTGTCCTCGGCCAGGTCGAAGTCGGTGATCAGGTCGCTGAAGTTGTCGCTTTCGGTGCGGTAGCTGTCGGTCA
CUT457_18... AGATCGATCCTGTCCTCGGCCAGGTCGAAGTCGGTGATCAGGTCGCTGAAGTTGTCGCTTTCGGTGCGGTAGCTGTCGGTCA
CUT456_18... AGATCGATCCTGTCCTCGGCCAGGTCGAAGTCGGTGATCAGGTCGCTGAAGTTGTCGCTTTCGGTGCGGTAGCTGTCGGTCA
1149 1230
TOPO AcAl... GCGCGCTGAAGCGGAAGGTGTCGGCACCCTCGCCGCCGGCGAGCTGGTCGCGCCCGTGGCCGCCGGCCAGGTTGTCGGCACC
CUT457_18... GCGCGCTGAAGCGGAAGGTGTCGGCACCCTCGCCGCCGGCGAGCTGGTCGCGCCCGTGGCCGCCGGCCAGGTTGTCGGCACC
CUT456_18... GCGCGCTGACGCGGAAGGTGTCGGCACCCTCGCCGCCGGCGAGCTGGTCGCGCCCGTGGCCGCCGGACAGGTTGTCGGCACC
1231 1312
TOPO AcAl... GGCACCGCCGTTCAGCACATCGTTGCCCACGCCGCCCGCCAGGCTGTCGTCGCCGCCGGCGCCGTCGAGGCTTTCCGCCGCC
CUT457_18... GGCACCGCCGTTCAGCACATCGTTGCCCACGCCGCCCGCCAGGCTGTCGTCGCCGCCGGCGCCGTCGAGGCTTTCCGCCGCC
CUT456_18... GGCACCGCCGTTCAGCACATCGTTGCCCACGCCGCCCGCCAGGCTGTCGTCGCCGCCGGCGCCGTCGAGGCTTTCCGCCGCC
1313 1394
TOPO AcAl... ACGCTGCCGAGCAGGCTGTCGTCGTCCTTGCCGCCGGCGATGGCGCTGCGCTCGAAGATCAGGTTGCCGCTGTCGAGCAGGC
CUT457_18... ACGCTGCCGAGCAGGCTGTCGTCGTCCTTGCCGCCGGCGATGGCGCTGCGCTCGAAGATCAGGTTGCCGCTGTCGAGCAGGC
CUT456_18... ACGCTGCCGAGCAGGCTGTCGTCGTCCTTGCCGCCGGCGATGGGCCTGCCCTCCAAGATCAGGTTGCCGCTGTCAAACAGGC
1395 1476
TOPO AcAl... CGCTGAAGTTGCCTTCGAGGGCCAGCGTGAAGCGCCGGCCGTCGGCGTCCGCCTCGTAGCTCCTCAGGTAGGTGCAAGGGCG
CUT457_18... CGCTGAAGTTGCCTTCGAGGGCCAGCGTGAAGCGCCGGCCGTCGGCGTCCGCCTCGTAGCTCCTCAGGTAGGTGCAAGGGCG
CUT456_18... CCCTGAAGTTGCCTTCCAGGGCCAAGGTGGAAGGGCCGGCCGATTGGCTTCCGCCTCGTAACTCCTCAGGGAGGTGCAGGGG

pSTH23

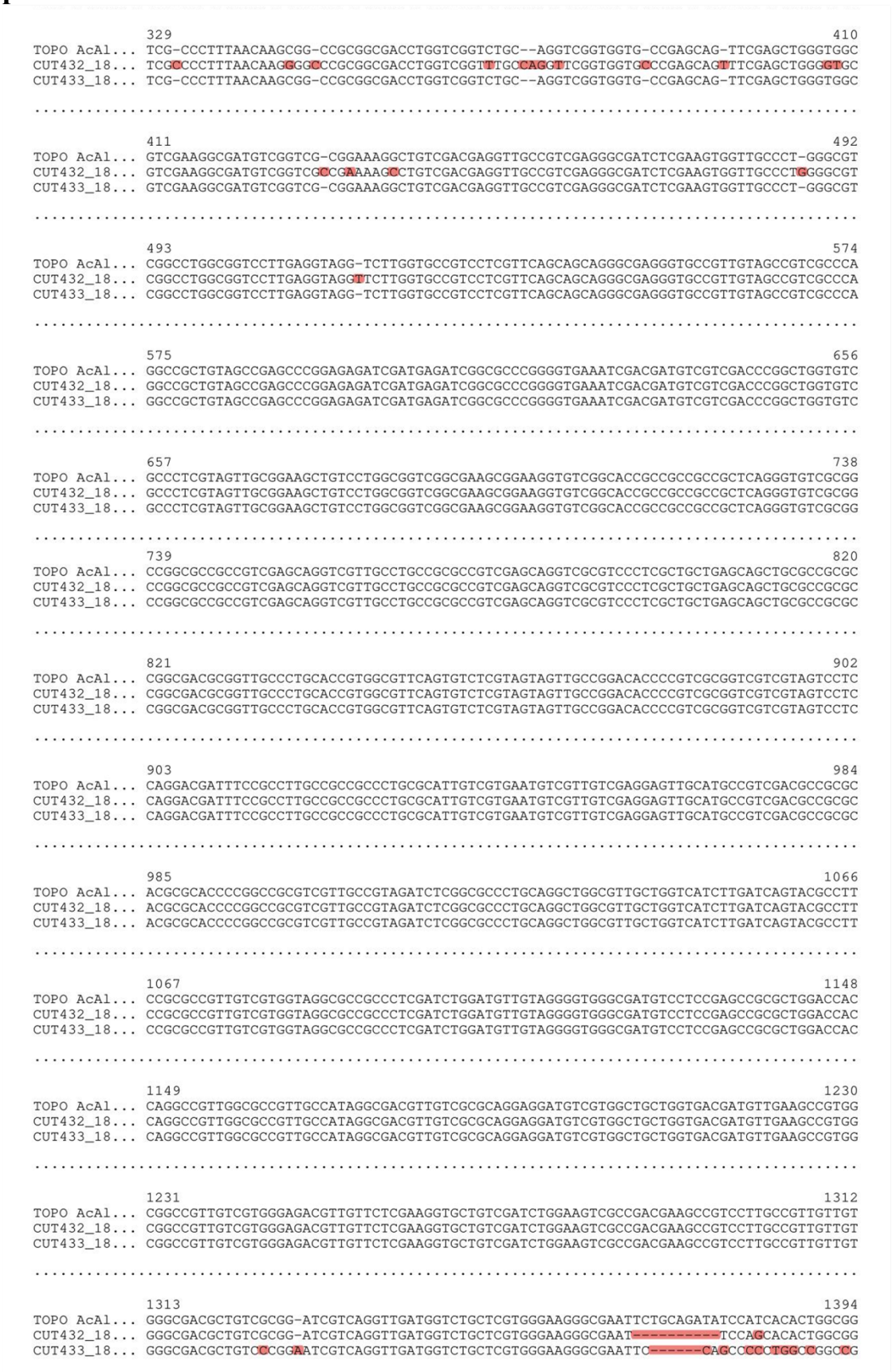
329 410
TOPO AcAl... TCG-CCCTTTAACAAGCGG-CCGCGGCGACCTGGTCGGTCTGC--AGGTCGGTGGTG-CCGAGCAG-TTCGAGCTGGGTGGC
CUT432_18... TCGCCCCTTTAACAAGGGGCCCGCGGCGACCTGGTCGGTTTGCCAGGTTCGGTGGTGCCCGAGCAGTTTCGAGCTGGGGTGC
CUT433_18... TCG-CCCTTTAACAAGCGG-CCGCGGCGACCTGGTCGGTCTGC--AGGTCGGTGGTG-CCGAGCAG-TTCGAGCTGGGTGGC
411 492
TOPO AcAl... GTCGAAGGCGATGTCGGTCG-CGGAAAGGCTGTCGACGAGGTTGCCGTCGAGGGCGATCTCGAAGTGGTTGCCCT-GGGCGT
CUT432_18... GTCGAAGGCGATGTCGGTCGCCGAAAAGCCTGTCGACGAGGTTGCCGTCGAGGGCGATCTCGAAGTGGTTGCCCTGGGGCGT
CUT433_18... GTCGAAGGCGATGTCGGTCG-CGGAAAGGCTGTCGACGAGGTTGCCGTCGAGGGCGATCTCGAAGTGGTTGCCCT-GGGCGT
493 574
TOPO AcAl... CGGCCTGGCGGTCCTTGAGGTAGG-TCTTGGTGCCGTCCTCGTTCAGCAGCAGGGCGAGGGTGCCGTTGTAGCCGTCGCCCA
CUT432_18... CGGCCTGGCGGTCCTTGAGGTAGGTTCTTGGTGCCGTCCTCGTTCAGCAGCAGGGCGAGGGTGCCGTTGTAGCCGTCGCCCA
CUT433_18... CGGCCTGGCGGTCCTTGAGGTAGG-TCTTGGTGCCGTCCTCGTTCAGCAGCAGGGCGAGGGTGCCGTTGTAGCCGTCGCCCA
575 656
TOPO AcAl... GGCCGCTGTAGCCGAGCCCGGAGAGATCGATGAGATCGGCGCCCGGGGTGAAATCGACGATGTCGTCGACCCGGCTGGTGTC
CUT432_18... GGCCGCTGTAGCCGAGCCCGGAGAGATCGATGAGATCGGCGCCCGGGGTGAAATCGACGATGTCGTCGACCCGGCTGGTGTC
CUT433_18... GGCCGCTGTAGCCGAGCCCGGAGAGATCGATGAGATCGGCGCCCGGGGTGAAATCGACGATGTCGTCGACCCGGCTGGTGTC
657 738
TOPO AcAl... GCCCTCGTAGTTGCGGAAGCTGTCCTGGCGGTCGGCGAAGCGGAAGGTGTCGGCACCGCCGCCGCCGCTCAGGGTGTCGCGG
CUT432_18... GCCCTCGTAGTTGCGGAAGCTGTCCTGGCGGTCGGCGAAGCGGAAGGTGTCGGCACCGCCGCCGCCGCTCAGGGTGTCGCGG
CUT433_18... GCCCTCGTAGTTGCGGAAGCTGTCCTGGCGGTCGGCGAAGCGGAAGGTGTCGGCACCGCCGCCGCCGCTCAGGGTGTCGCGG
739 820
TOPO AcAl... CCGGCGCCGCCGTCGAGCAGGTCGTTGCCTGCCGCGCCGTCGAGCAGGTCGCGTCCCTCGCTGCTGAGCAGCTGCGCCGCGC
CUT432_18... CCGGCGCCGCCGTCGAGCAGGTCGTTGCCTGCCGCGCCGTCGAGCAGGTCGCGTCCCTCGCTGCTGAGCAGCTGCGCCGCGC
CUT433_18... CCGGCGCCGCCGTCGAGCAGGTCGTTGCCTGCCGCGCCGTCGAGCAGGTCGCGTCCCTCGCTGCTGAGCAGCTGCGCCGCGC
821 902
TOPO AcAl... CGGCGACGCGGTTGCCCTGCACCGTGGCGTTCAGTGTCTCGTAGTAGTTGCCGGACACCCCGTCGCGGTCGTCGTAGTCCTC
CUT432_18... CGGCGACGCGGTTGCCCTGCACCGTGGCGTTCAGTGTCTCGTAGTAGTTGCCGGACACCCCGTCGCGGTCGTCGTAGTCCTC
CUT433_18... CGGCGACGCGGTTGCCCTGCACCGTGGCGTTCAGTGTCTCGTAGTAGTTGCCGGACACCCCGTCGCGGTCGTCGTAGTCCTC
903 984
TOPO AcAl... CAGGACGATTTCCGCCTTGCCGCCGCCCTGCGCATTGTCGTGAATGTCGTTGTCGAGGAGTTGCATGCCGTCGACGCCGCGC
CUT432_18... CAGGACGATTTCCGCCTTGCCGCCGCCCTGCGCATTGTCGTGAATGTCGTTGTCGAGGAGTTGCATGCCGTCGACGCCGCGC
CUT433_18... CAGGACGATTTCCGCCTTGCCGCCGCCCTGCGCATTGTCGTGAATGTCGTTGTCGAGGAGTTGCATGCCGTCGACGCCGCGC
985 1066
TOPO AcAl... ACGCGCACCCCGGCCGCGTCGTTGCCGTAGATCTCGGCGCCCTGCAGGCTGGCGTTGCTGGTCATCTTGATCAGTACGCCTT
CUT432_18... ACGCGCACCCCGGCCGCGTCGTTGCCGTAGATCTCGGCGCCCTGCAGGCTGGCGTTGCTGGTCATCTTGATCAGTACGCCTT
CUT433_18... ACGCGCACCCCGGCCGCGTCGTTGCCGTAGATCTCGGCGCCCTGCAGGCTGGCGTTGCTGGTCATCTTGATCAGTACGCCTT
1067 1148
TOPO AcAl... CCGCGCCGTTGTCGTGGTAGGCGCCGCCCTCGATCTGGATGTTGTAGGGGTGGGCGATGTCCTCCGAGCCGCGCTGGACCAC
CUT432_18... CCGCGCCGTTGTCGTGGTAGGCGCCGCCCTCGATCTGGATGTTGTAGGGGTGGGCGATGTCCTCCGAGCCGCGCTGGACCAC
CUT433_18... CCGCGCCGTTGTCGTGGTAGGCGCCGCCCTCGATCTGGATGTTGTAGGGGTGGGCGATGTCCTCCGAGCCGCGCTGGACCAC
1149 1230
TOPO AcAl... CAGGCCGTTGGCGCCGTTGCCATAGGCGACGTTGTCGCGCAGGAGGATGTCGTGGCTGCTGGTGACGATGTTGAAGCCGTGG
CUT432_18... CAGGCCGTTGGCGCCGTTGCCATAGGCGACGTTGTCGCGCAGGAGGATGTCGTGGCTGCTGGTGACGATGTTGAAGCCGTGG
CUT433_18... CAGGCCGTTGGCGCCGTTGCCATAGGCGACGTTGTCGCGCAGGAGGATGTCGTGGCTGCTGGTGACGATGTTGAAGCCGTGG
1231 1312
TOPO AcAl... CGGCCGTTGTCGTGGGAGACGTTGTTCTCGAAGGTGCTGTCGATCTGGAAGTCGCCGACGAAGCCGTCCTTGCCGTTGTTGT
CUT432_18... CGGCCGTTGTCGTGGGAGACGTTGTTCTCGAAGGTGCTGTCGATCTGGAAGTCGCCGACGAAGCCGTCCTTGCCGTTGTTGT
CUT433_18... CGGCCGTTGTCGTGGGAGACGTTGTTCTCGAAGGTGCTGTCGATCTGGAAGTCGCCGACGAAGCCGTCCTTGCCGTTGTTGT
1313 1394
TOPO AcAl... GGGCGACGCTGTCGCGG-ATCGTCAGGTTGATGGTCTGCTCGTGGGAAGGGCGAATTCTGCAGATATCCATCACACTGGCGG
CUT432_18... GGGCGACGCTGTCGCGG-ATCGTCAGGTTGATGGTCTGCTCGTGGGAAGGGCGAAT----------TCCAGCACACTGGCGG
CUT433_18... GGGCGACGCTGTCCCGGAATCGTCAGGTTGATGGTCTGCTCGTGGGAAGGGCGAATTC------CAGCCCCTGGCCGGCCG

Appendix C: Calculation of sequential parameters

The ^{1}H-NMR spectrum of alginate can be used to study the composition and block structures du to different shifts of the different residues, diads and triads (Figure 41).

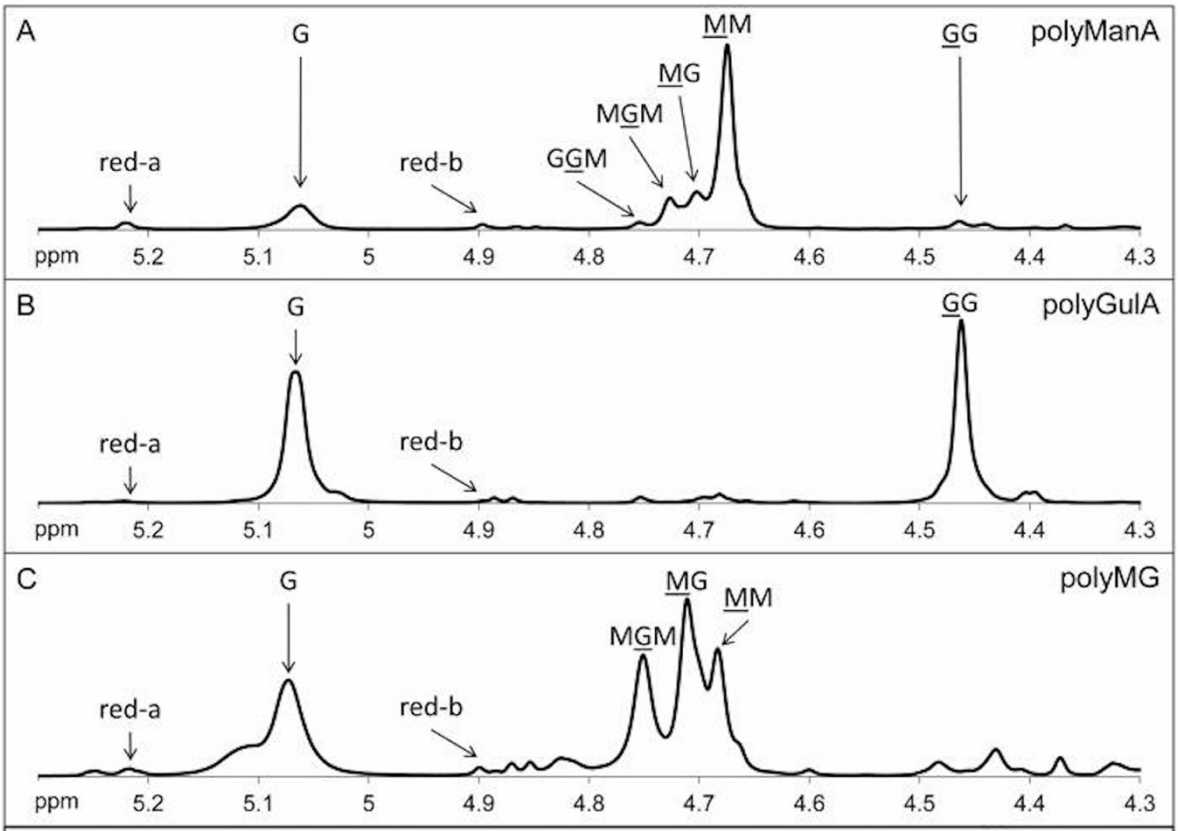

D

Substrate	F_G	F_M	F_{GG}	F_{MM}	$F_{MG,GM}$	F_{GGG}	F_{MGM}	$F_{GGM,MGG}$	DP_n
polyManA	0.17	0.83	0.05	0.71	0.12	0.04	0.11	0.01	18
polyGulA	0.93	0.07	0.87	0.01	0.06	0.85	0.03	0.02	19
polyMG	0.46	0.54	0.16	0.24	0.30	0.10	0.25	0.06	17

Figure 41: ^{1}H-NMR spectra of three alginate samples with different composition. 10 mg/ml mannuronan (A), poly-G (B) and poly-MG (C) was dissolved in D_2O. The sequence parameters are shown for the three different spectra (D). Copied from (111).

The integrals of the different peaks were determined by the NMR software (TopSpin 4.0.7 (Bruker BioSpin). These integrals were used to calculate the sequence parameters by the equations

$$F_G = \frac{I_G}{I_G + (I_{\boldsymbol{MG}} + I_{\boldsymbol{MM}})} = \frac{I_G}{I_{tot}}$$

$$F_M = 1 - F_G$$

$$F_{GG} = \frac{I_{G\boldsymbol{G}G+M\boldsymbol{G}G}}{I_{tot}}$$

$$F_{GGM} = \frac{I_{G\boldsymbol{G}M-5}}{I_{tot}}$$

$$F_{MGM} = \frac{I_{M\boldsymbol{G}M-5}}{I_{tot}}$$

$$F_{MG} = F_{GM}\,\frac{I_{\boldsymbol{M}G-1}}{I_{tot}}$$

$$F_{MM} = F_{GM}\,\frac{I_{\boldsymbol{M}M-1}}{I_{tot}}$$

$$F_{GGG} = F_{GG} - F_{GGM}$$

$$F_{G>1} = \frac{F_G - F_{MGM}}{F_{GGM}}$$

where I is the integral of the peaks and F is the fraction. $F_{G>1}$ is a measure of the average G-block length.

Appendix D: Enzyme assays

Enzyme assays were used to measure enzyme activity of AlgE-type mannuronan C-5-epimerases. Abs_{230} was plotted as a function of time (Figure 42-46)

Lyase assays of AcAlgE2 and AcAlgE3 to measure enzyme kinetics

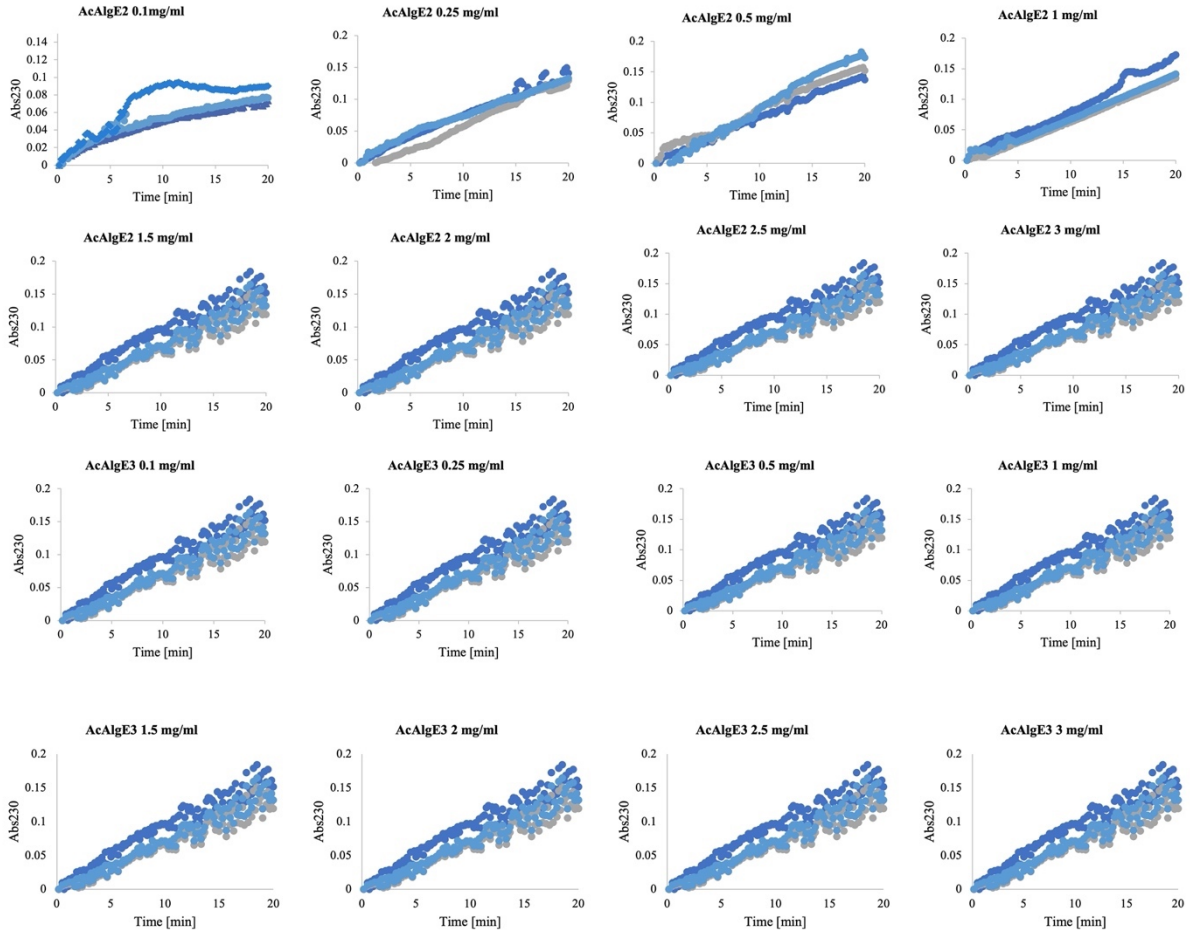

Figure 42: Abs_{230} measured every 10 sec for 20 min. AcAlgE2 or AcAlgE3 were working on sodium alginate (Sigma V-90) in 50 mM MOPS buffer, 1.5 mM $CaCl_2$. The enzymes had been purified by IEC and SEC. The enzyme and substrate concentration are given above the graphs. Three parallels were measured for each enzyme assay.

Lyase assays of AcAlgE2 and AcAlgE3 to measure salt dependency

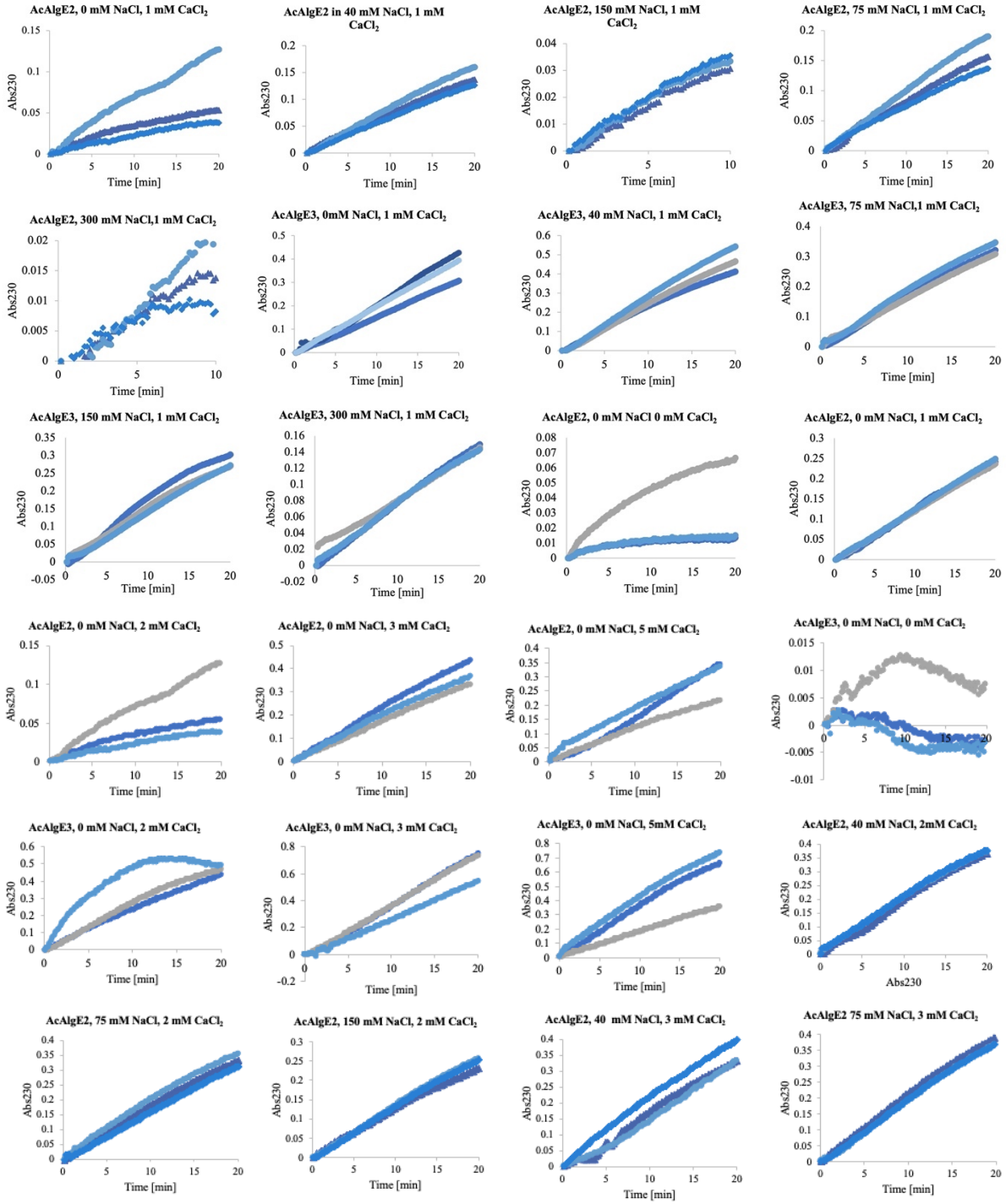

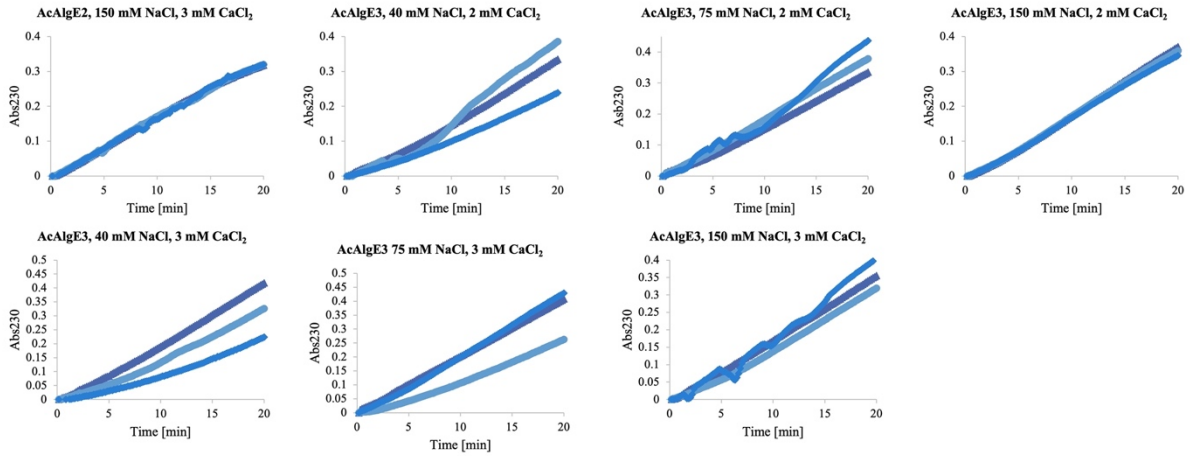

Figure 43: Abs_{230} measured every 10. sec for 20 min. Partially purified AcAlgE2 or AcAlgE3 were working on alginate (Sigma V-90). The reaction mix contained 1 mg/ml alginate, 50 mM MOPS buffer with variable concentrations of NaCl and $CaCl_2$. The enzyme, NaCl and $CaCl_2$ concentration is given above the graphs. Three parallels were measured for each enzyme assay.

Optimized epimerase assay – comparison of 200 and 75 mM NaCl

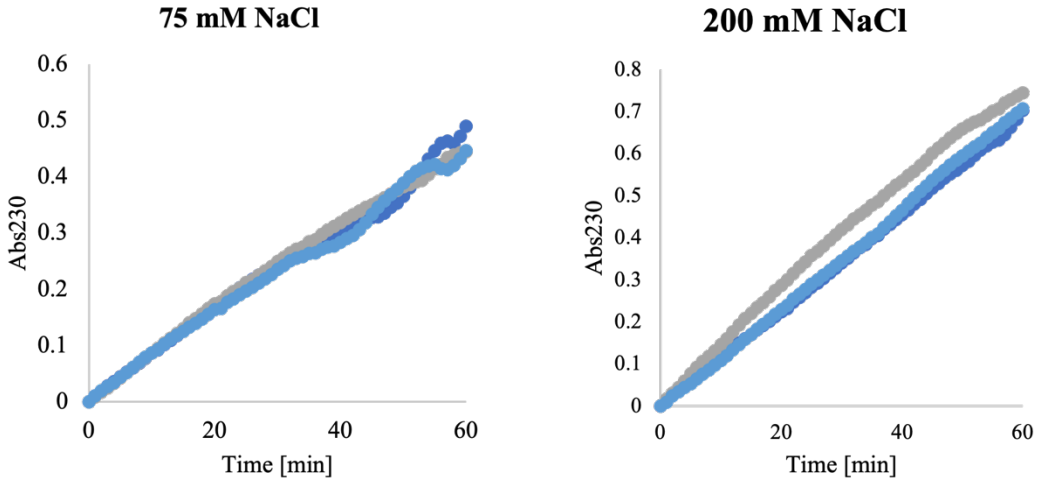

Figure 44: Abs_{230} measured every min for 60 min. A G-specific lyase was working on 1 mg/ml sodium alginate (Sigma V-90) in 50 mM MOPS buffer, 1.5 mM $CaCl_2$. The NaCl concentration is given above the graphs. Three parallels were measured for each enzyme assay.

Optimized epimerase assay – comparison of AlgE6 and mutant at different $CaCl_2$-concentrations

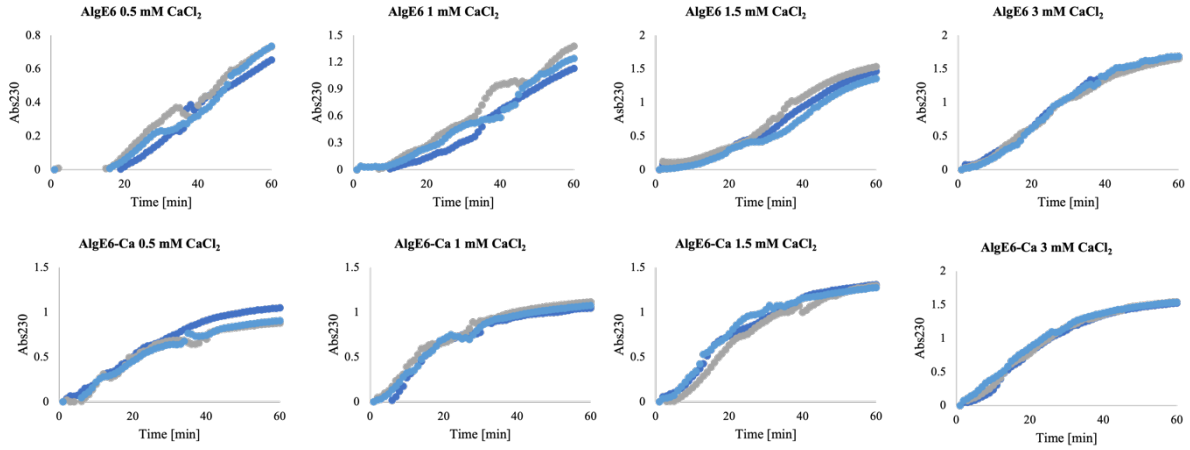

Figure 45: Abs_{230} measured every min for 60 min. Partially purified AlgE6 and AlgE6-Ca were working on 1 mg/ml mannuronan in 50 mM MOPS buffer and different $CaCl_2$ concentrations. The enzyme and $CaCl_2$ concentration are given above the graphs. Three parallels were measured for each enzyme assay.

Lyase assays of two AlgE6 mutants

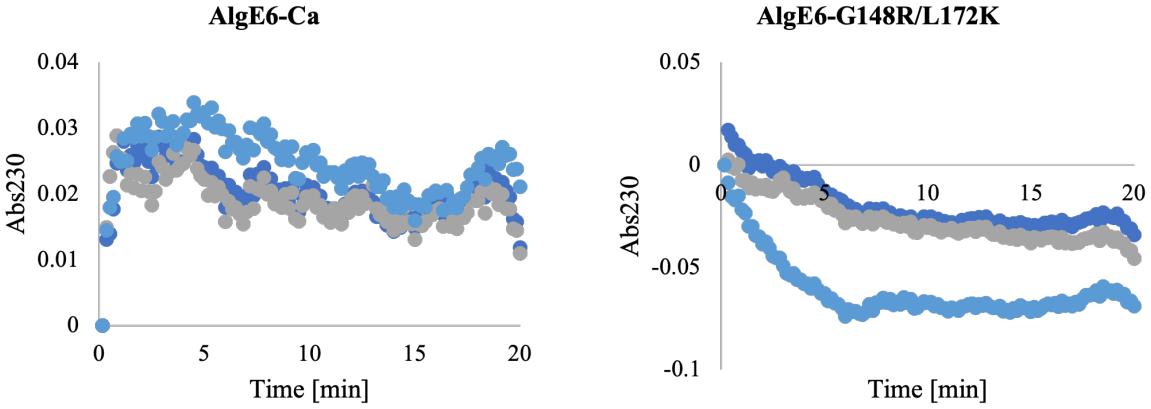

Figure 46: Abs_{230} measured every 10 sec for 20 min. Partially purified AlgE6-Ca and AlgE-G148R/L172K were working on 1 mg/ml sodium alginate (Sigma V-90) in 50 mM MOPS buffer and 1.5 mM $CaCl_2$. The enzyme is given above the graphs. Three parallels were measured for each enzyme assay.

Appendix E: Calculated enzyme activity

The lyase activity of AcAlgE2 and AcAlgE3 at different NaCl and $CaCl_2$ concentration was calculated (Table 12-14).

Table 12: Lyase activity of AcAlgE2 and AcAlgE3 at different NaCl-concentrations.[5]

Enzyme	NaCl concentration [mM]	Activity [U/mole]
AcAlgE2	0	$1.08 \times 10^7 \pm 5.37 \times 10^6$
	40	$2.67 \times 10^7 \pm 1.98 \times 10^6$
	75	$2.62 \times 10^7 \pm 2.56 \times 10^6$
	150	$1.20 \times 10^7 \pm 3.00 \times 10^5$
	300	$6.54 \times 10^6 \pm 2.44 \times 10^6$
AcAlgE3	0	$2.53 \times 10^7 \pm 7.75 \times 10^6$
	40	$3.96 \times 10^7 \pm 1.64 \times 10^6$
	75	$2.58 \times 10^7 \pm 1.47 \times 10^6$
	150	$2.43 \times 10^7 \pm 1.81 \times 10^6$
	300	$1.13 \times 10^7 \pm 1.19 \times 10^6$

Table 13: Lyase activity of AcAlgE2 and AcAlgE3 at different $CaCl_2$ concentrations.[6]

Enzyme	Ca [mM]	Activity [U/mole]
AcAlgE2	0	$3.21 \times 10^6 \pm 2.75 \times 10^6$
	1	$4.45 \times 10^7 \pm 2.31 \times 10^6$
	2	$4.87 \times 10^7 \pm 7.85 \times 10^6$
	3	$6.45 \times 10^7 \pm 5.82 \times 10^6$
	5	$5.41 \times 10^7 \pm 1.29 \times 10^7$
AcAlgE3	0	$7.94 \times 10^4 \pm 5.64 \times 10^4$
	1	$3.09 \times 10^7 \pm 5.82 \times 10^6$
	2	$4.65 \times 10^7 \pm 6.85 \times 10^6$
	3	$5.68 \times 10^7 \pm 9.34 \times 10^6$
	5	$4.60 \times 10^7 \pm 1.52 \times 10^7$

[5] The substrate was 1 mM alginate (Sigma V-90) in 50 mM MOPS, pH 6.9, 1 mM $CaCl_2$. The measured activity and standard deviation are based on triplicates for all samples. The activity is given in U/mol**e**, assuming pure protein samples.

[6] The substrate was 1 mM alginate (Sigma V-90) in 50 mM MOPS, pH 6.9 and there was no NaCl in the reaction mix. The results and standard deviation are based on triplicates for all samples. The activity is given in U/mol**e**, assuming pure protein samples.

Table 14: Lyase activity of AcAlgE2 and AcAlgE3 at different NaCl and $CaCl_2$ concentrations.[7]

Enzyme	NaCl[mM]	Activity [U/mole]		
		1 mM $CaCl_2$	**2 mM $CaCl_2$**	**3 mM $CaCl_2$**
AcAlgE2	0	$1.08 \times 10^7 \pm 5.37 \times 10^6$	$4.87 \times 10^7 \pm 7.85 \times 10^6$	$64.5 \times 10^7 \pm 5.82 \times 10^6$
	40	$2.67 \times 10^7 \pm 1.98 \times 10^6$	$5.59 \times 10^7 \pm 3.73 \times 10^6$	$6.45 \times 10^7 \pm 3.76 \times 10^6$
	75	$2.63 \times 10^7 \pm 2.56 \times 10^6$	$5.95 \times 10^7 \pm 4.47 \times 10^6$	$7.22 \times 10^7 \pm 2.79 \times 10^6$
	150	$1.20 \times 10^7 \pm 3.00 \times 10^5$	$4.96 \times 10^7 \pm 1.11 \times 10^6$	$6.54 \times 10^7 \pm 3.12 \times 10^6$
AcAlgE3	0	$2.53 \times 10^7 \pm 7.76 \times 10^6$	$4.33 \times 10^7 \pm 2.41 \times 10^6$	$5.68 \times 10^7 \pm 9.34 \times 10^6$
	40	$3.96 \times 10^7 \pm 1.64 \times 10^6$	$5.14 \times 10^7 \pm 6.63 \times 10^6$	$5.77 \times 10^7 \pm 3.87 \times 10^6$
	75	$2.58 \times 10^7 \pm 1.47 \times 10^6$	$5.73 \times 10^7 \pm 4.56 \times 10^6$	$6.36 \times 10^7 \pm 8.70 \times 10^6$
	150	$2.43 \times 10^7 \pm 1.81 \times 10^6$	$6.13 \times 10^7 \pm 2.42 \times 10^6$	$6.13 \times 10^7 \pm 6.31 \times 10^6$

The epimerase activity of AlgE6 and AlgE6-Ca at different $CaCl_2$ concentration is shown in Table 15.

Table 15: Epimerase activity of AlgE6 and AlgE6-Ca at different $CaCl_2$ concentrations.[8]

Enzyme	Ca^{2+} concentration [mM]	Activity [U/mole]
AlgE6	0.5	$3.53 \times 10^7 \pm 6.22 \times 10^6$
	1	$5.10 \times 10^7 \pm 1.41 \times 10^6$
	1.5	$7.49 \times 10^7 \pm 2.03 \times 10^6$
	3	$9.16 \times 10^7 \pm 1.24 \times 10^7$
AlgE6-Ca	0.5	$2.94 \times 10^7 \pm 6.40 \times 10^6$
	1	$3.31 \times 10^7 \pm 2.87 \times 10^6$
	1.5	$4.14 \times 10^7 \pm 6.58 \times 10^6$
	3	$5.82 \times 10^7 \pm 1.10 \times 10^7$

[7] The substrate was 1 mM alginate (Sigma V-90) in 50 mM MOPS, pH 6.9. The results and standard deviation are based on triplicates for all samples. The activity is given in U/mol**e**, assuming pure protein samples.
[8] The substrate was 1 mM mannuronan in 50 mM MOPS, pH 6.9, 75 mM NaCl. The measured activity and standard deviation are based on triplicates for all samples. The activity is given in U/mol**e**, assuming pure protein samples.

Appendix F: Lineweaver Burk-plot

To estimate the Michaelis-Menten constants K_m, V_{max} and k_{cat}, a Lineweaver Burk-plot was made by plotting $1/V_0$ against 1/[S] (Figure 47).

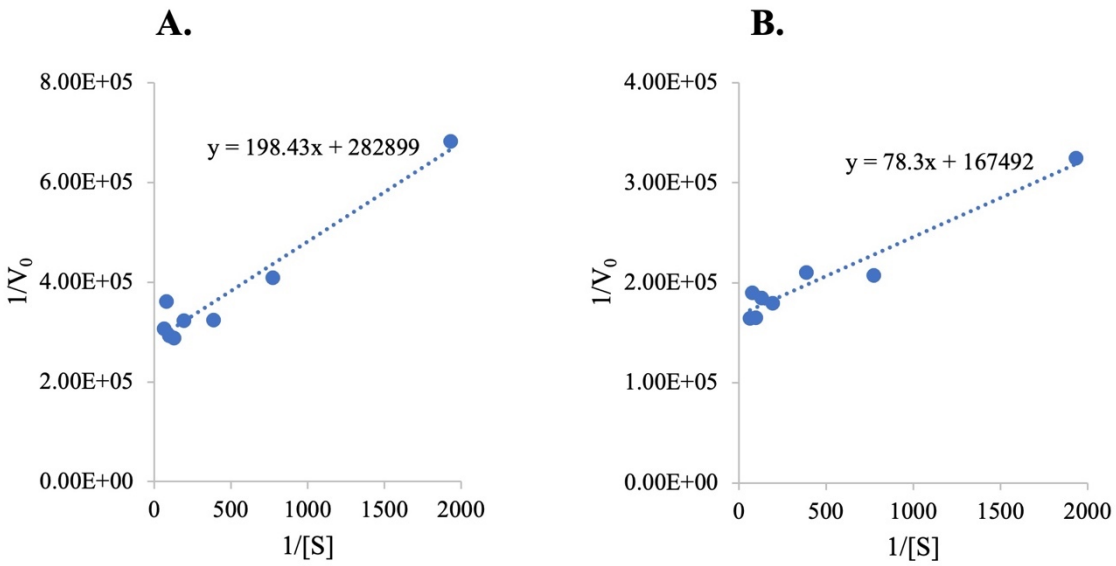

Figure 47: Lineweaver Burk-plots for the lyase activity of AcAlgE2 (A) and AcAlgE3 (B), based on the Michaelis-Menten plots in Figure 30 and the equations in Section 2.21.4.

Appendix G: Chromatograms from protein purification

The chromatograms from purification of AlgE-type mannuronan C-5-epimerases in this work are presented in Figure 48-54. UV absorption at 280 nm, given in Milli absorbance units (mAU), conductivity and concentration of B (Buffer B was used for IEC and Buffer D for IMAC) are shown as a function of volume (ml) eluted from the column.

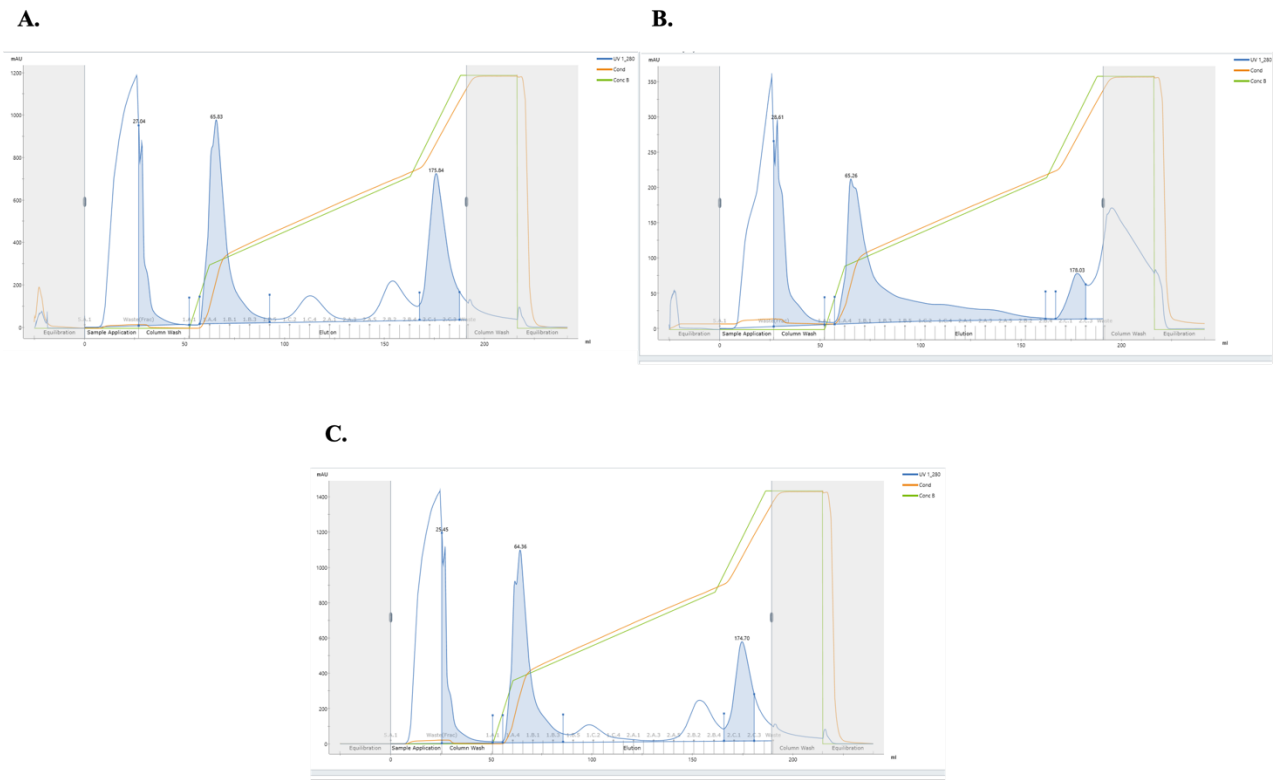

Figure 48: Chromatograms showing the elution profile (mAU UV absorption at 280 nm) of AcAlgE1 (A), AcAlgE2 (B) and AcAlgE3 (C) with C-terminal His-tags during purification by IEC.

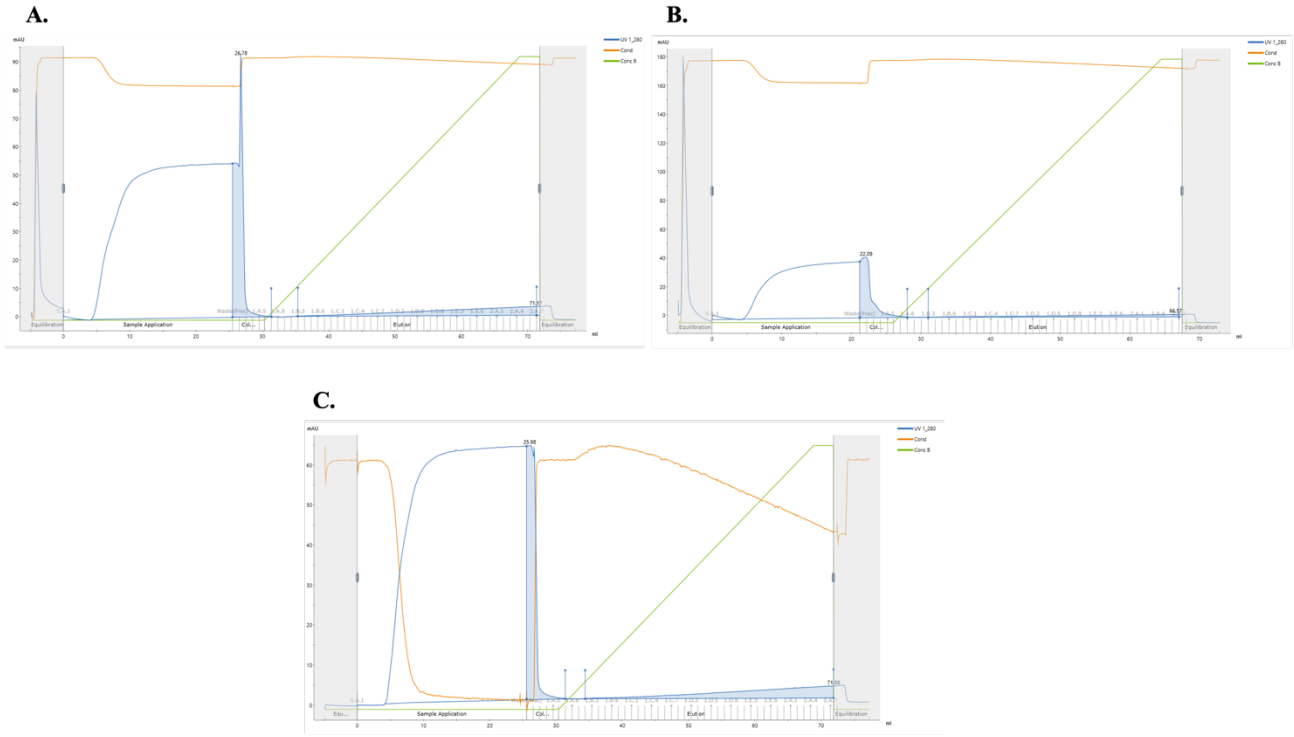

Figure 49: Chromatograms showing the elution profile (mAU UV absorption at 280 nm) of AcAlgE1 (A), AcAlgE2 (B) and AcAlgE3 (C) with C-terminal His-tags during purification by IMAC.

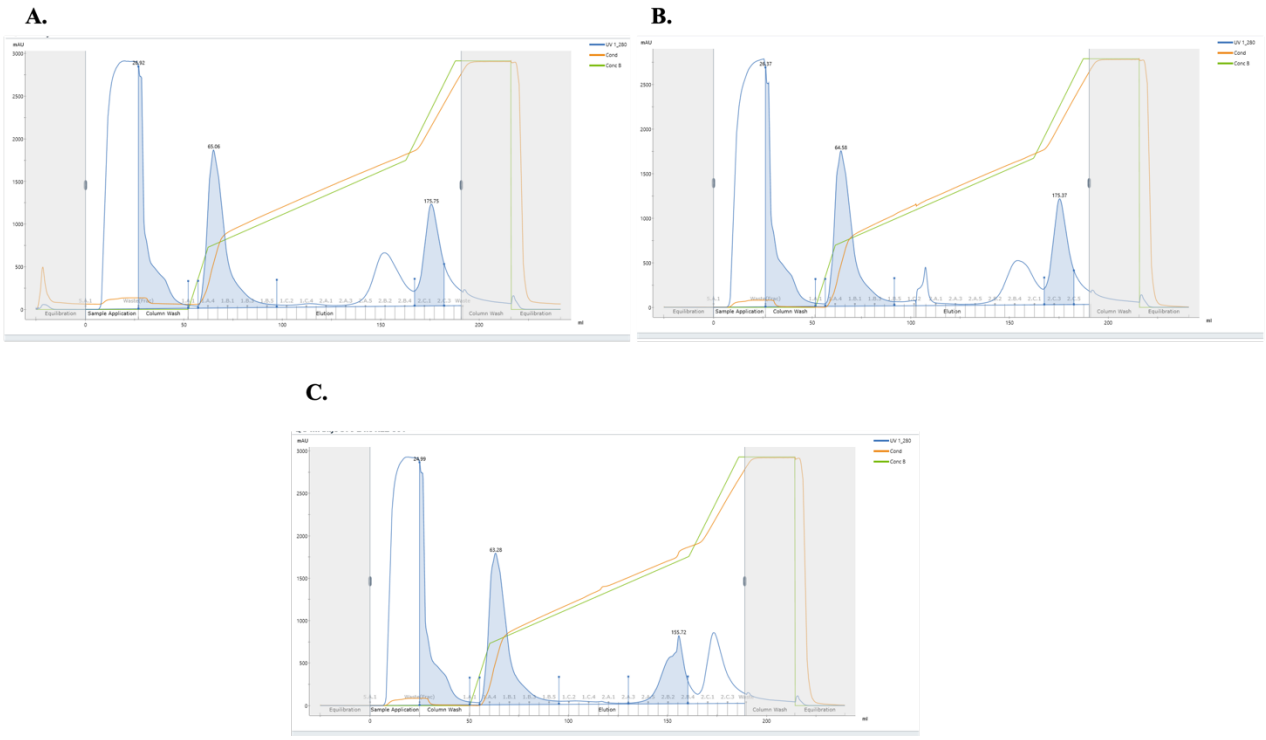

Figure 50: Chromatograms showing the elution profile (mAU UV absorption at 280 nm) of AcAlgE1 (A), AcAlgE2 (B) and AcAlgE3 (C) expressed in *E. coli* RV308 during purification by IEC.

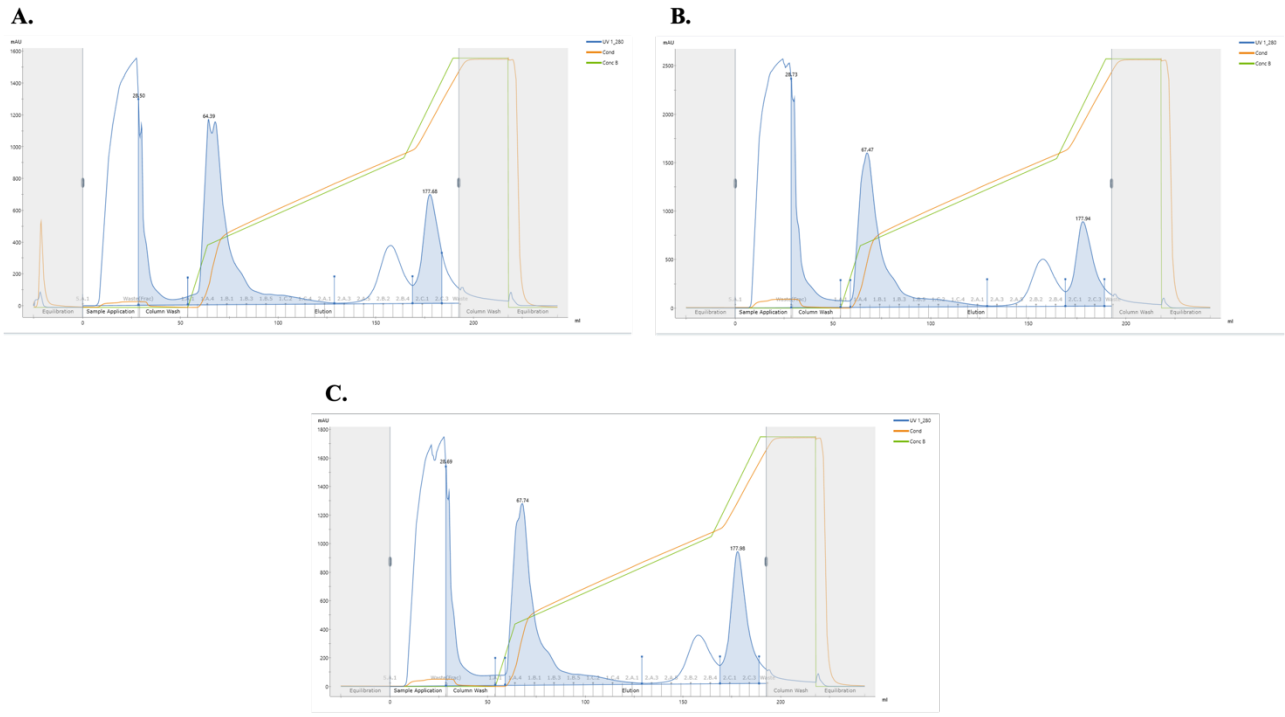

Figure 51: Chromatograms showing the elution profile (mAU UV absorption at 280 nm) of AcAlgE1 (A), AcAlgE2 (B) and AcAlgE3 (C) expressed in *E. coli* RV308 by HCDC during purification by IEC.

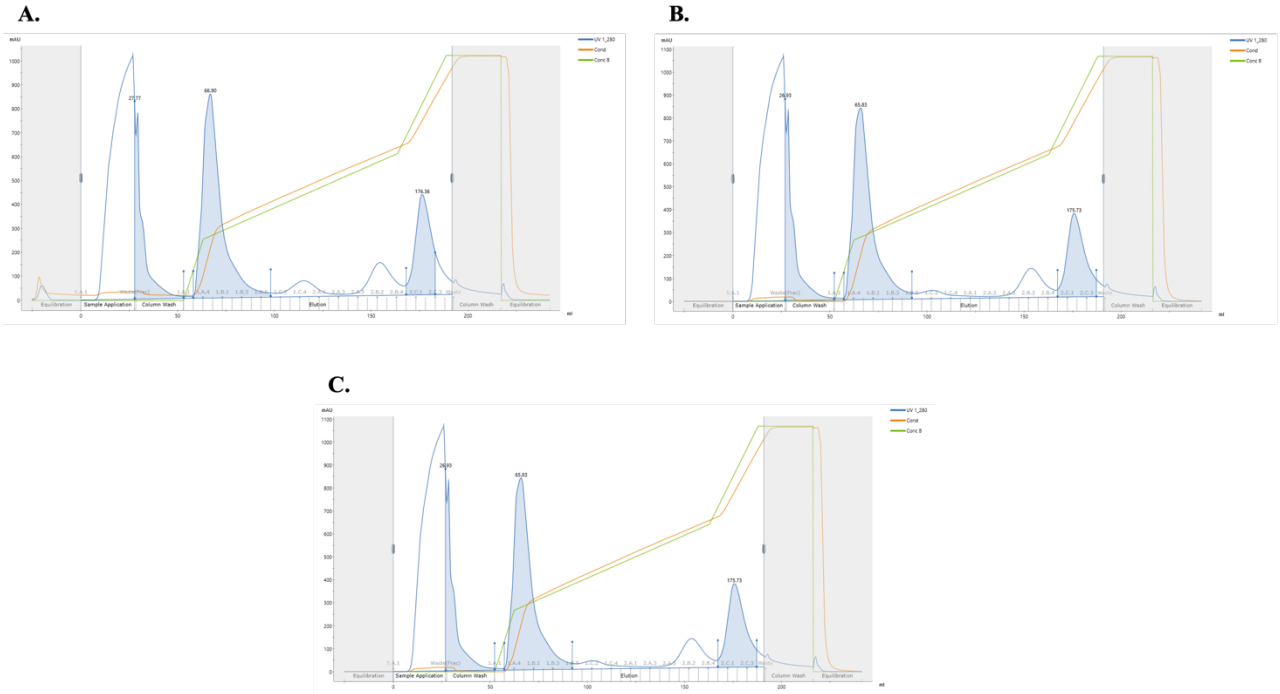

Figure 52: Chromatograms showing the elution profile (mAU UV absorption at 280 nm) of AcAlgE1 (A), AcAlgE2 (B) and AcAlgE3 (C) expressed in *E. coli* SHuffle T7 express during purification by IEC.

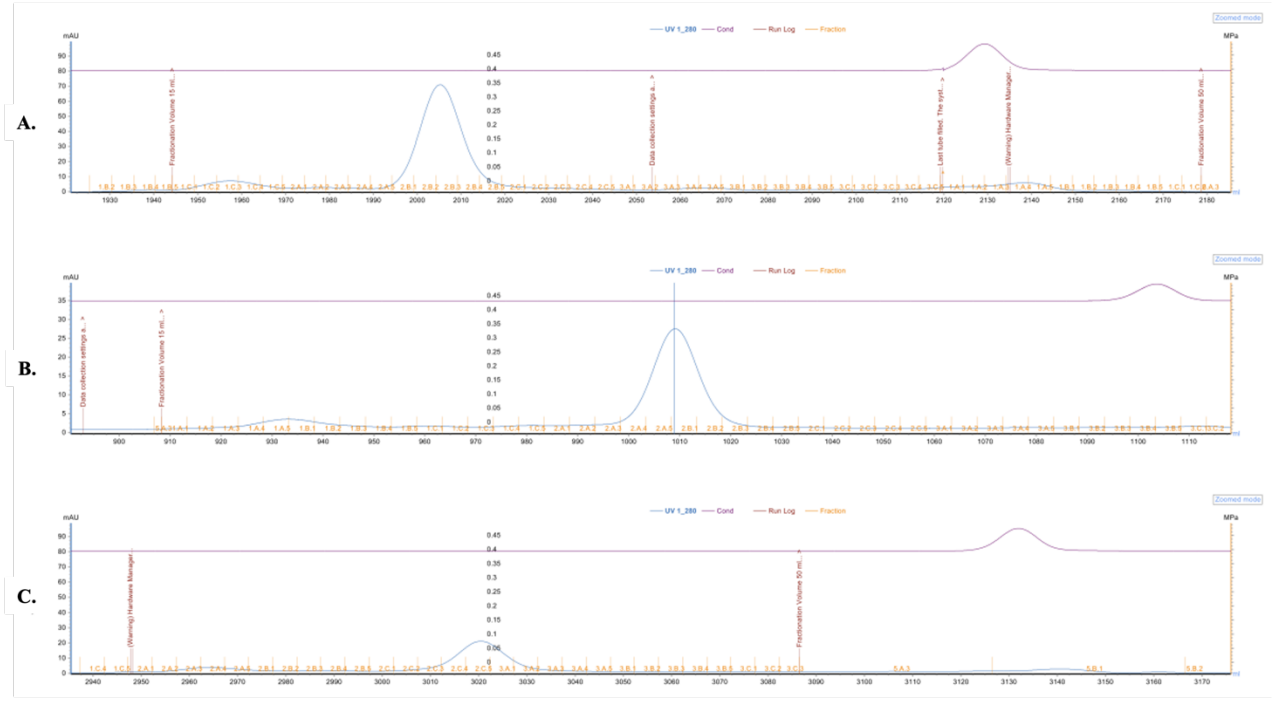

Figure 53: Chromatograms showing the elution profile (mAU UV absorption at 280 nm) of AcAlgE1 (A), AcAlgE2 (B) and AcAlgE3 (C) expressed in *E. coli* SHuffle T7 express during purification by SEC.

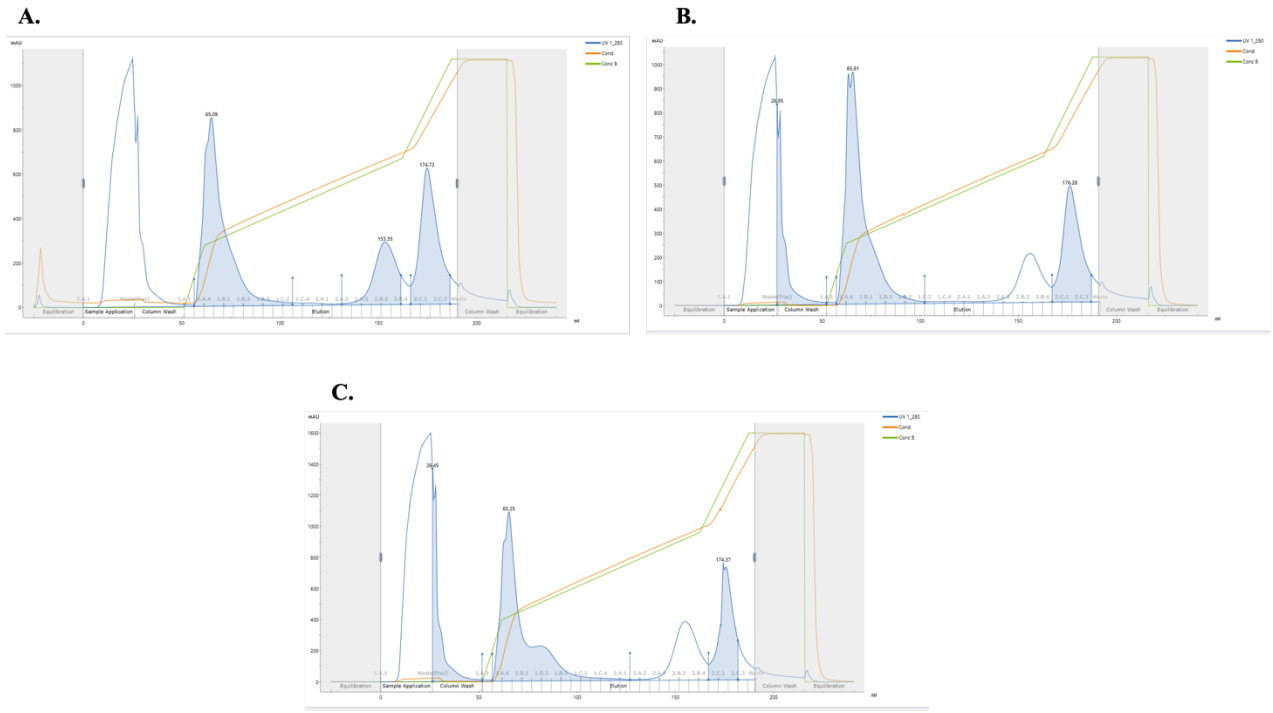

Figure 54: Chromatograms showing the elution profile (mAU UV absorption at 280 nm) of AlgE6 (A), AlgE6-G148R/L172K (B) and AlgE6-Ca (C) during purification by IEC.

Silje Trå Hervig

A study of AlgE-type mannuronan C-5-epimerases from *Azotobacter chroococcum* and *Azotobacter vinelandii*

NTNU
Kunnskap for en bedre verden